Non-invasive determination of myocardial oxygen consumption with ^{11}C-acetate and positron emission tomography

Michael A. Brown MBBS, FRACP

Department of Medicine
University of Adelaide

Submitted for the degree of
Doctor of Medicine
April, 1994

Awarded 1995

Table of Contents

Chapter

(iii) Abstract

Assessment of myocardial metabolism with radiolabelled substrates and positron emission tomography (PET) provides a potentially sensitive technique to investigate physiological and pathological cardiac states *in vivo*. However myocardial substrate utilization is dependent on a number of variables, including prevailing substrate concentrations, the hormonal environment and the presence of pathological states such as myocardial ischaemia. Prior studies have indicated that overall metabolic activity cannot be estimated from rates of utilization of any one particular substrate, for example glucose or fatty acid. Oxygen consumption would provide an ideal assessment of metabolic activity, however technical considerations preclude assessment of this with oxygen-15 and PET. It was hypothesized that acetate labelled with carbon-11 would provide an index of oxidative metabolism, based on fundamental biochemical principles. Acetate is predominantly metabolized in the citric acid cycle, with limited alternative metabolic pathways. The rate of production of $^{11}CO_2$ from ^{11}C-acetate would reflect citric acid cycle flux, and could be measured from the externally assessed clearance of total ^{11}C-radioactivity from myocardium using PET. Citric acid cycle flux is known to be tightly coupled to oxidative phosphorylation, and hence would provide an index of oxidative metabolism.

This hypothesis is confirmed in studies using isolated perfused rabbit hearts and closed chest canine studies. The rate of production and clearance of $^{14}CO_2$, resulting from oxidation of ^{14}C-acetate, was closely correlated with oxygen consumption in isolated perfused rabbit hearts. Similarly the rate of production and clearance of $^{11}CO_2$, resulting from oxidation of ^{11}C-acetate, was closely correlated with myocardial oxygen consumption in canine studies. Production and clearance of $^{11}CO_2$ could be measured externally by PET from the rate of clearance of total ^{11}C-radioactivity from myocardium. The technique has been validated over a wide range of cardiac work loads and under conditions of myocardial ischaemia, myocardial reperfusion following ischaemia and hypoxia. ^{11}C-acetate kinetics were found to be insensitive to changes in myocardial substrate supply.

Changes in oxidative metabolism were then evaluated in acute and chronic animal models of myocardial infarction. Myocardial oxygen consumption was impaired by 26 to 97% following 1 hour of coronary occlusion in acute studies and to a lesser extent in chronic studies. Oxygen consumption and contractility are known to be dissociated in "stunned" myocardium following acute myocardial ischaemia. Recovery of oxidative metabolism and contractility following 1 hour of coronary occlusion were found to occur in parallel over a 4 week period.

Preliminary experience with ^{11}C-acetate was also obtained in normal subjects and patients following acute myocardial infarction. Oxidative metabolism was related to work load in normal subjects, and was impaired in patients with myocardial infarction.

In summary the technique offers non-invasive assessment of myocardial oxidative metabolism on a regional basis using PET. These measurements can be made on a serial basis and in situations where assessment of oxygen consumption was previously not possible, particularly with respect to human studies.

(iv) This thesis contains no material which has been accepted for the award of any other degree or diploma in any university and that, to the best of my knowledge and belief, the thesis contains no material previously published or written by another person, except where due reference is made in the text of the thesis.

The author consents to this thesis being made available for photocopying and loan if accepted for the degree of Doctor of Medicine.

.....

M. A. Brown

(v) I would like to thank Professor Burton Sobel and Dr. Steven Bergmann of the Cardiovascular Division, Department of Medicine of Washington University, St. Louis, Missouri for their inspiration, enthusiasm and support while this work was in progress. I acknowledge my colleagues at Washington University, in particular Carla Weinheimer and Howard James for technical support with animal experiments, Jim Bakke for technical support with biochemical assays, David Marshall and the staff of the Washington University Medical Cyclotron for preparation of positron emitting tracers, Joanne Markham for assistance with mathematical modelling and Pilar Hererro for partial volume and spillover correction analyses. I also acknowledge Dr. Julio Perez for his contribution to the studies requiring assessment of left ventricular function with echocardiography. Initial patient studies were performed in collaboration with Dr. Mary Walsh.

Chapter 1.

Introduction.

Evaluation of myocardial oxidative metabolism may provide a potentially sensitive index for evaluating the impact of cardiac disease on metabolic function and the efficacy of therapeutic interventions. Cardiac contractility has previously been used as the major index of cardiac function, although past and recent studies have highlighted the disparity between myocardial viability and contractility which may occur. The rapid loss of contractility during acute ischaemia was first recognised by Tennant and Wiggers in 1935 [1], and recent studies have also demonstrated a dissociation between viability (or preservation of myocardial metabolism) and contractility in "stunned" myocardium [2] and "hibernating" myocardium [3]. Stunned myocardium may occur following repetitive brief ischaemic insults, with transient loss of contractility which may recover to normal over a period of days to weeks. Hibernating myocardium may occur in chronically ischaemic myocardium, where myocardial blood flow is insufficient to support energy production for contractility but sufficient to maintain viability. Recognition of this dissociation in patients with chronic coronary artery disease will lead to optimal therapy with revascularization in patients who demonstrate impaired ventricular contractility.

Potentially a non-invasive index of overall myocardial metabolism, when evaluated on a regional basis, would be useful to delineate the extent and distribution of jeopardized myocardium. The response to interventions such as coronary thrombolysis for acute myocardial infarction and to coronary angioplasty or coronary artery bypass surgery for chronic myocardial ischaemia could potentially be predicted with greater sensitivity and reliability. Similarly the efficacy of physiologic or pharmacological interventions designed to enhance myocardial metabolism could be characterized in a variety of disease states.

Positron emission tomography has allowed the non-invasive evaluation of the regional myocardial distribution over time of selected physiologic tracers labelled with positron emitting radionuclides. The application of this technique to the aforementioned disease states has resulted in confirmation of the concept of hibernating

myocardium in humans, which would otherwise not be possible [4]. Previous studies have largely utilized carbon-11 (^{11}C) palmitate or fluorine-18 (^{18}F) deoxyglucose to assess myocardial metabolism. However, myocardial energy requirements are fulfilled by a complex pattern of utilization of substrates depending on the prevailing substrate, oxygen and hormone concentrations in arterial blood. Hence total energy utilization cannot be predicted from the utilization of any one major substrate alone [5]. Technical limitations in imaging the heart preclude the use of oxygen-15 (^{15}O) oxygen to measure regional myocardial oxygen consumption, although this method is successful in the brain [6]. An alternative method of measuring oxygen consumption would be to measure citric acid cycle flux, since oxidative phosphorylation is tightly coupled to the citric acid cycle. Hence directional changes in oxygen consumption and energy production would be reflected by similar changes in citric acid cycle flux. Since myocardial energy requirements are predominantly met by aerobic metabolism during both normoxia and ischaemia [7], assessment of citric acid cycle flux would potentially indicate overall myocardial energy production. A variety of radiolabelled tracers were considered for their ability to reflect citric acid cycle flux, including acetate, acetoacetate or β hydroxybutyrate, pyruvate and lactate. Anticipated problems with each of these tracers are discussed below. Acetate was the most likely tracer based on known cardiac metabolic pathways, and had previously been labelled with carbon-11. It was hypothesized that ^{11}C-acetate would primarily be metabolized in the citric acid cycle, producing $^{11}CO_2$, and that alternative metabolic routes would be minor. The rate of production and clearance of $^{11}CO_2$ from the heart would reflect the activity of the citric acid cycle, which could be measured by PET from the rate of external clearance of the ^{11}C-radiolabel from the heart. Hence it was hypothesized that the use of ^{11}C-acetate with PET would provide an indirect assessment of oxidative metabolism in the heart, and that this technique could be validated by comparison with directly measured myocardial oxygen consumption. It was also hypothesized that since initial sequestration of ^{11}C-acetate by the heart is an energy dependant process requiring activation to ^{11}C-acetylCoA, accumulation early after administration would

require viable myocardium. Hence administration of ^{11}C-acetate in patients with acute or chronic myocardial infarction would provide an index of infarct size.

Background

a. Myocardial Metabolism

Myocardial contractility relies on the production of adenosine triphosphate (ATP) within the mitochondria to activate the actomyosin complex, resulting in myofibrillar shortening. Cellular stores of ATP are limited, requiring continuous production of ATP to ensure cardiac contraction. The majority of ATP during normoxia is produced by oxidative phosphorylation of adenosine diphosphate [7]. Investigation of the source of ATP production during myocardial ischaemia in a open chest canine model indicates that the pattern of metabolism remains predominantly oxidative, with over 90% of ATP produced by oxidative phosphorylation rather than anaerobic metabolism [7]. Oxidative phosphorylation is tightly coupled to the citric acid cycle, hence changes in energy requirements are reflected by parallel changes in citric acid cycle activity. The citric acid cycle is the major source of reducing equivalents for oxidative phosphorylation. The subsequent transfer of electrons from reducing equivalents in the form of NADH and $FADH_2$ results in the transfer of electrons along the electron carrying chain and reduction of oxygen, with the phosphorylation of ADP to ATP. The citric acid cycle depends on the oxidation of acetyl CoA, which may be produced from diverse substrates including fatty acids, glucose, amino acids (such as glutamate), lactate and ketone bodies. The relative contribution of each substrate group will depend on the arterial concentration of each substrate [8], the metabolic environment (particularly myocardial ischaemia), and the hormonal environment. This is in contrast to substrate utilization within the brain, which is predominantly reliant on glucose. Under normal conditions in a non fasting animal, fatty acids are the preferred cardiac substrate. Hence addition of fatty acids to perfused hearts results in a reduction of glucose metabolism [4], as does the addition of ketone bodies [9]. In contrast glucose utilization predominates after glucose loading (or following a high carbohydrate meal) in association with high insulin levels.

It has been recognized for over 50 years that the heart is able to also utilize ketone bodies [10]. Previous studies have demonstrated that acetoacetate may be a preferred cardiac substrate, since acetoacetate is able to suppress the utilization of glucose in perfused hearts [11,12]. Acetoacetate is also able to suppress the utilization of free fatty acids by the heart in *in vivo* canine studies [13], supporting the concept of a preferred or at least readily utilized substrate.

The diversity of substrate utilization under normoxic conditions results in an inability to measure overall energy requirements using any one particular substrate [5]. Although fatty acids may be the major cardiac substrate during normoxia, fatty acid oxidation is preferentially inhibited during ischaemia due to the inhibition of beta oxidation of long chain fatty acids. Glycolysis is stimulated during ischaemia, relying on both exogenous sources of glucose and glycogen breakdown. Accumulation of metabolites during ischaemia, particularly lactate and NADH, subsequently inhibit glycolysis due to inhibition of glyceraldehyde 3-phosphate dehydrogenase. Although anaerobic glycolysis is enhanced, the majority of ATP production continues from oxidation of acetyl CoA and oxidative phosphorylation [7].

Acetate is readily activated to acetyl CoA by the heart, and in isolated perfused hearts is able to support normal cardiac function without reliance on exogenous glucose or fatty acid metabolism [14]. Arterial concentrations of acetate are normally low in humans, approximately 40 to 300 μM and hence acetate results in a small contribution to overall energy requirements [15,16]. A hormonal influence has also been demonstrated, with insulin increasing the utilization of acetate [14]. Supra physiological levels of acetate have been found to inhibit the utilization of glucose in perfused rat hearts [14,17], indicating the ready utilization of acetate.

b. Potential tracers of citric acid cycle flux

Potential tracers of citric acid cycle flux are those myocardial substrates which undergo limited intermediary metabolism prior to the formation of acetyl CoA, for example ketone bodies, pyruvate, lactate or acetate. Conversely, glucose undergoes extensive intermediary metabolism involving gluconeogenesis and glycolysis.

Metabolic products of glycolysis will eventually include carbon dioxide, via the citric acid cycle, and fatty acids, amino acids and lactate.

Pyruvate is converted to acetyl CoA by pyruvate dehydrogenase. Alternative major metabolic pathway are the formation of lactate by lactic dehydrogenase, a reaction which at equilibrium is well in favour of lactate production at a pH of 7.0 [18], or the formation of glycolytic intermediates [17]. Pyruvate is readily utilized by the perfused rat heart [14], and at high concentrations may account for approximately 90% of oxidative metabolism. However an appreciable quantity of pyruvate, approximately 30%, disappearing from the perfusion medium is converted into lactate [14]. The efflux of radiolabelled lactate, in addition to radiolabelled CO_2, following the metabolism of radiolabelled pyruvate would then prevent assessment of radiolabelled CO_2 production and hence the rate of citric acid cycle flux. In addition radiolabelled glycolytic intermediates would also increase the complexity of interpretation of clearance kinetics.

Lactate is utilized by the heart under normoxic conditions, however the same limitations true for pyruvate are also true for lactate. In addition ischaemic hearts are net producers of lactate, and metabolism to pyruvate under these circumstance is unlikely.

Ketone bodies, either acetoacetate or β hydroxybutyrate, are readily utilized by the heart during normoxia, as described above. Acetate is formed as an intermediary step prior to the production of acetyl CoA. However studies of isolated rat hearts perfused with acetoacetate have demonstrated that 50% of acetoacetate removed from the medium can be accounted for by the formation of β hydroxybutyrate [11]. Hence the variable rate of production of radiolabelled β hydroxybutyrate and radiolabelled CO_2 would prevent the assessment of citric acid cycle flux.

Acetate is directly activated to acetyl CoA, and hence would appear to be an ideal agent for the study of citric acid cycle turnover. A detailed summary of potential biochemical pathways involving acetate is shown below.

c. Biochemical Pathways of Acetate Metabolism

Acetic acid is a carboxylic acid with the structure CH_3-COOH, and is ubiquitous in nature. Metabolism requires activation to acetyl CoA, which may occur in all tissues.

acetate + ATP + CoASH ⇒ acetyl CoA + AMP + PPi

where ATP = adenosine triphosphate, CoASH = Coenzyme A, AMP = adenosine monophosphate and PPi = pyrophosphate. This reaction in myocardial tissue is mediated by acetyl CoA synthetase within mitochondria, and the reaction is uni-directional. In contrast, activation of acetate within other tissues such as liver or adipose tissue occurs within cellular cytoplasm [19].

The initial activation of acetate to acetyl CoA would appear to be poorly regulated, in contrast to the intermediary metabolism of other substrates, as suggested by the tenfold increase in acetyl CoA levels found in isolated perfused rat hearts when perfused with 5 mM acetate [20]. This arterial concentration is supra physiological compared to normal levels of 40 - 300 μM in man [16,21]. Acetyl CoA hydrolase, which may reverse the direction of this reaction when the ratio of acetyl CoA/CoA is high, is found in liver and adipose tissue [22], and has also been reported in rat and sheep heart [23]. However the activity of acetyl CoA hydrolase in the latter tissues is 4 (rat heart) to 14 fold (sheep heart) less than the activity of acetyl CoA synthetase, possibly indicating that acetate utilization is more important in these tissues than acetate production.

Acetyl CoA is subsequently predominantly oxidized in the citric acid cycle, ultimately forming carbon dioxide and water. Rapid expansion of the normally small metabolic pool of acetyl CoA within the mitochondria may result in the reversible conversion to acetylcarnitine within the cytoplasm by a carnitine dependent acyl transferase system [22]. During cardiac arrest in perfused rat hearts, when myocardial energy demand is low and citric acid cycle flux inhibited, approximately 50% of the carbon-14 label from carbon-14 labelled acetate has been reported in acylcarnitine [24]. Alternative metabolic routes of metabolism of acetyl CoA appear to be minor in contrast to metabolism in the citric acid cycle. Although potential pathways are myriad, the major pathways are discussed below.

The production of acetyl CoA from pyruvate (catalyzed by a multienzyme complex, the pyruvate dehydrogenase complex) is essentially irreversible [25], preventing the ultimate metabolism of acetate to pyruvate and limiting the diversity of further metabolic products such as lactate. However anapleurotic reactions, postulated to replenish the level of citric acid cycle intermediates following their removal, may potentially form pyruvate as shown below [18].

oxaloacetate + ADP + H_3PO_4 ⇔ pyruvate + ATP + H_2O

(catalyzed by pyruvic carboxylase)

malate + NADPH + H^+ ⇔ pyruvate + $NADP^+$

(catalyzed by malic enzyme)

Both oxaloacetate and malate are citric acid cycle intermediates, and hence these metabolic pathways are potential metabolic pathways of acetate. However previous studies of the metabolism of ^{13}C-acetate have demonstrated no incorporation of the ^{13}C label from ^{13}C-acetate into alanine, using nuclear magnetic resonance spectroscopy [26]. Since isotope equilibration between pyruvate and alanine is rapid [27], this finding has suggested that anapleurotic reactions producing pyruvate are limited in their extent.

Ketone bodies, acetoacetate and β hydroxybutyrate, may potentially be produced from acetyl CoA by mitochondrial bound enzymes as shown below.

2 acetyl CoA ⇔ acetoacetyl CoA + CoA

(catalyzed by acetoacetyl CoA transferase, although the equilibrium is far to the left [22])

acetoacetyl CoA ⇔ acetoacetate ⇔ 3-hydroxybutyrate

(catalyzed by 3-oxoacid-CoA transferase and 3-hydroxybutyrate dehydrogenase respectively)

Ketone bodies are readily utilized by the heart for energy production, and these steps do not appear to be subject to any particular control [28]. The heart has not previously been regarded as a ketogenic organ , unlike other organs such as the liver [15,29]. However studies demonstrating ketone production by myocardial tissue have

been reported in pig heart extracts [30], isolated rat heart mitochondria [31] and dog hearts rendered hypoxic [29].

Alternatively acetyl CoA can be utilized within the mitochondria or the cytosol to form fatty acids by *de novo* synthesis or by chain elongation. Although fatty acid biosynthesis in organs such as liver and adipose tissue predominantly occurs within the cell cytoplasm, fatty acid biosynthesis in the heart may either occur within the mitochondria or cytosol. Conflicting results have previously been reported [32] with respect to the major site of production. Studies examining the utilization of carbon-14 labelled acetate during normoxia in isolated perfused rat hearts have demonstrated *de novo* synthesis of palmitate and at least partial production of stearate by chain elongation [32]. The majority of incorporated radioactivity was found in C_{14}, C_{16} and C_{18} fatty acids, and these fatty acids were distributed predominantly in phospholipids (78%,) and triglycerides (17%) [32]. *De novo* synthesis of palmitate from acetyl CoA is shown below.

$$\text{acetyl CoA} + 7\ \text{malonyl CoA} + 14\ H^+ \Rightarrow$$
$$\text{palmitate} + 8\ \text{CoA} + 7\ CO_2 + 14\ NADP^+ + 6\ H_2O$$

The mitochondrial membrane is impermeable to acetyl CoA, however acetyl CoA is transported to the cytosol by a carnitine dependent acyl transferase system [22], enabling free fatty acid synthesis in the cytosol. Alternatively acetyl CoA is synthesised within the cytosol from the citric acid cycle intermediate citrate, which can be transported to the cytosol from the mitochondrial matrix.

$$\text{citrate} + \text{ATP} + \text{CoA} \Rightarrow \text{acetyl CoA} + \text{oxaloacetate} + \text{ADP} + \text{Pi}$$

Additionally the major class of C_{18} fatty acids (such as stearic, oleic and linoleic acids) may be formed predominantly by chain elongation from palmitate, as shown below.

$$\text{palmitoyl CoA} + \text{malonyl CoA} \Rightarrow \text{stearoyl CoA}$$

(in a complex series of metabolic steps)

where malonyl CoA is formed from acetyl CoA

$$\text{acetyl CoA} + HCO_3^- + \text{ATP} \Rightarrow \text{malonyl CoA} + \text{ADP} + \text{Pi}$$

(catalyzed by acetyl CoA carboxylase).

Hence acetate may be incorporated into fatty acids by either of these mechanisms. However the extent of this is less than 1% of metabolized acetate during normoxia in isolated hearts [20]. The extent of incorporation of labelled acetate into neutral lipid and phospholipid may increase 3 to 4 fold during 60 minutes of severe hypoxia, compared to 60 minutes of normoxic perfusion [33]. Hence these studies suggest little incorporation of radiolabelled acetateinto lipid, either during normoxia or ischaemia.

Citric acid cycle intermediates, formed originally from acetate, may also be metabolized to amino acids. The primary example is the production of glutamate from α-ketoglutarate, a citric acid cycle intermediate.

$$\alpha\text{-ketoglutarate} + NH_3 + NADH + H^+ \Leftrightarrow \text{L-glutamic acid} + NAD^+ + H_2O$$

(catalyzed by glutamate dehydrogenase)

Additionally glutamate may be formed from α-ketoglutarate by transamination.

α-ketoglutarate + amino acid ⇔ glutamate + keto acid

(catalyzed by glutamic amino transferase)

Similarly oxaloacetate may be metabolized to aspartate by transamination.

oxaloacetate + alanine ⇔ aspartate + pyruvate

(catalyzed by a transaminase)

Rapid ^{14}C isotope equilibration between α-ketoglutarate and glutamate has been reported in isolated rat heats perfused with ^{14}C-acetate [20]. However in the same study poor isotope equilibration was reported between oxaloacetate and aspartate, suggesting a low rate of aspartate transamination in this model.

A detailed assessment of potential acetate metabolism, as discussed above, is necessary to determine the complexity of radiolabelled substrate kinetics. Positron emission tomography is able to define the concentration and distribution of the radiolabel in the region of interest, but is not able to distinguish between the various metabolites containing the radiolabel. Hence interpretation of tracer kinetics depends on a limited number of metabolic pathways which are predictable under a wide variety of metabolic conditions.

The concept of using radiolabelled acetate to assess citric acid cycle flux depends on oxidation to radiolabelled carbon dioxide. Synthesis of acetate using ^{11}C in the carboxyl group of the acetate molecule would result in metabolism to $^{11}CO_2$ in the citric acid cycle. The rate of production of $^{11}CO_2$ from ^{11}C-acetate will reflect citric acid cycle flux, which may be potentially measured from the externally derived clearance of ^{11}C-acetate from myocardium. Oxidative phosphorylation (for the production of high energy phosphates) is known to be tightly coupled to citric acid cycle flux and hence assessment of the latter will provide an index of oxidative metabolism.

However the ratio between citric acid cycle flux and oxygen consumption will vary depending on the substrate used for myocardial energy consumption. For example, oxidation of glucose, lactate and palmitate consume 3.0, 3.0 and 2.9 moles of oxygen per mole of acetyl CoA utilized, respectively. Using palmitate as a reference, oxygen consumption calculated from citric acid cycle flux would be underestimated by 4% if glucose were the only substrate utilized. The same underestimation would be encountered if lactate were the only substrate utilized. This potential error in measuring oxygen consumption must be considered in assessing the validity of a technique using citric acid cycle flux, however the magnitude of this error would appear to be small.

Chapter 2.

Positron Emission Tomography.

Positron emitting radionuclides currently in use for cardiac studies are either cyclotron or generator produced. Examples of cyclotron produced radionuclides are oxygen-15 (half life ($t_{1/2}$) of 2.1 minutes), carbon-11 ($t_{1/2}$ 20.4 minutes), nitrogen-13 ($t_{1/2}$ 10.0 minutes) and fluorine-18 ($t_{1/2}$ 110 minutes), while an example of a generator radionuclide is rubidium 82 ($t_{1/2}$ 76 seconds). Cyclotron produced radionuclides are isotopes of naturally occurring elements of physiological cardiac substrates, and are chemically indistinguishable. Hence metabolism of a radiolabelled substrate is identical to the unlabelled substrate. This is in contrast to conventional nuclear studies utilizing gamma emitting radionuclides, which are not physiological substrates. The short half life of positron emitting radionuclides enables serial studies with different agents (for example, assessing myocardial blood flow and metabolism) with low radiation dosimetry to the patient.

Positrons are emitted from the radionuclide, travel a short distance in the tissue under study prior to interaction with an electron, which results in annihilation. The resulting energy is carried by two photons with an energy of 511 keV each, which travel at near 180 degrees to each other. Simultaneous detection of two photons indicates that the interaction of positron and electron must have arisen on a line between the sites of detection. Resulting localization by coincidence detection results in high spatial resolution and high detection efficiency. Further localization may be achieved by measuring the time difference between detection of two annihilation photons, so called time of flight systems.

The majority of tomographic units employ multiple rings of detectors in circular arrays to allow the simultaneous acquisition of data from multiple planes. Instruments used in this study were PETT VI and Super PETT 1, the latter a time of flight machine. Potential limitations of PET are attenuation of photons by tissue, partial volume effects and spillover of radiation from region to region. Attenuation is compensated by attenuation correction involving an external source of positrons, enabling quantitative radionuclide concentrations to be calculated from image data. Partial volume effects

occur when the dimensions of the tissue imaged are less than half the spatial resolution of the instrument used. For example, accurate recovery of counts from the left ventricular wall would require a left ventricular wall thickness of 24 mm in a tomographic unit with a full width at half maximum (FWHM) resolution of 12 mm. Since left ventricular wall thickness is substantially less, recovery of counts is less than anticipated. Given the technical limitations of current generation tomographic units, reduced counts can only be compensated by the application of a mathematical model. Hence counts in myocardial tissue in this study are corrected using assumed and fixed dimensions for left ventricular wall thickness and left ventricular cavity diameter, as described in Appendix A. Spillover refers to the effect of a region containing radioactivity on the region of interest. An adjacent region containing higher radiation will increase count rates in the region of interest, for example high count rates in the left ventricular cavity will "spillover" onto the adjacent left ventricular wall. Accurate quantification requires correction for both partial volume effects and spillover, using a mathematical model.

Positron Emitting Substrates.

A number of positron emitting tracers of cardiac metabolism have been thoroughly investigated, in particular ^{11}C-palmitate and ^{18}F-fluorodeoxyglucose. The limitations revealed, particularly with respect to ^{11}C-palmitate, influence the method of investigation of future substrates and hence are worthwhile discussing.

a. ^{11}C-palmitate.

Palmitate is a saturated long chain (16:0) fatty acid, which represents one of the major fatty acids in plasma. The cellular uptake of free fatty acids has previously been considered to be due to passive diffusion, however recent reports in isolated rat cardiomyocytes have indicated a carrier dependent system [34]. The tracer kinetics of ^{11}C-palmitate have been well characterized in a variety of animal models. Essentially clearance consists of three phases. The first is due to washout of non-extracted tracer and to backdiffusion of non-metabolized tracer. Subsequent clearance is biexponential, suggesting that the ^{11}C-label has entered two distinct metabolic pools. The second phase consists of a early, rapidly clearing phase while the third phase consists of a late,

slowly clearing phase. The relative magnitude of the two phases differs, depending on cardiac workload, substrate conditions, and coronary flow. Early studies indicated that the clearance half time of the early phase was inversely proportional to work load [35,36]. These findings were consistent with the expected metabolic fate of palmitate. The early major phase was due to oxidation of ^{11}C-palmitate to $^{11}CO_2$, which was cleared from the heart. The late minor phase was due to incorporation of ^{11}C-palmitate into triglyceride and phospholipid, which demonstrated a slow turnover. Increased cardiac work resulted in a greater proportion of ^{11}C-palmitate undergoing oxidation. Clearance of ^{11}C-label from the heart represented the sequential steps of beta oxidation, oxidation in the citric acid cycle and clearance from the heart. However, the last factor makes no significant contribution as tissue clearance times are constant over a wide range of flow rates [36]. Subsequent open chest canine studies have demonstrated a correlation between the amount and rate of $^{11}CO_2$ release from myocardium and the clearance half time of the early clearance phase [37]. The same studies with ^{11}C-palmitate have also demonstrated inhibition of free fatty acid oxidation after glucose loading [37]. The size of the rapid phase decreased and the clearance half time increased after glucose loading, suggesting preferential utilization of glucose over free fatty acids. Myocardial ischaemia in perfused hearts also results in a prolonged clearance half time of the rapid phase [38], consistent with inhibition of fatty acid oxidation. Further detailed studies of the metabolic fate of the ^{11}C label during myocardial ischaemia have demonstrated that "backdiffusion" of extracted but non-metabolized ^{11}C-palmitate is responsible for a major proportion of clearance of the ^{11}C label [39]. Under control conditions in open chest anaesthetised dogs, 45% of initially extracted ^{11}C-palmitate was metabolized to $^{11}CO_2$, whereas 6% backdiffused. Under ischaemic conditions, 17% of initially extracted ^{11}C-palmitate was metabolized to $^{11}CO_2$, and 16% backdiffused. Hence estimates of metabolic activity based on residue clearance of ^{11}C-palmitate underestimate the extent of reduction of fatty acid oxidation during ischaemia. Subsequent studies confirm these results and document increased incorporation of the ^{11}C label into lipid fractions during ischaemia [40]. Metabolism of

^{11}C-palmitate during reperfusion after transient myocardial ischaemia is discussed in Chapter 6.

^{11}C-palmitate has also been used to assess left ventricular infarct size in canine studies 48 hours after coronary occlusion, comparing infarct size tomographically with morphometric estimates of infarct size and with infarct size from creatine kinase depletion [41]. Close correlations were obtained, indicating ^{11}C-palmitate can be used to assess infarct size in this model of persistent coronary occlusion. Similarly tomographic estimates of infarct size with ^{11}C-palmitate are closely correlated with enzymic estimates of infarct size based on the serial plasma CK-MB method [41].

b. ^{18}F-fluorodeoxyglucose.

Glucose is a major myocardial substrate, particularly under certain conditions such as ischaemia. Glucose is taken up by a facilitated, carrier mediated process. Subsequently glucose is phosphorylated by hexokinase, and involved in either gluconeogenesis or glycolysis. The rapid metabolism of glucose and the wide variety of metabolic products has limited the use of radiolabelled glucose in PET, although the use of ^{11}C-glucose has been investigated. An alternative approach has been to use analogs of glucose, in particular deoxyglucose. Deoxyglucose is phosphorylated by hexokinase, but is not subject to further metabolism and hence the diversity of metabolic end products is avoided. Labelling of deoxyglucose with fluorine-18 has enabled measurement of overall myocardial utilization of glucose, as assessed by positron emission tomography using Patlak graphical analysis [42,43]. A potential limitation of the technique may occur with dephosphorylation of ^{18}F-fluorodeoxyglucose-6-phosphate and subsequent egress of ^{18}F-fluorodeoxyglucose from the myocardium. The accuracy of this technique has not been defined in situations where this may occur, for example myocardial ischaemia. Although this technique is generally able to assess regional glucose utilization, no assessment of overall substrate utilization can be made due to the variable contribution of individual substrates, as discussed in Chapter 1.

The major role of ^{18}F-fluorodeoxyglucose to date has been the determination of myocardial viability post myocardial infarction, a technique pioneered by Schelbert [44]. ^{18}F-fluorodeoxyglucose is extracted by viable myocardium, and a comparison of regional myocardial uptake of this tracer compared to the uptake of a tracer used for indicating myocardial flow (such as N13-ammonia) used to differentiate viable from non-viable myocardium. Currently this tracer is widely accepted as the "gold" standard in defining myocardial viability in chronic coronary artery disease, although its role in acute myocardial infarction has not been validated. Uptake may occur in experimental models of transmural myocardial infarction, where no viable myocardium remains [45], and recent studies have demonstrated variable uptake in patients with viable myocardium post infarction [46].

c. ^{11}C-acetate.

Initial reports of synthesis of ^{11}C-acetate occurred during World War II, however a resurgence of interest in production of ^{11}C labelled radiopharmaceuticals occured in the early 1970's[47,48]. A modification of early techniques was further reported in 1982 [49]. Diffuse whole body uptake in dogs was initially reported in 1973 [48], and imaging of 2-^{11}C-acetate studied in a baboon and one human in the same year [47]. Both studies showed substantial uptake of ^{11}C-acetate in myocardium, and the externally derived clearance rate was found to be mono-exponential in one human subject with a half time of 3.3 minutes. Canine studies at the Royal Postgraduate Medical School in London, reported in abstract form in 1980, demonstrated retention of ^{11}C-acetate in regions of myocardial ischaemia [50]. The authors suggested that ^{11}C-acetate may be useful for detection of myocardial ischaemia [50], and similar findings were reported in 5 patients with coronary artery disease [51]. Subsequent studies by the same group demonstrated that externally derived clearance rates of ^{11}C from myocardium were influenced by cardiac pacing in canine studies and exercise in man, possibly reflecting changes in myocardial oxygen consumption [52]. The mean clearance half time was reported to be 10.7 minutes in 5 patients at rest, decreasing to 6.8 minutes with exercise. These studies of ^{11}C-acetate kinetics in myocardium described above were reported in abstract form, with no known subsequent publication of detailed findings.

Experimental studies reported in the following Chapters were undertaken at Washington University between 1985 and 1988. These data have largely been published from 1987 onwards [53,54,55,56,57].

Chapter 3

Delineation of myocardial oxygen utilization with ^{11}C-acetate in isolated perfused rabbit hearts.

Initial studies of the cardiac utilization of radiolabelled acetate were performed in the isolated perfused rabbit heart. This model allowed the precise control of a number of factors such as myocardial flow, myocardial oxygen utilization, cardiac work and delivery of radiolabelled tracer and allowed the venous effluent to be collected for characterization of the metabolic end products of radiolabelled acetate. Because of the short half life of ^{11}C tracers (20.4 minutes), ^{14}C-acetate was used in initial studies to determine the metabolic end products containing the ^{14}C label.

The aims of this initial *ex-vivo* study were to **a.** define the extraction and metabolism of ^{14}C-acetate under diverse conditions of flow and metabolism, **b.** determine the relationship between the rate of efflux of $^{14}CO_2$ in venous effluent (reflecting oxidation of ^{14}C-acetate) and oxygen consumption, and **c.** define the relationship between the externally detectable clearance of myocardial ^{11}C radioactivity and myocardial oxygen consumption in isolated perfused rabbit hearts.

The result of these studies would give the theoretical basis for the clinical application of ^{11}C-acetate with PET. A number of conditions must be met for the technique to have clinical application. A moderate to high myocardial extraction fraction of tracer present during diverse coronary flow conditions would be necessary for the left ventricle to be imaged tomographically. The rate of $^{11}CO_2$ production from ^{11}C-acetate and rate of efflux of $^{11}CO_2$ from the heart must reflect turnover of the citric acid cycle and myocardial oxygen consumption. Finally the end products of ^{11}C-acetate metabolism other than $^{11}CO_2$ would have to be minor in order for the externally detectable clearance of myocardial ^{11}C radioactivity to reflect the rate of $^{11}CO_2$ production, since PET is not able to discriminate between the metabolic end products in which the ^{11}C label is eventually incorporated.

Methods

Male New Zealand white rabbits weighing 3 to 5 pounds were stunned with a blow to the head. Hearts were rapidly excised and perfused with non recirculating,

oxygenated (95% O_2/5% CO_2) modified Krebs Henseleit perfusate containing 400 μM palmitate, 5mM glucose, and 70 mU/liter insulin. Hearts were paced at a rate of 180 beats/min with a right atrial bipolar electrode. Left ventricular pressure was monitored continuously with a fluid filled latex balloon inserted through the left atrium. The first derivative of left ventricular pressure (dP/dt) and coronary perfusion pressure were also recorded. The left ventricular pressure-time index was calculated from the product of the area under the left ventricular systolic pressure curve and heart rate [58]. The pulmonary artery was cannulated for collection of coronary venous effluent. Oxygen utilization was calculated from the product of arterio-venous oxygen difference per millilitre of perfusate and flow, normalized for heart weight.

Experimental procedure. To determine the steady-state extraction fraction of ^{14}C-acetate and production of $^{14}CO_2$ under diverse conditions, 11 hearts were perfused with 20 μCi/litre 1-^{14}C-acetate (specific activity 56 mCi/mmol; New England Nuclear) over a period of 30 minutes. The extraction fraction was calculated from the arterio-venous ^{14}C-acetate difference as a percentage of arterial ^{14}C-acetate.

High pressure liquid chromatography (see below) was used to separate ^{14}C-acetate, which was then quantified by gamma counting. Conditions investigated were normal flow (20 ml/min), and reduced flow (2 ml/min) with and without the addition of 50 μM of unlabelled sodium acetate. The extraction fraction was measured after 20 to 30 minutes of perfusion in control hearts and at both 10 and 20 minutes following the onset of ischaemia (2 ml/min flow). The extraction fraction was also measured in hearts reperfused at control flow rates after 60 minutes of ischaemia (n = 3), 20-30 minutes after commencement of ^{14}C-acetate infusion.

In 16 additional hearts studied under control conditions, with hypoxia (flow rate of 20 ml/min with hypoxic media), with ischaemia, or with reperfusion after ischaemia, the rate of oxidation of ^{14}C-acetate was determined based on the measured rate of efflux of $^{14}CO_2$ in the venous effluent over a 40 minute interval after a 2 minute infusion of 15 μCi ^{14}C-acetate. The 2 minute infusion period was selected based on results of pilot studies (data not shown) in rabbits of the arterial time-activity curve after intravenous

administration of tracer, indicating that tracer was largely cleared from the arterial circulation by this time.

After the completion of these initial studies, 0.5 mCi's of ^{11}C-acetate and 15 μCi's of ^{14}C-acetate were infused simultaneously over 2 minutes in 10 hearts. Clearance of ^{11}C-radioactivity was measured externally by residue detection, and the rates of efflux of total ^{14}C radioactivity and $^{14}CO_2$ were determined in the venous effluent over 20 to 40 minutes. In four of these hearts , the ^{11}C myocardial residue time-activity curve was determined at three different workloads induced by changing preload and heart rate (low and medium workload) and by infusion of isoproterenol (5×10^{-7}M) to produce a high workload state.

Measurement of $^{14}CO_2$ radioactivity. Coronary venous effluent was collected at 1 minute intervals into tubes containing sodium hydroxide to trap $^{14}CO_2$. Total ^{14}C radioactivity was measured by placing 1 ml of perfusate in 1 ml of Protosol (New England Nuclear) and adding 10 mls of Aquasol II (New England Nuclear) before ß-scintillation spectrometry. A duplicate sample was treated with 0.25 ml of 5N HCl and allowed to stand overnight on ice before spectrometry. These conditions were found to be necessary to prevent the loss of ^{14}C-acetate which occurred at room temperature, while allowing the loss of $^{14}CO_2$. Assay of controls verified greater than 99.9% loss of ^{14}C-bicarbonate (New England Nuclear) after acidification and greater than 98% retention of ^{14}C-acetate . The $^{14}CO_2$ content per millilitre of perfusate was calculated as the difference between total and residual radioactivity after treatment with HCl.

Measurement of ^{14}C-labelled metabolites in venous effluent. To characterize conversion of labelled acetate to metabolites other than labelled CO_2, albumen was precipitated in samples of venous effluent with an equal volume of 10% perchloric acid. The samples were centrifuged , and supernatant fractions were allowed to stand on ice overnight (as described above) for dissipation of $^{14}CO_2$. Samples were then stored at -70°C prior to analysis. Metabolites were separated with a Spectra Physics high pressure liquid chromatography (HPLC) system (San Jose, CA) and detected with a Waters Differential Refractometer. Optimal separation of acetate from citric acid cycle intermediates was accomplished with two organic acid columns in sequence (Biorad

Aminex HPX 87H and Benson OA850) with 0.01N H_2SO_4 at a flow rate of 0.5 ml/min at room temperature [59]. Retention times of individual citric acid cycle intermediates were determined, as were those for pyruvate, lactate, acetoacetate and ß-hydroxybutyrate. Because retention times for some species overlapped, additional separation for acetate and acetoacetate was accomplished with a C18 reverse phase column (LiChrosorb RP18, E.Merk, Darmstadt, W.Germany) in combination with an organic acid column. Fractions of venous effluent separated on the basic of measured retention times of each standard were collected for assay of ^{14}C-radioactivity.

Lactate and glucose were assayed conventionally with commercially available enzymatic assay kits (Behring Diagnostic, La Jolla, CA). Utilization and production of substrate were calculated from the product of arterio-venous concentration differences and flow, and normalized for heart weight. Myocardial lipid was extracted by the Bligh and Dyer procedure [60], and the percentage of ^{14}C radioactivity in the lipid phase relative to total ^{14}C myocardial radioactivity was determined.

Residue detection of ^{11}C-acetate. Annihilation photons were detected with two sodium iodide crystals placed symmetrically at 180 degrees across the isolated perfused rabbit heart. Coincidence counts were detected with an Ortec fast coincidence counter. Singles counts from one sodium iodide crystal and coincidence counts from both were recorded on-line with a Digital Equipment Corp. RX-08 mini computer. Data were subsequently decay corrected off-line, using a half time of 20.4 minutes for ^{11}C-radioactivity. Clearance data were fitted with a multi exponential curve fitting routine using the Marquardt algorithm. Although an attempt was made to fit biexponential solutions to all data, only monoexponential solutions were apparent in ischaemic and hypoxic hearts. The biological half time ($t_{1/2}$) was calculated from the rate constant (k) and the relationship $t_{1/2} = \ln 2/k$. The relative magnitude of each phase of a biexponential curve was calculated by back extrapolation of the monoexponential phase to the time of completion of infusion of ^{11}C-acetate as a percentage of the sum of both phases at that time.

Statistical analyses. Data in this and subsequent chapters are expressed as mean ± SD, unless otherwise specified. Multiple comparisons of paired or unpaired data

were analysed by analysis of variance followed by t tests corrected for the number of comparisons by the Bonferroni method [61]. Linear regression was calculated by the least squares method.

Isolated perfused rabbit heart studies were approved by the Animal Studies Committee of Washington University and conformed to the policies of the American Heart Association.

Results

Haemodynamics, flow and oxygen consumption. Haemodynamics and substrate utilization for steady-state studies (Group 1) and clearance studies following a 2 minute infusion (Group 2) with ^{14}C-acetate are presented in Table 3.1, shown on the following page. Haemodynamics were constant throughout the interval of evaluation of control hearts. In both Group 1 and Group 2 flow was reduced by 85 to 90% in ischaemic hearts, and myocardial oxygen consumption was diminished proportionately. Heart rate diminished by approximately 40-50% despite atrial pacing due to the development of atrio-ventricular block following the reduction of coronary flow. Hearts reperfused after 60 minutes of ischaemia showed a mild reduction of left ventricular pressure-time index and oxygen consumption compared to control hearts at a marginally higher left ventricular end-diastolic pressure, indicating substantial recovery of contractility despite the prolonged period of ischaemia.

Utilization of glucose was depressed in ischaemic hearts. However, the reduction was not statistically different compared with control hearts in part because of the increased extraction fraction at low flow. Also, glucose utilization varied considerably in control hearts because of low extraction fraction at high flow rates.

Hypoxic hearts showed a disproportionate reduction in left ventricular pressure time index compared to oxygen consumption, suggesting a greater role of anaerobic glycolysis. The higher glucose utilization in these hearts and the higher lactate production associated with hypoxia confirmed the possibility of increased anaerobic metabolism.

Steady-state utilization of ^{14}C-acetate. The steady-state extraction fraction of ^{14}C-acetate was determined in 11 hearts subjected to a wide range of flows,

Table 3.1 Haemodynamic variables, oxygen consumption, and glucose and lactate utilization during studies of ^{14}C-acetate extraction (**Group 1**) and radiolabelled acetate clearance (**Group 2**).

	HR (beats/ min)	**LVEDP** (mm Hg)	**dP/dT** (mm Hg/ sec)	**LVPTI** (mm Hg/ sec/min)	**Flow** (ml/g/min)	**MVO_2** (ml/g/min)	**Glucose** uptake (mg/g/min)	**Lactate** production (mg/g/min)
Group 1								
Control (n=4)	193±7	10±2	870±150	2360±660	4.04±0.58	0.061±0.013	-	0.099±0.067
Ischaemia (n=4)	117±44*	7±3	200±60*	680±300*	0.61±0.22*	0.009±0.004*	-	0.095±0.021
Reperfusion (n=3)	184±7	12±8	935±140	1920±30	4.37±0.76	0.057±0.011	-	0.040±0.018
Group 2								
Control (n=10)	187±19	8±4	970±180	2580±490	5.35±0.93	0.069±0.01	0.21±0.26	0.076±0.019
Ischaemia (n=10)	86±12*	9±2	140±50*	550±260*	0.48±0.1*	0.008±0.001*	0.055±0.014	0.091±0.035
Hypoxia (n=3)	185±5	8±2	530±58*	1100±740*	4.73±0.92	0.011±0.002*	0.435±0.044	0.389±0.071*
Reperfusion (n=3)	190±4	13±5	910±170	2050±620	4.62±0.41	0.055±0.006	0.147±0.138	0.083±0.111

HR = heart rate; LVEDP = left ventricular end diastolic pressure; dP/dT = first derivative of left ventricular pressure; LVPTI = left ventricular pressure-time index; MVO_2 = myocardial oxygen consumption. Values are mean ± SD, * $p < 0.01$ compared to control.

resulting in a spectrum of altered metabolic states. Extraction fraction of ^{14}C-acetate in hearts perfused at control flow rates of 20 ml/min with media without unlabelled sodium acetate averaged 63.4 ± 9.5%. In ischaemic hearts this averaged 94.9 ± 1.1%. Addition of a physiologic concentration (50 μM) of unlabelled sodium acetate had no significant effect on the extraction fraction (59.6 ±1.6% in control hearts, 93.4 ± 0.7% in ischaemic hearts). Thus, in hearts perfused with media with or without unlabelled acetate, the extraction fraction was significantly higher with ischaemia ($p < 0.001$). The extraction fraction of ^{14}C-acetate remained constant over 30 minutes in ischaemic hearts. Hearts reperfused at control flow rates after 60 minutes of ischaemia exhibited extraction fractions similar to those in the control group (54.8 ± 4.0%; n = 3, p = ns compared to control studies).

Steady-state production of $^{14}CO_2$, resulting from oxidation of ^{14}C-acetate, in control and reperfused hearts generally occurred within 15 minutes after onset of perfusion with ^{14}C-acetate and accounted for 86 ±7% of ^{14}C-acetate uptake over the duration of the infusion. The rate of production of $^{14}CO_2$ in ischaemic hearts continued to increase throughout the period of infusion but appeared to reach steady state by 25 minutes. This delay to equilibrium was possibly caused by the slower rate of turnover of the citric acid cycle during ischaemia.

Rate of oxidation of ^{14}C-acetate. The rate of efflux of $^{14}CO_2$ in the venous effluent was characterized under a variety of conditions after a 2 minute infusion of ^{14}C-acetate. Efflux of $^{14}CO_2$ reached a maximum 2.3 ± 0.8 min after the end of infusion in control hearts (n = 10) but was delayed to 11.8 ± 2.6 min in ischaemic hearts (n = 10). Efflux was subsequently biexponential in control and reperfused hearts (Figure 3.1 a), consisting of a dominant rapid phase and a smaller slow phase of efflux. Efflux was monoexponential in ischaemic and hypoxic hearts (Figure 3.1 b). The half-times of efflux calculated from the rapid phase were 3.2 ± 0.9 min for control (n = 7), 1.9 ± 0.4 min for isoproterenol stimulated (n = 3), 15.0 ± 0.4 min for ischaemic (n = 10), 9.3 ± 2.2 min for hypoxic (n = 3), and 3.1 ± 0.2 min for reperfused hearts (n = 3). The rates of efflux of $^{14}CO_2$ under these diverse conditions studied correlated closely with the rate of oxygen consumption in each heart (Figure 3.2, $r = 0.97$, $p < 0.001$). The rate of efflux also correlated closely with indices of cardiac work such as left ventricular

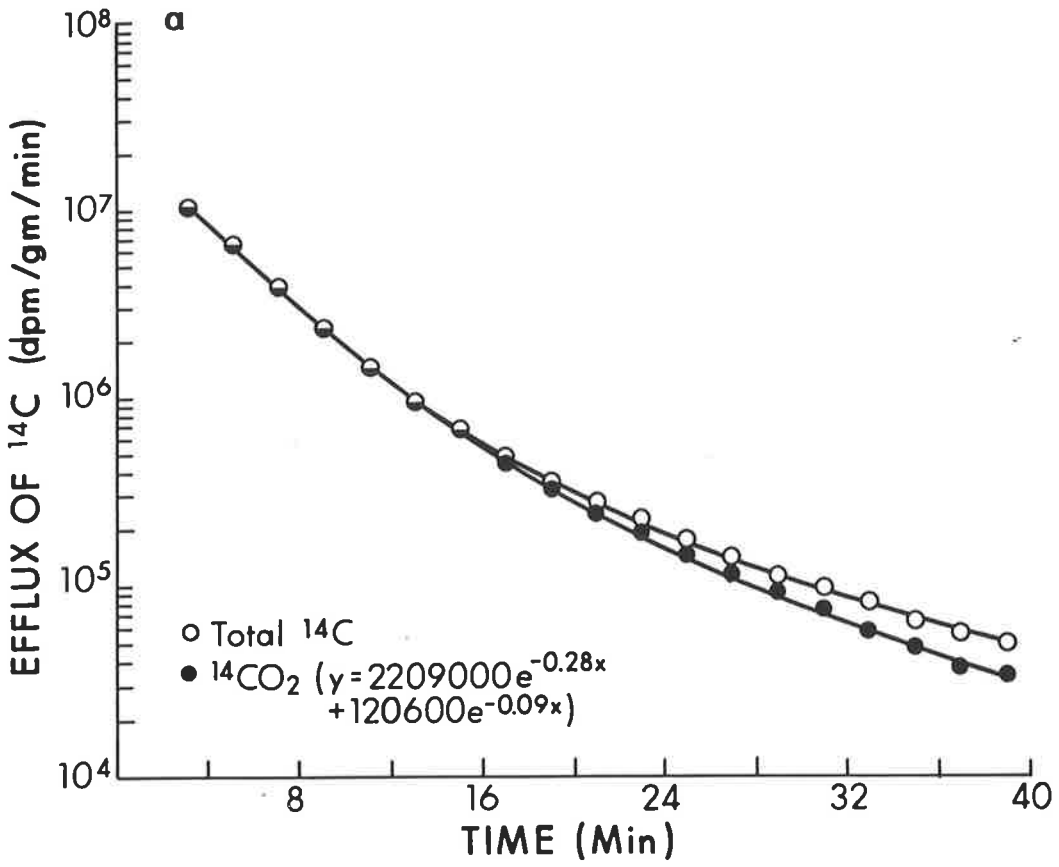

Figure 3.1. Efflux of total ^{14}C and $^{14}CO_2$ as a function of time after ^{14}C-acetate from **a.** one control heart and **b.** one ischaemic heart. Efflux of $^{14}CO_2$ was biexponential in all control hearts and monoexponential in all ischaemic hearts as shown in these examples with the solid lines fitted from peak efflux of $^{14}CO_2$. Rate constants for the rapid phase (0.28 min^{-1}) and slow phase (0.09 min^{-1}) in the control and ischaemic heart ((0.036 min^{-1}) are shown, The rate of efflux of total ^{14}C is very similar to the rate of $^{14}CO_2$ efflux.

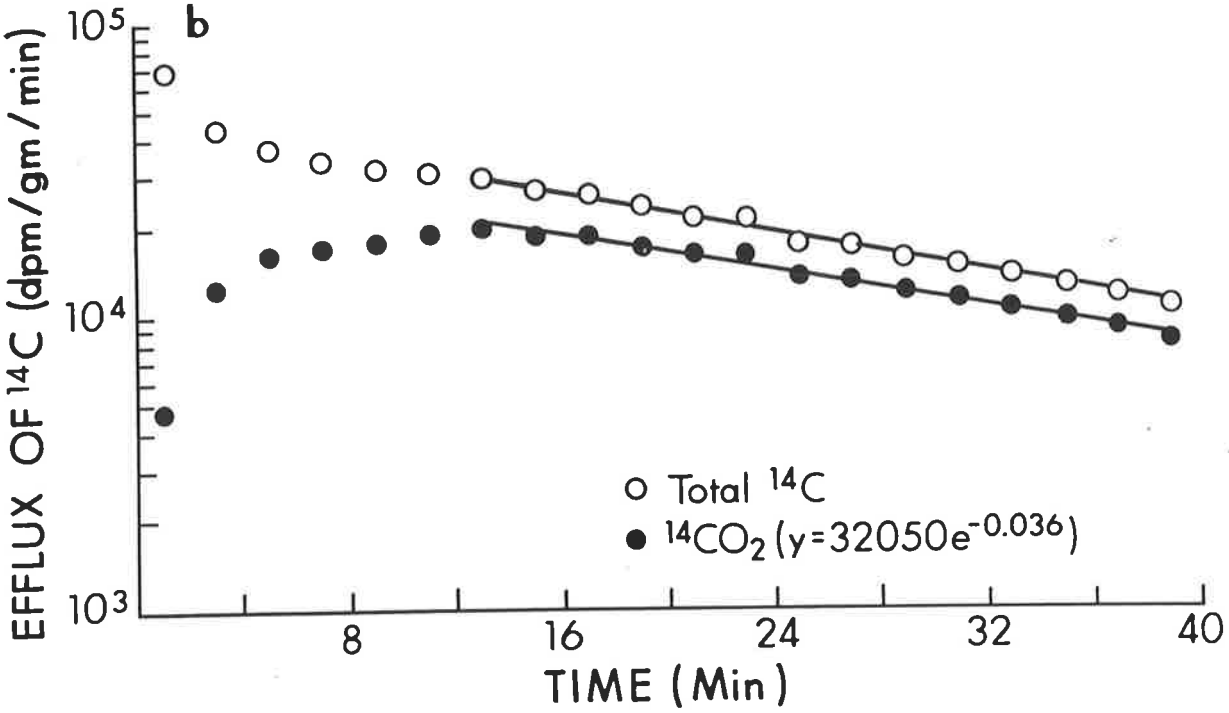

Figure 3.1 (cont) Efflux of total ^{14}C and $^{14}CO_2$ as a function of time after ^{14}C-acetate from **a.** one control heart and **b.** one ischaemic heart. Efflux of $^{14}CO_2$ was biexponential in all control hearts and monoexponential in all ischaemic hearts as shown in these examples with the solid lines fitted from peak efflux of $^{14}CO_2$. Rate constants for the rapid phase (0.28 min^{-1}) and slow phase (0.09 min^{-1}) in the control and ischaemic heart ((0.036 min^{-1}) are shown. The rate of efflux of total ^{14}C is very similar to the rate of $^{14}CO_2$ efflux.

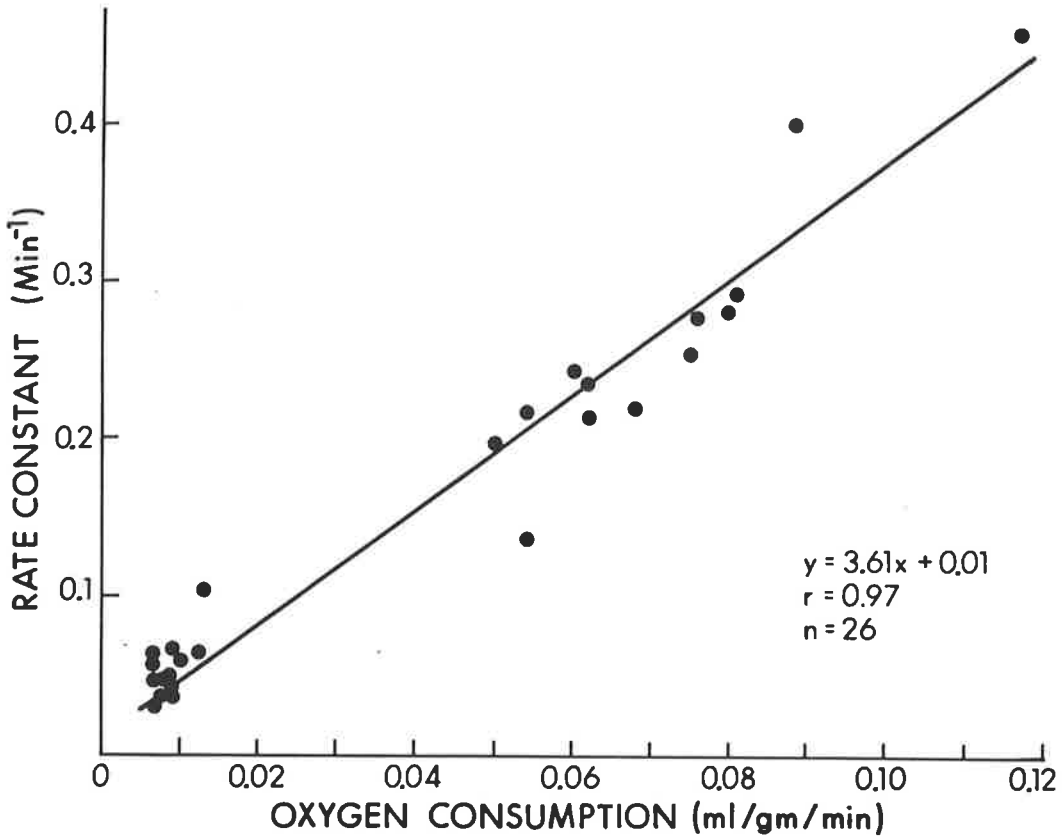

Figure 3.2 Correlation between myocardial oxygen consumption and the rate constant of the rapid phase of venous efflux of $^{14}CO_2$. The latter is indicative of the rate of oxidation of ^{14}C-acetate ($r = 0.97$, $p < 0.001$).

pressure-time index ($r = 0.86$, $p < 0.001$) and left ventricular dP/dt ($r = 0.97$, $p < 0.001$). Studies during hypoxia showed a relationship between oxygen consumption and rate constant of the rapid phase of efflux of $^{14}CO_2$ similar to that seen in all other studies, indicating that reduced clearance seen with ischaemia was caused by impaired oxygen delivery resulting in impaired oxygen utilization, rather than reduced clearance as a result of low flow per se. Reduced clearance of $^{14}CO_2$ could potentially occur during low coronary flow causing a discrepancy between myocardial oxygen consumption and rate of efflux of $^{14}CO_2$, invalidating the use of externally derived clearance rates by PET. However no evidence of this was present.

Prediction of $^{14}CO_2$ efflux based on total venous efflux of ^{14}C-radioactivity. The rate of efflux of total ^{14}C-radioactivity in the venous perfusate was used to estimate the rate of $^{14}CO_2$ efflux, which in turn was used to determine whether acetate oxidation could be measured externally by residue detection of myocardial ^{11}C-acetate. Because dynamic studies with PET define total clearance of tracer from myocardium but not clearance of $^{11}CO_2$ specifically, this comparison was performed to identify potential limitations of estimating oxidation of ^{11}C-acetate from analysis of myocardial residue time activity curves.

Half times of the major phase of $^{14}CO_2$ efflux and total ^{14}C efflux were almost identical in control hearts whether or not stimulation with isoproterenol was used (Figure 3.3). A similar concordance was seen in reperfused hearts and in hypoxic hearts. In ischaemic hearts, the half-times for $^{14}CO_2$ efflux (15.8 ± 4.8 min) were slightly longer than those for total ^{14}C efflux (14.7 ± 3.4 min) although the difference was not statistically significant.

This modest discrepancy was attributable to a lower fraction of $^{14}CO_2$ comprising total ^{14}C radioactivity in the venous effluent (Figure 3.4). In control and reperfused hearts, nearly all ^{14}C-radioactivity ($96.0 \pm 1.1\%$) in the venous effluent was in the form of $^{14}CO_2$ during the first 20 minutes (Figure 3.4). In contrast, in ischaemic hearts $^{14}CO_2$ contributed $75.7 \pm 7.2\%$ of total venous radioactivity during the period of monoexponential clearance of $^{14}CO_2$ 10-30 minutes after the completion of the ^{14}C-acetate infusion (Figure 3.4). The period of 10-30 minutes was used since the rate of

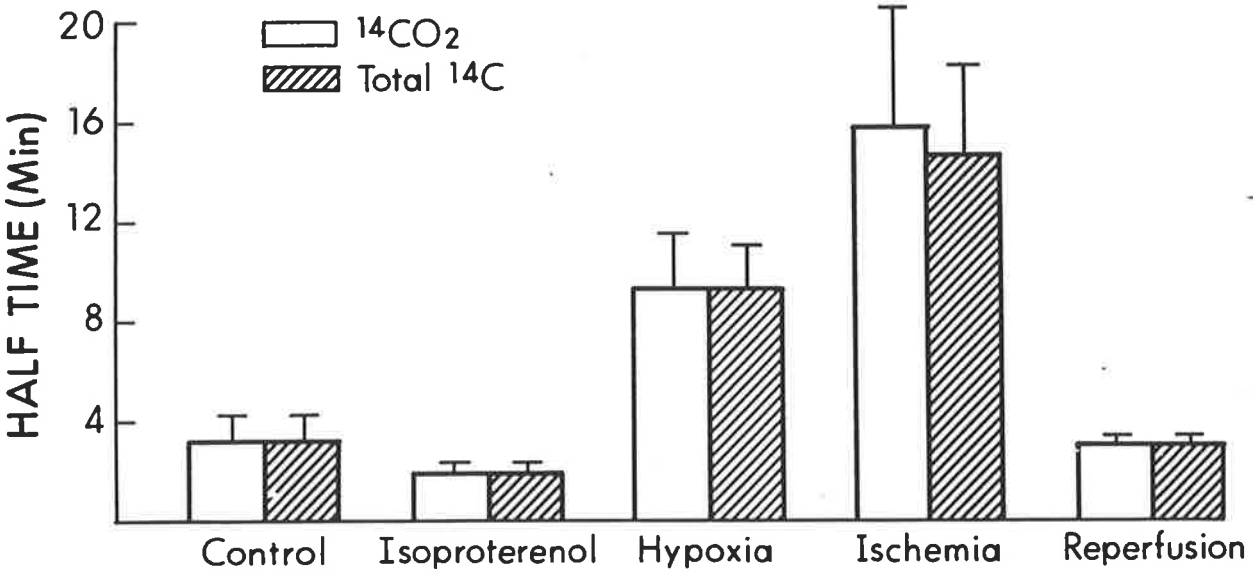

Figure 3.3 Half times of the rapid phase of $^{14}CO_2$ (open bars) and total ^{14}C efflux (hatched bars) over a wide range of flows and metabolic conditions. The half time of $^{14}CO_2$ efflux was inversely proportional to workload and oxygen consumption. No significant difference was found between the half times for $^{14}CO_2$ and for total ^{14}C efflux within each group.

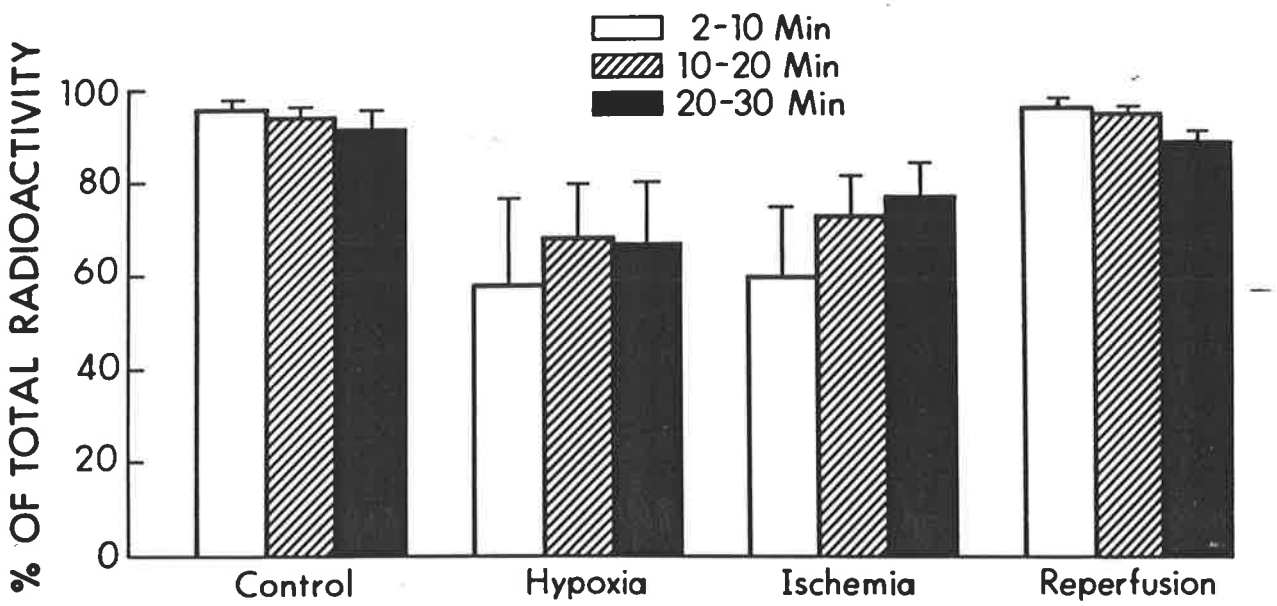

Figure 3.4 Contribution of $^{14}CO_2$ radioactivity to total venous radioactivity during the intervals shown after completion of infusion of ^{14}C-acetate. Limited myocardial release of metabolites of ^{14}C-acetate occurred in hypoxic and ischaemic hearts as discussed in the text.

efflux of $^{14}CO_2$ was calculated from peak production of $^{14}CO_2$, which was delayed during ischaemia. However despite the presence of back diffused ^{14}C-acetate or metabolites of ^{14}C-acetate in the venous effluent of ischaemic hearts, the disparity between calculated rates of $^{14}CO_2$ efflux and total ^{14}C efflux was small.

Metabolites of ^{14}C-acetate. The metabolites in the coronary venous effluent were separated by HPLC to determine whether ^{14}C-radioactivity that was not accounted for by $^{14}CO_2$ was attributable to back diffused ^{14}C-acetate or to metabolites. Prior studies using ^{14}C-palmitate had demonstrated that non-metabolized back diffused ^{14}C-palmitate occurred to a major extent during ischaemia, as discussed in Chapter 2. In the effluent of control hearts, 4 minutes after the completion of the infusion of ^{14}C-acetate, 96% of the venous effluent was in the form of $^{14}CO_2$. Non metabolized ^{14}C-acetate comprised 19% of non $^{14}CO_2$ activity or 0.8% of total effluent radioactivity. Thirty-five percent of non-$^{14}CO_2$ activity was attributable to ^{14}C-ß hydroxybutyrate (accounting for 24%) and ^{14}C acetoacetate (accounting for 11%). In ischaemic hearts at 4 minutes after the completion of tracer infusion , 44% of coronary venous effluent was in the form of $^{14}CO_2$. Back diffused ^{14}C-acetate contributed 3.3 ± 1.3% of non $^{14}CO_2$ activity , whereas ^{14}C-ß hydroxybutyrate accounted for 73.7 ± 6.4% and ^{14}C-acetoacetate for 0.7 ± 1.2% (n = 3). At 14 minutes, 80% of total radioactivity was in the form of $^{14}CO_2$. Of non-$^{14}CO_2$ activity , 1.0 ± 0.9% was attributable to ^{14}C-acetate, whereas ^{14}C-ß hydroxybutyrate comprised 40.6 ± 10.6% and ^{14}C-acetoacetate 3.6 ±2.7%. The remaining ^{14}C metabolites were largely citrate, succinate and lactate with the percentages of each increasing at the later period of assay (Table 3.2).

The distribution of the ^{14}C label between the aqueous and lipid fraction of myocardium was determined in 4 hearts after completion of the ^{14}C-acetate clearance studies. The majority of residual activity was contained in the aqueous phase of control hearts, with 0% and 12.6% of activity contained in the lipid phase of 2 control hearts. A similar percentage was found in the lipid phase of 2 ischaemic hearts, 2.8% and 5.5%.

External assessment of clearance of ^{11}C-acetate. Clearance of ^{11}C-acetate was measured in six control and four ischaemic hearts by analysis of myocardial residue time-activity curves measured externally and compared with the clearance of

Table 3.2

Percentage of total non-$^{14}CO_2$ coronary venous radioactivity due to labelled metabolites after a 2 minute infusion of ^{14}C-acetate in three ischaemic hearts.

Time	Acetate	Hydroxybutyrate	Acetoacetate	Citrate	Succinate	Lactate
2-4 min	3.3 ± 1.3	73.7 ± 6.4	0.7 ± 1.2	5.7 ± 2.6	3.4 ± 2.5	4.6 ± 4.7
12-14 min	1.0 ± 0.9	40.6 ± 10.6	3.6 ± 2.7	12.0 ± 3.3	20.2 ± 9.8	13.8 ± 1.8

Values are mean ± SD.

In control hearts, nearly all radioactivity in the venous effluent was in the form of $^{14}CO_2$. In ischaemic hearts, 2 to 4 minutes after ^{14}C-acetate infusion, 44% of effluent was in the form of $^{14}CO_2$. This production increased to greater than 80% (see Figure 3.4) after 14 minutes.

^{14}C-acetate measured by direct assay of radioactivity in the coronary venous effluent. In control hearts, ^{11}C-acetate clearance was measured at 14 workloads and compared with oxygen consumption. The decline in myocardial residue counts as a function of time was biphasic (Figures 3.5, a and b) and data from control hearts could be closely fitted with biexponential solutions. The rate constant of the major phase of clearance increased with higher work load in parallel with increased oxygen consumption (Figure 3.5, a and b). No change in the rate constant of the minor phase was seen with increased workload ($t_{1/2}$ 28.5 ± 16.0 min). The biexponential clearance of the myocardial residue suggested that the ^{11}C label was present within the myocardial cell in at least two intracellular pools, one clearing rapidly and one slowly. The relative size of each was approximated from the size of each phase of the biexponential curve. Clearance was predominantly due to the rapid phase, since the slowly clearing pool accounted for only 7.4 ± 3.0% of total ^{11}C radioactivity. No significant change in the size of this pool was seen with changes in cardiac work or oxygen consumption.

The myocardial residue time-activity curve in four ischaemic hearts, analysed over the same interval as that used to calculate rates of $^{14}CO_2$ efflux (ie., 10 to 40 minutes after completion of the ^{14}C-acetate infusion), was monoexponential (Figure 3.5, c).

In each heart, the rate of clearance of total ^{11}C-radioactivity measured externally (rate constant, major phase) was very similar to the rate of efflux of total ^{14}C radioactivity (rate constant, major phase) measured from the coronary venous effluent. A close correlation was seen between these two methods of measuring acetate metabolism, as shown in Figure 3.6 a, $r = 0.99$, $p < 0.001$).

Consistent with the close correlations found between the rate of total ^{14}C efflux, $^{14}CO_2$ efflux and oxygen consumption, externally derived ^{11}C-acetate clearance and oxygen consumption correlated closely as well (Figure 3.6 b, $r = 0.95$, $p < 0.001$).

^{11}C-acetate residue curves in ischaemic hearts were analyzed over the interval in which efflux of $^{11}CO_2$ was monoexponential. Thus approximately the first 10 minutes of each curve were excluded. However sampling intervals may be difficult to discern in clinical studies from inspection of ^{11}C-radioactivity residue curves only. To determine the error involved when an earlier period was used, the first 20 minutes of the residue

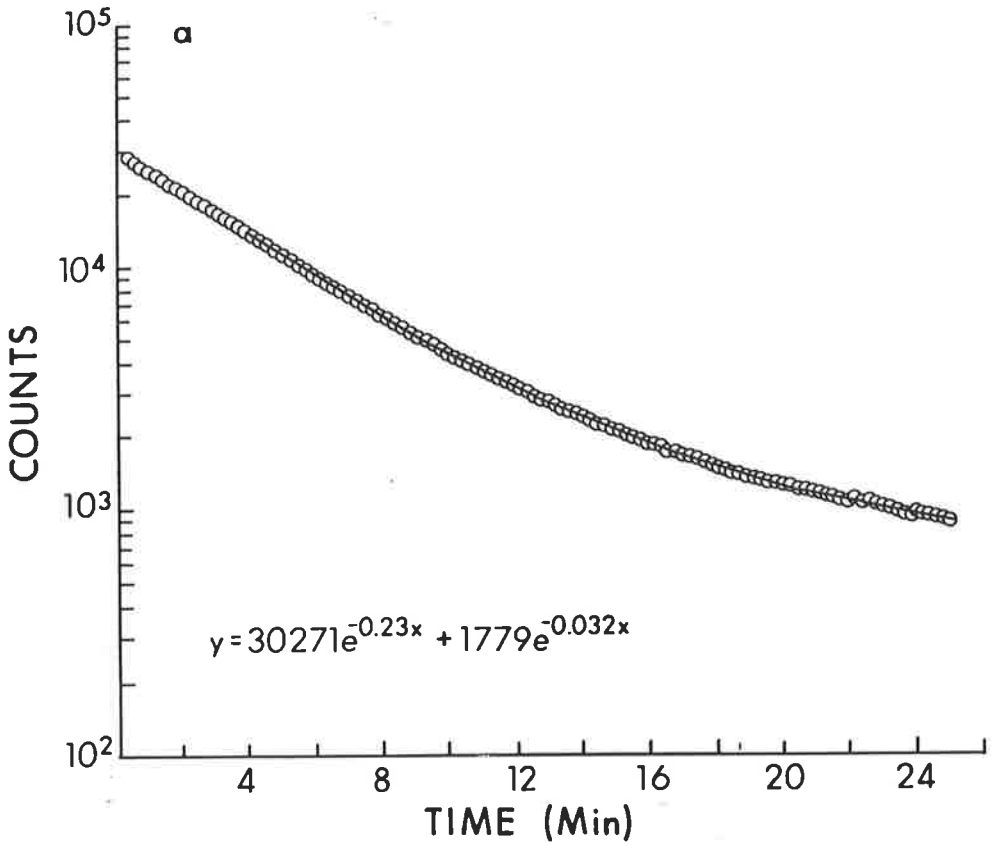

Figure 3.5 Externally detected myocardial residue time-activity curves after infusion of ^{11}C-acetate. Clearance from a control heart **a.** before and **b.** after stimulation with isoproterenol was biexponential as shown by the solid line. The rate constant of the rapid phase increased from 0.23 to 0.49 min^{-1} with isoproterenol. Clearance from the ischaemic heart **c.** was monoexponential. Fits were made to coincide with the monoexponential efflux of $^{11}CO_2$, from 14 to 40 minutes in this example, as shown by the solid line.

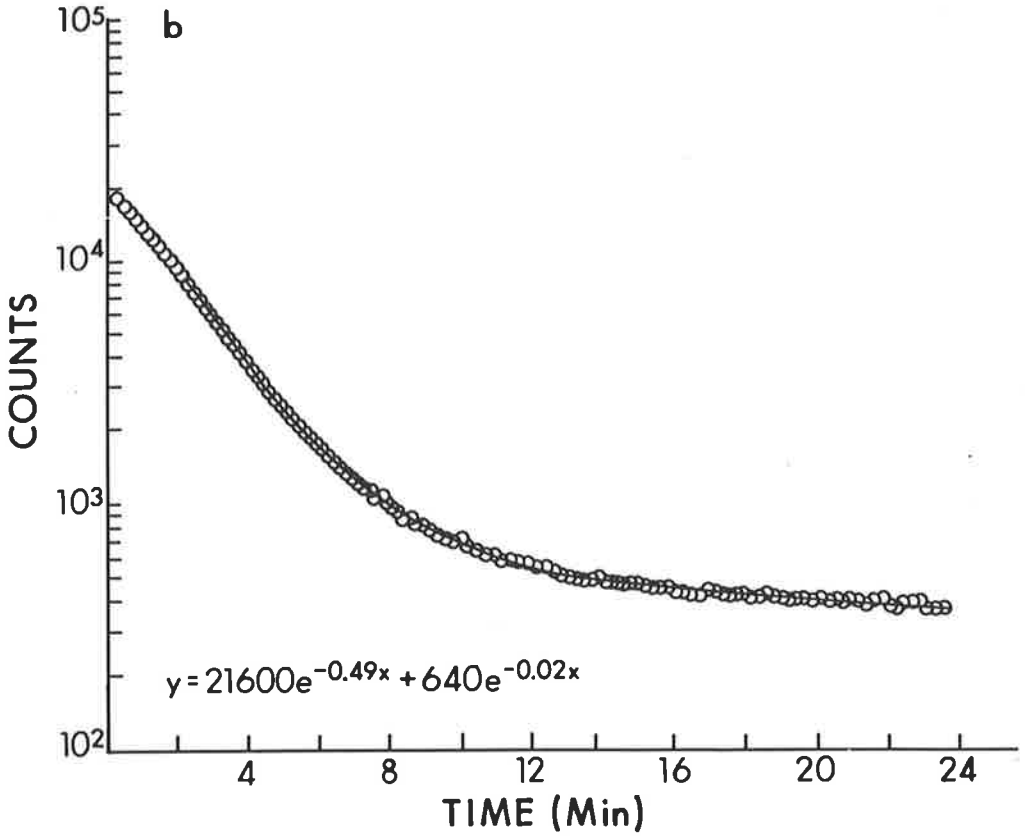

Figure 3.5 (cont) Externally detected myocardial residue time-activity curves after infusion of ^{11}C-acetate. Clearance from a control heart **a.** before and **b.** after stimulation with isoproterenol was biexponential as shown by the solid line. The rate constant of the rapid phase increased from 0.23 to 0.49 min^{-1} with isoproterenol. Clearance from the ischaemic heart **c.** was monoexponential. Fits were made to coincide with the monoexponential efflux of $^{11}CO_2$, from 14 to 40 minutes in this example, as shown by the solid line.

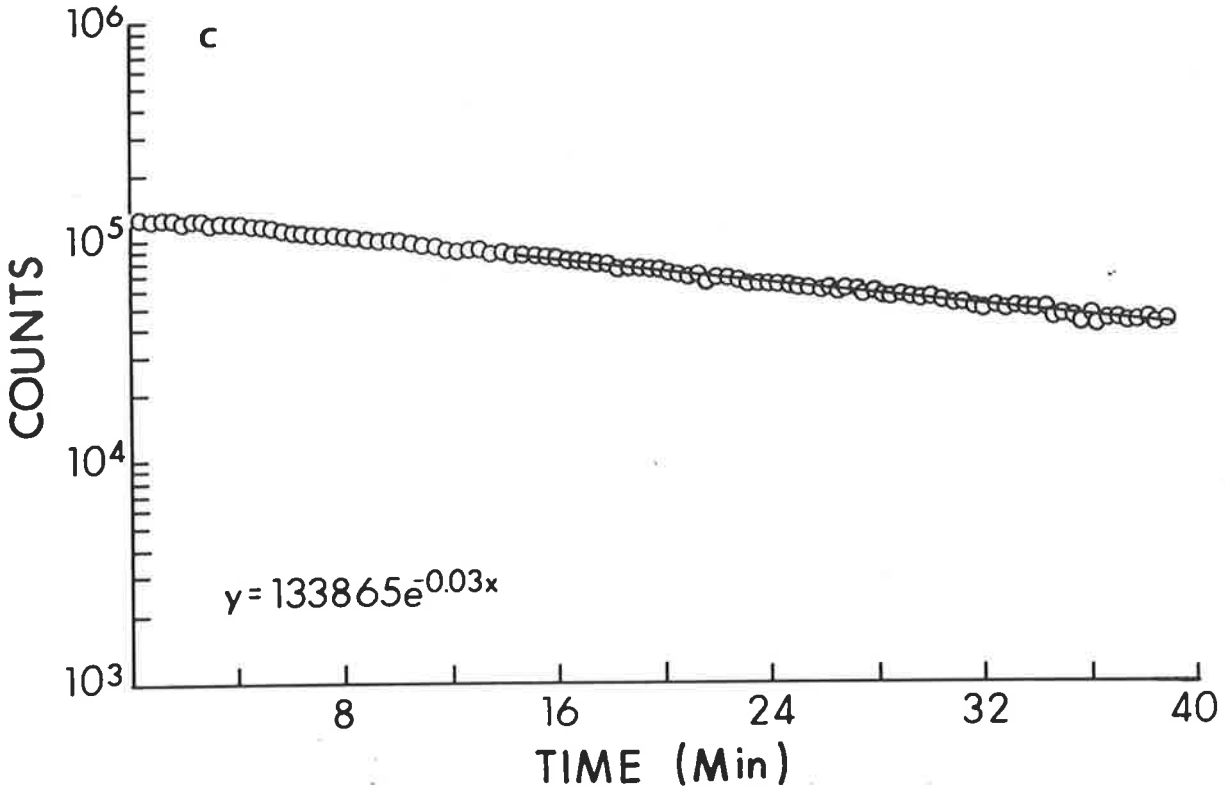

Figure 3.5 (cont) Externally detected myocardial residue time-activity curves after infusion of ^{11}C-acetate. Clearance from a control heart **a.** before and **b.** after stimulation with isoproterenol was biexponential as shown by the solid line. The rate constant of the rapid phase increased from 0.23 to 0.49 min^{-1} with isoproterenol. Clearance from the ischaemic heart **c.** was monoexponential. Fits were made to coincide with the monoexponential efflux of $^{11}CO_2$, from 14 to 40 minutes in this example, as shown by the solid line.

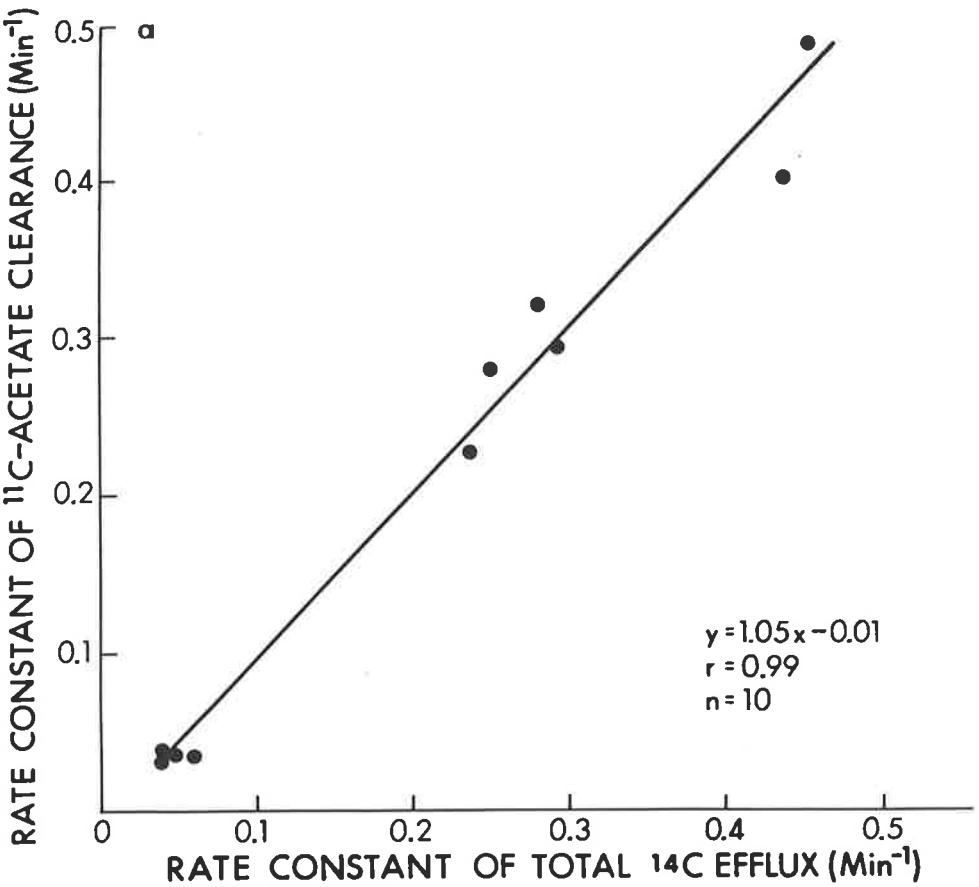

Figure 3.6 a. Correlation between the rate constants for total ^{14}C efflux and the rate constants of the ^{11}C residue time-activity curve from 10 hearts. Both rate constants were calculated from the rapid phase of biexponential curves.

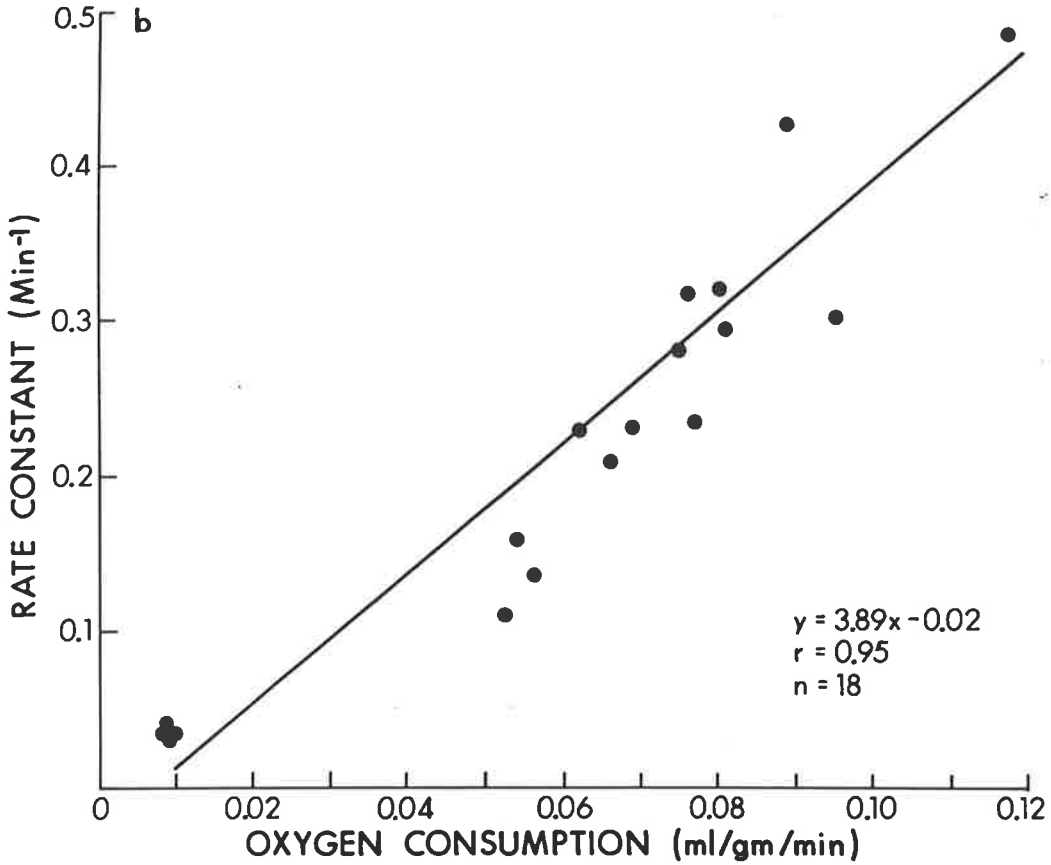

Figure 3.6 b. Correlation between myocardial oxygen consumption and the rate constant of the rapid phase of the externally detected myocardial residue time-activity curves in 18 studies after infusion of ^{11}C-acetate.

curves were analyzed as an arbitrary period rather than the later selected period, commencing at the time of maximal $^{14}CO_2$ efflux as discussed above. No significant differences were observed for half times from this interval (19.9 ± 2.5 min compared to 20.3 ± 1.9 min). Thus, although oxidation of acetate and production of CO_2 are delayed during ischaemia, the interval selected for calculation of the externally derived rate constant does not appear to be critical.

Discussion

In this model, during normoxic conditions the steady state extraction fraction of radiolabelled acetate was approximately 63% despite the high flow rates required to achieve normoxia. Extraction fraction increased further during ischaemia due to the increased transit time of tracer, at a time prior to significant injury to the myocardium by ischaemia. This relatively high extraction fraction (in comparison to other substrates) is consistent with the previously reported extraction fraction of unlabelled acetate of approximately 44% found at rest in volunteers or patients with cardiac disease [15], a factor which potentially enhances the imaging potential of ^{11}C-acetate. For comparison, the extraction fraction of free fatty acid and glucose in the same study was reported to be 15% and zero respectively [15].

Following a brief infusion of ^{14}C-acetate, designed to approximate the period of high levels of tracer found in the arterial circulation prior to clearance, the rate of efflux (major phase) of $^{14}CO_2$ from myocardium depended on oxygen consumption. Peak $^{14}CO_2$ efflux occurred earlier and the subsequent rate of efflux was faster at higher oxygen consumption. The close correlation found between the rate of efflux of $^{14}CO_2$ and oxygen consumption confirmed the original hypothesis that the rate of oxidation of radiolabelled acetate would provide an indirect measurement of oxygen consumption, at least in this model under constant substrate conditions. Furthermore the rate of efflux of $^{14}CO_2$ was indicated by the rate of efflux of total ^{14}C radioactivity over a wide range of metabolic conditions, since $^{14}CO_2$ was the major component under ischaemic and hypoxic conditions and almost the entire component under normoxic conditions.

Analysis of the non-$^{14}CO_2$ fraction produced from ischaemic hearts indicated that the majority of ^{14}C-metabolites were due to ketone bodies, either ^{14}C-ß hydroxybutyrate or ^{14}C-acetoacetate. The heart has previously not been regarded as a ketogenic organ [62], however review of previous studies indicate that these results are consistent with analyses of pig heart extracts [30], isolated rat heart mitochondria [31] and dog hearts rendered hypoxic [29]. Additionally in this study ^{14}C-labelled citric acid cycle intermediates were found to a minor degree, predominantly succinate and citrate. ^{14}C-labelled lactate was also found, presumably produced from these intermediates as the conversion of pyruvate to acetyl CoA is essentially irreversible in animal tissues [25]. Although back diffusion of these ^{14}C-labelled metabolites constitute up to 20 to 25% of total ^{14}C-radioactivity cleared from the heart during ischaemia, this resulted in only a minor and non statistically significant over-estimation of the rate of $^{14}CO_2$ efflux based on measurement of total ^{14}C efflux. Virtually no difference was present during normoxic conditions, either in controls or following prolonged ischaemia.

The biexponential clearance of ^{11}C-radioactivity from myocardium suggests that the label was incorporated into at least two distinct intracellular pools, and was released for metabolism in the citric acid cycle at differential rates. It is likely that the major phase represents incorporation of the label into acetyl CoA, acetylcarnitine and citric acid cycle intermediates. As previously discussed in Chapter 1, alternative metabolic routes are incorporation into amino acids, such as glutamate and incorporation into lipids. The minor phase may reflect slow turnover of these ^{14}C-labelled pools with subsequent reformation of ^{14}C-acetyl CoA and metabolism in the citric acid cycle.

Importantly for the future application of this technique to the non invasive evaluation of citric acid cycle flux by PET, the externally measured rate of clearance of ^{11}C-radioactivity from myocardium was in close agreement with the rate of radiolabelled CO_2 production measured invasively. The latter measurement was calculated from the time of peak efflux of $^{14}CO_2$ (see Figure 3.1, b) and the corresponding ^{11}C myocardial time activity curve was fitted over the same period. The time of peak $^{14}CO_2$ efflux will correspond to the time at which the rate of decrease of the myocardial residue is maximal. This may be difficult to determine when clearance is slow due to low work load or

ischaemia, however inspection of the ^{11}C residue curves indicates (Figure 3.5, c) that the likely impact of fitting an inappropriate portion of the curve will be small, confirmed by comparison of results between an arbitrary and appropriate period as discussed in Results.

Hence this initial study confirms the initial hypothesis that the rate of oxidation of ^{14}C-acetate, reflecting citric acid cycle flux, is closely related to directly measured myocardial oxygen consumption under a variety of metabolic conditions. Since the metabolism of ^{14}C-acetate and ^{11}C-acetate is identical, this conclusion can be extended to ^{11}C-acetate. The externally derived clearance rates of the ^{11}C label after administration of ^{11}C-acetate are also closely related to directly measured oxygen consumption, due to the limited metabolic end products of acetate metabolism described.

These results were published in 1987, and were the first to validate the use of ^{11}C-acetate as a tracer of oxidative metabolism following preliminary studies in abstract form by this author [63] and Buxton et al [64].

Subsequent studies published by Buxton et al [65] in 1988 have confirmed these data in an isolated perfused rat heart model. A good correlation was found between the initial rate constant of $^{14}CO_2$ clearance and myocardial oxygen consumption, after administration of ^{14}C-acetate. In this series of experiments oxygen consumption was varied over a fourfold range by hypoxia and phenylephrine stimulation. Rate constants for clearance of $^{14}CO_2$ and total ^{14}C-radioactivity were very similar and did not vary significantly under all conditions tested, similar to the results described herein.

Chapter 4

Delineation of myocardial oxygen consumption with ^{11}C-acetate in *in vivo* canine hearts.

The previously described isolated perfused rabbit heart studies confirm that the rate of oxidation of ^{11}C-acetate in this model provided an indirect assessment of oxygen utilization. However extrapolation to the *in vivo* situation is limited by a number of potential constraints of this model. The ability to image the myocardium with PET remains unclear, given a lack of data concerning the relative uptake and clearance of ^{11}C-acetate from myocardium, lung and blood pool. However initial reports were encouraging [52]. Prolonged recirculation of tracer within arterial blood and *in vivo* metabolism of ^{11}C-acetate could potentially distort the aforementioned findings in the *in vitro* model. Variation of substrate utilization by the heart could potentially alter the extraction of ^{11}C-acetate, hence affecting image quality or alter the relationship between the rate of ^{11}C-acetate oxidation and oxygen consumption.

To examine some of these potential limitations the metabolism of ^{11}C-acetate was studied in a canine model by PET. The aim of this study was to determine the utility of ^{11}C-acetate as a tracer of oxidative metabolism over a range of metabolic states *in vivo*. The specific aims were to **a.** determine the imaging characteristics of ^{11}C-acetate in a canine model, **b.** determine whether the rate of oxidation of ^{11}C-acetate could be measured from the externally detected rate of clearance of ^{11}C-radioactivity from the myocardium and **c.** determine whether the externally detected rate of clearance of ^{11}C-radioactivity provided an index of myocardial oxidative metabolism *in vivo*.

Methods

Experimental Preparations. Eight mongrel dogs weighing 17-31 kg were premedicated with subcutaneous morphine (1 mg/kg body weight) and anaesthetized with intravenous thiopental (12.5 mg/kg) and α-chloralose (60 mg/kg). Catheters were placed under fluoroscopic guidance into the descending aorta for measurement of blood pressure and for arterial sampling, the coronary sinus for coronary venous sampling and the left atrium retrograde across the mitral valve for administration of radiolabelled microspheres. Additional catheters were placed into both femoral veins for administration

of radiolabelled tracers and administration of drug infusions. Aortic pressure and heart rate were monitored continuously. The rate-pressure product, an index of cardiac work, was calculated from the product of systolic blood pressure and heart rate.

Experimental protocol. A control and an intervention study were performed in each dog. Control studies were obtained after intravenous administration of ^{11}C-acetate under baseline conditions. After allowing for decay of previously injected tracer (approximately 100 minutes), an intervention designed to either increase or decrease cardiac work load was initiated. High work load was induced in 6 dogs with a continuous infusion of either norepinephrine or phenylephrine at an infusion rate sufficient to elevate systolic blood pressure to greater than 200 mm Hg. Low work load was induced in two dogs with intravenous propranolol (1 mg/kg as a slow bolus injection) and a sodium nitroprusside infusion sufficient to lower systolic blood pressure to less than 80 mm Hg (commencing at 3 μg/kg/min).

Positron emission tomography. All animal studies were carried out in PETT VI, a small aperture positron emission tomograph with four rings of detectors in a circular array permitting simultaneous collection of seven slices with a centre to centre separation of 1.44 cm, and a total axial field of view of 11 cm (encompassing the total canine heart) [66]. Detailed phantom studies showed a resolution (full width half maximum) of 12 mm with the configuration used for clinical studies.

After vascular instrumentation, dogs were placed in a Plexiglas shell designed to fit within PETT VI. The position of the apex of the heart was marked during fluoroscopy, and a low power laser subsequently used to position the apex at the appropriate level within the tomograph ensuring that the heart was imaged from base to apex. Once in the tomography unit animals were maintained under general anaesthesia in the same position, hence tomographic images of two serial ^{11}C-acetate studies could be directly compared.

Attenuation of radiation within the thorax was measured with a ring source of the positron emitter germanium-68/gallium-68. Attenuation correction factors were calculated from data with and without the animal within the ring source. Collection of emission data was commenced simultaneously with a bolus injection of approximately 0.8 mCi's of ^{11}C-acetate into the femoral vein. Serial tomograms were acquired every 1 to 2 minutes

for 20-40 minutes. A period of approximately 100 minutes (five half lives) between ^{11}C-acetate scans allowed for decay of the previously injected tracer.

Analysis of Tomographic Data. For data analysis a mid ventricular tomographic slice was selected from the reconstructed tomograms. One large region of interest was assigned to the entire left ventricular wall. In addition, three individual regions of interest (volume approximately 0.9 cm^3) were assigned to each of the lateral, anterior and septal walls (ie., nine regions per slice) to assess regional variability. A region of interest was also assigned to the centre of the left ventricular cavity to assess the activity of tracer in arterial blood. Counts from each region were corrected for decay and for partial volume and spillover effects (see Appendix A).

A multi exponential curve fitting routine (Marquardt algorithm) was used to fit decay, partial volume and spillover corrected myocardial time-activity curves from the time of maximal efflux of $^{11}CO_2$, the latter determined from aortic and coronary sinus blood sampling data (see discussion to follow).

External clearance of ^{11}C-radioactivity from canine myocardium was biphasic and could be closely fitted with biexponential solutions, suggesting incorporation of the label into two distinct metabolic pools within the myocardium. The relative size of each phase was calculated by back extrapolation of each monoexponential to the time of peak myocardial radioactivity, and expressed as a percent of the peak counts.

Analysis of blood ^{11}C-radioactivity and $^{11}CO_2$ content. Aortic and coronary sinus samples were collected at 10, 20, 40, 60, 90 and 120 seconds after the intravenous injection of ^{11}C-acetate, and then at 1 minute intervals for 14 minutes and at 2 minute intervals thereafter for the duration of imaging. Total ^{11}C-radioactivity and non-$^{11}CO_2$ radioactivity were measured in each sample as previously described [39]. Briefly, blood samples were divided in half and haemolyzed with isopropyl alcohol. Total ^{11}C-radioactivity was measured in alkalinized blood. Non-$^{11}CO_2$ radioactivity was measured after blood was acidified with 6N HCl and bubbled with nitrogen for 10 minutes to release $^{11}CO_2$. The $^{11}CO_2$ content of each sample was calculated from the difference between total ^{11}C-radioactivity and non-$^{11}CO_2$ radioactivity. Standards showed 95% retention of ^{11}C-acetate and a 98% loss of ^{11}C-labelled bicarbonate in

identically treated samples. Myocardial production of $^{11}CO_2$ per ml of blood was calculated from the $^{11}CO_2$ content of coronary sinus blood minus the $^{11}CO_2$ content of arterial blood. The decline in myocardial production of $^{11}CO_2$ as a function of time was monoexponential , and least squares analysis was used to calculate the rate constant of $^{11}CO_2$ production. This rate constant was equivalent to the rate of efflux of $^{11}CO_2$ from the heart. Myocardial extraction on non-$^{11}CO_2$ radioactivity per ml of blood was calculated from the non-$^{11}CO_2$ content of aortic blood minus the non-$^{11}CO_2$ content of coronary sinus blood.

Direct measurement of substrate utilization. Aortic and coronary sinus blood samples were taken simultaneously immediately before and after each ^{11}C-acetate scan and the results averaged. Oxygen tension, oxygen saturation and haemoglobin were measured in each sample (Instrumentation Laboratory Co-Oximeter 282) and oxygen content was calculated as shown below.

Oxygen content of blood

$$= 1.39 * Hb * \text{Hb saturation fraction} * 0.003 * pO_2$$

where Hb = Haemoglobin (gm/dl), pO_2 = oxygen partial pressure (mm Hg)

Oxygen extraction per ml of blood was calculated from the aortic and coronary sinus difference. Myocardial blood flow was measured immediately before each scan as described below. Post mortem, contiguous myocardial samples of approximately 1 to 2 grams each were removed from the septum, anterior and lateral left ventricular walls corresponding to regions analyzed on reconstructed tomograms. Myocardial blood flow per sample was calculated, and left ventricular oxygen consumption (micromoles of oxygen per gram per minute) calculated from the product of flow and directly measured oxygen extraction.

Samples of arterial and coronary venous blood were obtained before and after each tomographic study for analysis of fatty acid, glucose, lactate and acetate. Fatty acid in plasma was assayed with a colorimetric assay previously described [67]. Lactate and glucose were assayed as described in Chapter 3. Acetate was assayed using a commercially available kit (Boehringer Mannheim Biochemicals, Indianapolis) as described by Bergmeyer and Mollering [68].

Calculation of blood flow with microspheres. Radiolabelled microspheres (15 μm labelled with scandium-46, chromium-51, strontium-85 or cerium-141) were injected into the left atrium. Arterial blood from the femoral artery was withdrawn at a constant flow rate of 10 ml/min starting 15 seconds prior to microsphere injection and continued for 2 minutes thereafter. Approximately 2 to 3 million microspheres were injected. Samples of left ventricular myocardium obtained post mortem were divided into endocardial and epicardial segments, and regional blood flow for each sample was calculated using the standard reference technique [69].

These canine studies and those described in later Chapters were approved by the Animal Studies Committee of Washington University and conformed to the policies of the American Heart Association.

Results

Eight dogs were evaluated at both control work load and either low or high work load. However, two studies after sympathomimetic drug administration could not be completed due to death in one dog and unstable haemodynamics in another, leaving a total of 14 ^{11}C-acetate studies for analysis.

Haemodynamics and substrate utilization. A wide range of baseline aortic systolic pressures and heart rates were seen during control studies. High work load states were associated with higher levels of systolic blood pressure, rate-pressure product, blood flow and myocardial oxygen consumption compared with control levels (Table 4.1). Systolic pressure, heart rate, rate-pressure product, blood flow and myocardial oxygen consumption all decreased in low work load studies.

No significant change in the arterial plasma level of non esterified fatty acid, lactate or acetate occurred with either high or low work load interventions (Table 4.2). However, arterial glucose levels increased from 4.8 ± 0.4 to 9.2 ± 3.3 mmol/litre during high work load induced by sympathomimetic agents.

Table 4.1 Haemodynamics, myocardial blood flow and oxygen consumption for control, high work load and low work load canine studies.

		Control	High Work Load	Low Work Load
SBP	(mm Hg)	132 ± 25	201 ± 13*	61
HR	(min^{-1})	122 ± 53	128 ± 53	99
RRP	(mm Hg min^{-1})	16081 ± 7248	25560 ± 10490	6056
Flow	(ml/g/min)	0.77 ± 0.24	3.87 ± 2.43	0.41
MVO_2	(µmol/g/min)	3.4 ± 1.0	6.5 ± 3.2*	1.5

*$p < 0.05$ compared with control. Values represent mean ± SD. Only the mean is shown for low work load studies (n = 2). SBP = systolic blood pressure, HR = heart rate, RPP = rate pressure product, MVO_2 = myocardial oxygen consumption.

The extraction fraction of non esterified fatty acid and acetate at baseline was similar, approximately 33-34%, while the extraction fraction of lactate and glucose was 23% and 10% respectively. No significant change in the extraction fraction of any substrate occurred with alterations of work load.

Table 4.2 Effect of alterations in work load on arterial substrate concentration and myocardial utilization.

	Control	High Work Load	Low Work Load
Arterial concentration			
NEFA (µmol/litre)	546 ± 184	697 ± 497	387
Glucose (mmol/litre)	4.8 ± 0.4	9.2 ± 3.3*	9.7
Lactate (mmol/litre)	1.6 ± 0.6	3.1 ± 2.1	3.2
Acetate (µmol/litre)	87 ± 28	96 ± 31	63

(continued next page)

Table 4.2 (cont) Effect of alterations in work load on arterial substrate concentration and myocardial utilization.

	Control	High Work Load	Low Work Load
Extraction fraction (%)			
NEFA	34.3 ± 10.6	36.9 ± 9.5	28.8
Glucose	9.5 ± 7.8	11.0 ± 10.9	4.7
Lactate	22.8 ± 16.8	9.5 ± 10.9	26
Acetate	33.2 ± 8.7	37.2 ± 9.9	29.4

*$p < 0.05$ compared with control. Values represent mean ± SD. Only the mean is shown for low work load studies (n = 2). NEFA = non esterified fatty acids.

Tomography after ^{11}C-acetate administration. Total ^{11}C-radioactivity cleared from arterial blood in two phases. Initial clearance of ^{11}C-acetate to less than 5 to 10% of peak concentration was rapid and usually completed in < 2 minutes (Figure 4.1). Subsequent clearance was slow (mean half time 19 ± 7 min). During this slow phase, the major proportion of ^{11}C-radioactivity was in the form of $^{11}CO_2$, which peaked at a mean of six minutes after intravenous administration of ^{11}C-acetate in all studies. During the period from 6 to 20 minutes, $^{11}CO_2$ accounted for 62 ± 4% of total ^{11}C-radioactivity in arterial blood in control studies, 46 ± 11% in high work load studies and 52 ± 11 % in low work load studies.

Tomographic images of the left ventricle following ^{11}C-acetate were of excellent quality, and examples are shown in Chapter 7 to avoid repetition. The ventricular wall was obscured by ^{11}C-acetate within the blood pool during the first minute after tracer injection, but good contrast between the left ventricular wall and left ventricular cavity was seen by the second to third minute because of rapid clearance of ^{11}C-acetate from arterial blood and high extraction of ^{11}C-acetate by the myocardium. At this time the ratio of ^{11}C-radioactivity in myocardium to that in the left ventricular cavity was 2.0 ± 0.5. Contrast was reduced over the period of the scan because of more rapid clearance of

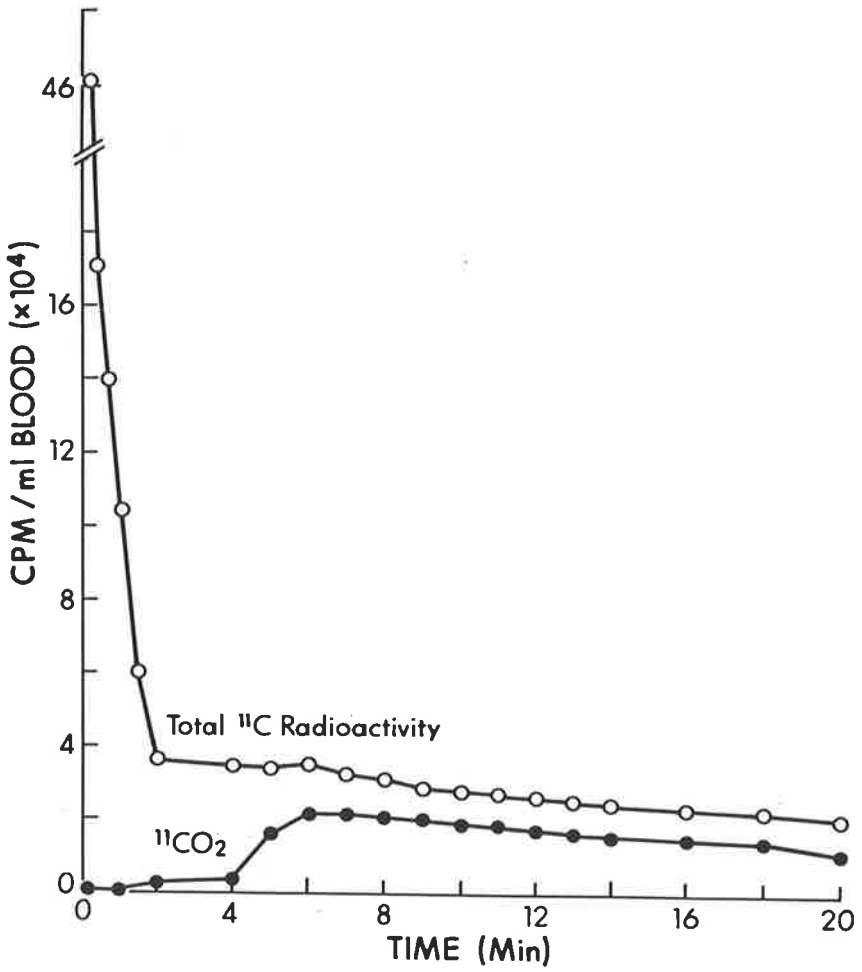

Figure 4.1 Concentration of directly measured arterial total ^{11}C-radioactivity and $^{11}CO_2$ is shown as a function of time. Early clearance of total ^{11}C radioactivity from the blood, initially representing ^{11}C-acetate, was rapid and generally completed by 2 minutes after intravenous administration of ^{11}C-acetate. Later, a major proportion of total ^{11}C radioactivity was due to $^{11}CO_2$ produced from oxidation of ^{11}C-acetate. CPM = counts per minute.

^{11}C-radioactivity from myocardium compared with blood (ratio 1.5 ± 0.3 by 20 minutes in control studies). Good contrast was also seen between myocardium and lung with a ratio of 2.3 ± 0.9 at 3 minutes. However, by 20 minutes myocardium was less well delineated from lung because of more rapid clearance from myocardium (ratio 1.1 ± 0.2 by 20 minutes in control studies).

Myocardial clearance of ^{11}C-radioactivity. Clearance of ^{11}C-radioactivity from myocardium was relatively homogeneous throughout the duration of the scan as shown by the homogeneity of concentration of ^{11}C-radioactivity in the ventricular wall over time. Myocardial time-activity curves were constructed from a region of interest encompassing the entire left ventricular wall in one mid-ventricular tomographic slice, and thus data represent mean left ventricular wall counts per voxel (volume element) per minute. Data from control and high work load studies, corrected for decay, partial volume effects and spillover effects, could be closely fitted with biexponential solutions (Figure 4.2, a-d). Clearance occurred predominantly during the major phase because the rate constant from the minor phase was close to zero in most studies. One low work load study could only be fitted with a monoexponential solution because of the slow rate of clearance.

The biexponential clearance suggested that the ^{11}C label was distributed in at least two major pools, as discussed previously. The major pool cleared rapidly and accounted for 81 ± 9% of the ^{11}C-radioactivity in control studies, based on the relative size of the two phases. A similar percentage (83 ± 4%) was found in high work load studies.

Mean half time of the major phase in control studies was 5.4 ± 2.2 minutes, decreased because of more rapid clearance in high work load studies (2.8 ± 1.3 min) and increased due to slower clearance in low work load studies (11.1 ± 1.3 min).

The rate of efflux of $^{11}CO_2$ from myocardium was calculated from serial aortic and coronary sinus blood samples to provide a measure of the rate of oxidation of ^{11}C-acetate. The time of maximal $^{11}CO_2$ efflux varied according to workload. In control, high and low work load studies, peak efflux of $^{11}CO_2$ was observed at 4.5 ± 1.9, 2.4 ± 2.5 and 10.2 ± 1.2 minutes respectively. The subsequent rate of efflux of $^{11}CO_2$ was monoexponential. Data from a representative control study comparing the efflux of

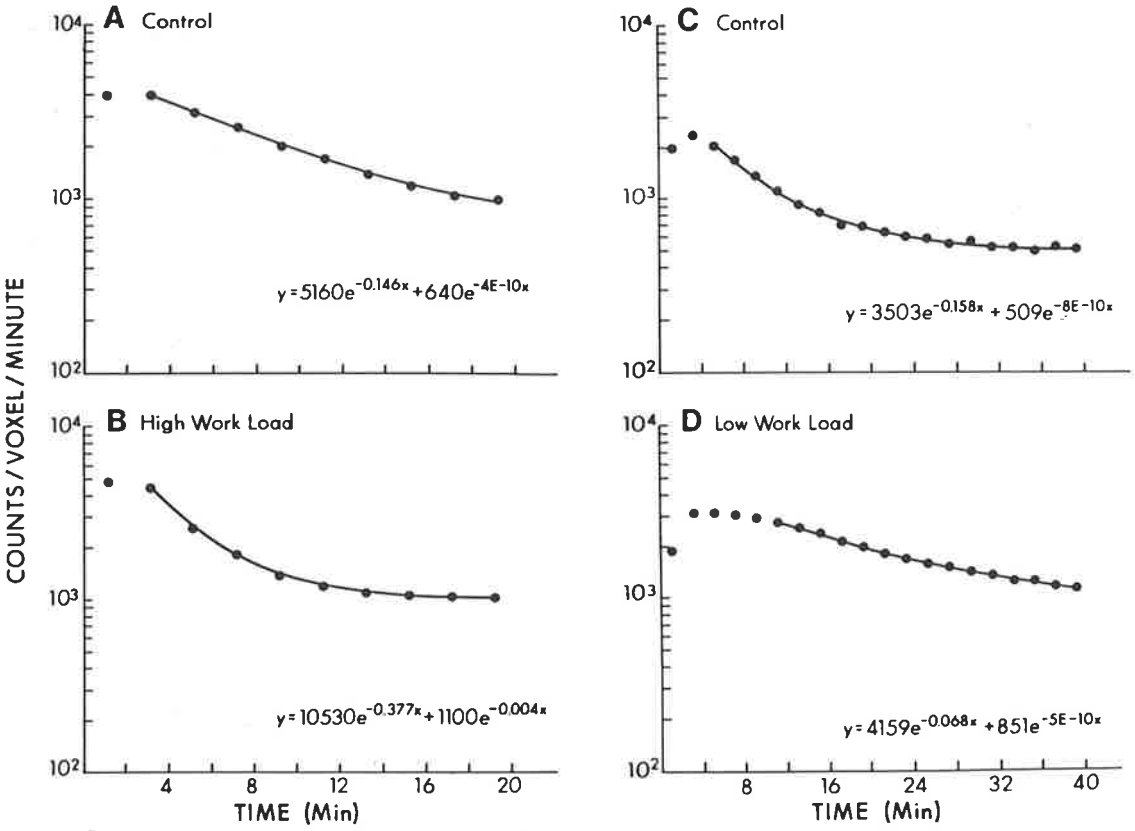

Figure 4.2 Myocardial time-activity curves obtained from serial 2 minute tomographic scans for a high work load study (**A**, control; **B**, high work load) and a low work load study (**C**, control; **D**, low work load). Control clearance curves were obtained at baseline in each study before intervention. Biexponential solutions, shown by the solid lines, were fitted from the time of maximal efflux of $^{11}CO_2$. The rate constant of the rapid phase varied directly with work load and therefore with myocardial oxygen consumption.

$^{11}CO_2$ with myocardial clearance of ^{11}C-radioactivity are shown in Figure 4.3 a. As discussed, the ^{11}C residue curve consists of a major rapid phase and a minor slow phase. The component due only to the rapid monoexponential phase, shown by the dashed line in Figure 4.3 a, was similar to the rate of efflux of $^{11}CO_2$ (rate constant 0.142/min and 0.137/min respectively). The overall correlation between the two measurements was 0.94 (Figure 4.3 b,n = 12, $p < 0.001$), and although the slope of this relationship was greater than one, no significant difference between rate constants measured by either technique was found (t test). Hence the rate of oxidation of ^{11}C-acetate could be measured externally from the rate of clearance of myocardial ^{11}C-radioactivity.

The relation between the rate of clearance of total ^{11}C-radioactivity from myocardium (rate constant, major phase) and myocardial oxygen consumption measured directly was examined to determine if the rate of clearance could be used as an index of myocardial oxidative metabolism. A close correlation was found (Figure 4.4 a, $r = 0.90$, $p < 0.001$), with increased rate of clearance at higher levels of oxygen consumption. Similarly, the rate constant correlated with the rate pressure product during each study (Figure 4.4 b, $r = 0.95$, $p < 0.001$). As expected, rate pressure product was closely correlated with oxygen consumption ($r = 0.84$, $RPP = 3334 * MVO_2 + 4083$, $p < 0.001$)

The clearance rates of myocardial ^{11}C-radioactivity could be potentially affected by the method of data analysis. Residue data used for curve fitting were corrected for partial volume effects and spillover using fixed cardiac dimensions. It was anticipated that possible error involved in using assumed dimensions was small because of the rapid clearance of ^{11}C-radioactivity from arterial blood. Rate constants calculated from residue data corrected only for decay without correction for partial volume effects and spillover were only slightly less than those calculated from fully corrected data ($95.9 \pm 7.8\%$).

Biexponential solutions were fitted to myocardial ^{11}C data from the time of peak efflux of $^{11}CO_2$. However, in clinical studies the time of peak efflux of $^{11}CO_2$ would not be known. The time of maximal decline of myocardial ^{11}C-radioactivity (due to efflux of $^{11}CO_2$) corresponded approximately to the time of peak efflux of $^{11}CO_2$ (6.2

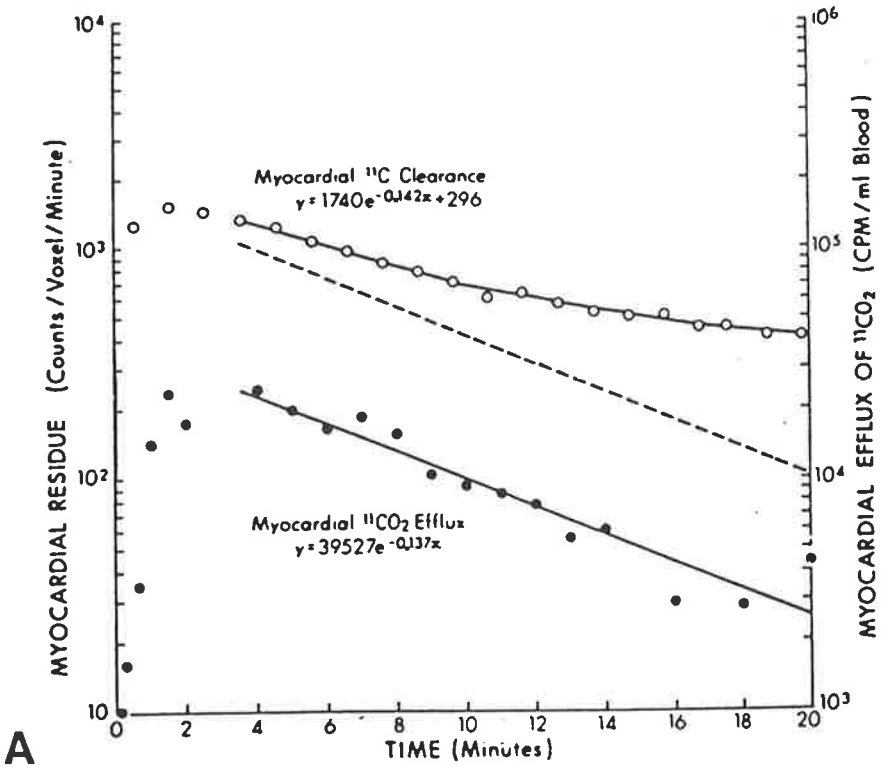

A

Figure 4.3 A Comparison of myocardial ^{11}C residue time-activity data measured by PET and $^{11}CO_2$ efflux measured from direct coronary sinus sampling in one control study. A biexponential solution was closely fitted to the myocardial ^{11}C clearance data. The dashed line represents clearance due to only to the rapid phase (0.142/min) and is similar to the rate constant of $^{11}CO_2$ efflux (0.137/min). CPM = counts per minute

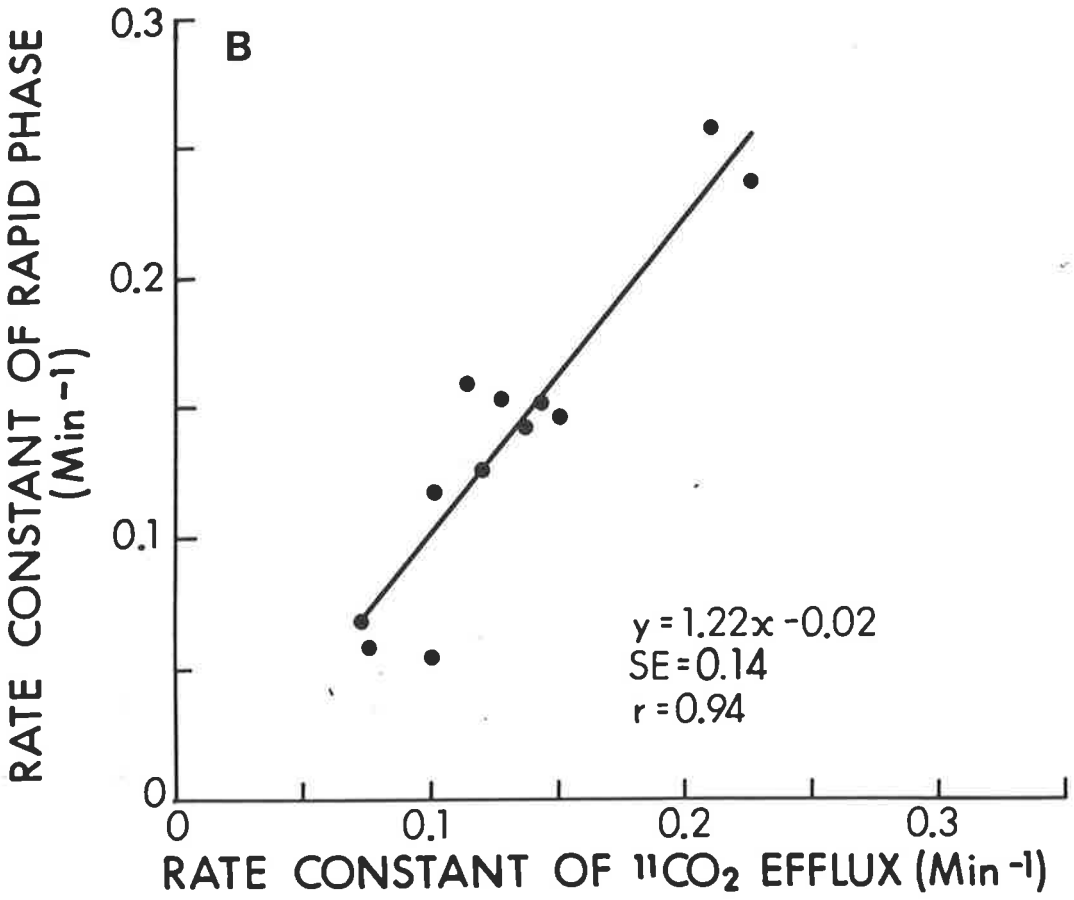

Figure 4.3 B The correlation between the rate constant of $^{11}CO_2$ efflux and the rate constant of the rapid phase of myocardial clearance of ^{11}C radioactivity was close in 12 studies ($p < 0.001$). Two high work load studies could not be analyzed due to technical difficulties with assays. The standard error of the slope is shown.

CPM = counts per minute

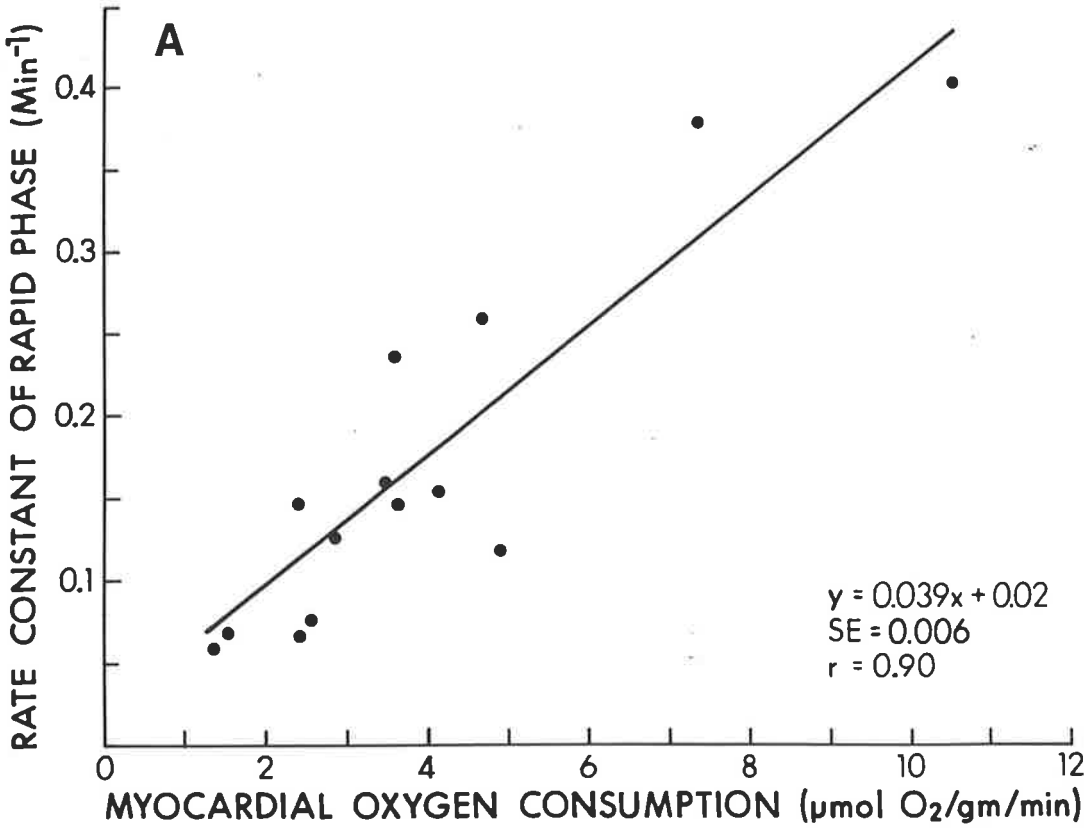

Figure 4.4 A Myocardial oxygen consumption was closely correlated with the rate constant of the rapid phase of clearance of ^{11}C radioactivity from myocardium (n = 14, $p < 0.001$). The standard error of the slope is shown. BP = blood pressure; HR = heart rate.

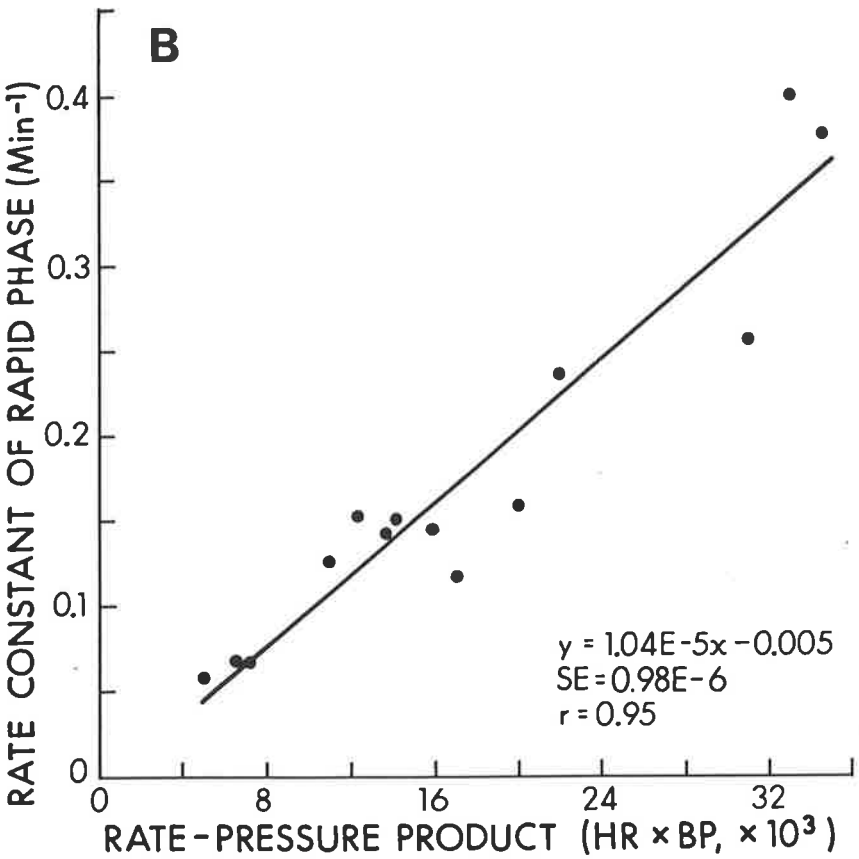

Figure 4.4 B Rate-pressure product (HR * systolic BP) was closely correlated with the rate constant of the rapid phase of clearance of ^{11}C radioactivity from myocardium ($n = 14$, $p < 0.001$). The standard error of the slope is shown. BP = blood pressure; HR = heart rate.

± 3.2 min and 4.7 ± 3.2 min, respectively), with a minor difference expected because of different sampling intervals for data derived from PET and that derived from blood sampling. In clinical studies, the time of maximal clearance of the ^{11}C residue would be appropriate as the initial point in curve fitting.

Regional tomographic data. Myocardial time-activity curves were also constructed for each of nine regions from the same mid ventricular slice used for assessing global left ventricular clearance rates in each ^{11}C-acetate study. Comparison of the rate constants of the major phase showed no significant difference among lateral, anterior and septal walls, indicating that clearance was homogeneous throughout the left ventricular wall (Table 4.3). The mean rate constant from nine regions within each slice was very similar to the rate constant measured from the mean data derived from the entire left ventricular wall. The variation of clearance within each slice, assessed by the coefficient of variation, was 16 ± 10% in control studies and was little affected by altered work load (Table 4.3).

Table 4.3 Rate constants of clearance of the rapid phase of ^{11}C myocardial residue time-activity curves are shown for each region of the left ventricular wall, at different work loads..

	Control	High Work Load	Low Work Load
Rate constant (min^{-1})			
Global	0.145 ± 0.053	0.292 ± 0.118*	0.063
Lateral	0.152 ± 0.057	0.339 ± 0.167*	0.045
Anterior	0.148 ± 0.061	0.278 ± 0.118*	0.055
Septal	0.142 ± 0.061	0.266 ± 0.125*	0.064
COV (%)	16.1 ± 9.5	17.0 ± 8.8	17.6

* $P < 0.05$ compared to control. COV = coefficient of variation. Data for low work load studies are shown as mean only.

Myocardial extraction of non-$^{11}CO_2$ radioactivity. The initial extraction fraction of non-$^{11}CO_2$ radioactivity, representing extraction of ^{11}C-acetate, was not calculated because of the rapid changes occurring at this time. Late extraction fraction (6-

20 min), as a percent of total ^{11}C-radioactivity, was relatively constant over time and was not significantly different among groups. Mean extraction fraction of radiolabel during this latter period was only 3.2 ± 3.6%, indicating that ^{11}C-radioactivity myocardial residue time-activity curves predominantly represented efflux of $^{11}CO_2$ rather than the result of continued uptake and clearance of ^{11}C-radioactivity.

Discussion

Positron emission tomography with ^{11}C-acetate to assess myocardial oxygen consumption. The use of ^{11}C-acetate with PET resulted in images of high quality. Mean steady state extraction fraction of unlabelled acetate in these canine studies was 33%. The unidirectional extraction fraction of ^{11}C-acetate is likely to be greater than this steady state (or bidirectional extraction fraction) and this high extraction fraction coupled with the rapid clearance of ^{11}C-acetate from blood allowed the early delineation of the left ventricular wall from the left ventricular cavity. Regions of interest were readily placed on the left ventricular wall, allowing myocardial time-activity curves to be generated from serial tomographic images.

Results of this study confirm the previous isolated perfused rabbit heart studies, given that more error will be encountered with the methodology employed for *in vivo* studies. The results confirm that the clearance of total ^{11}C-radioactivity from myocardium after ^{11}C-acetate administration largely reflect clearance of $^{11}CO_2$, and that this was biexponential and qualitatively similar to that seen in isolated perfused rabbit hearts. Estimates of the relative size of these two phases suggest that the major rapidly clearing phase account for approximately 81% of the ^{11}C label. No change in this figure was noted with increasing work, similar to results seen in the isolated perfused rabbit hearts. In the majority of canine ^{11}C-acetate studies essentially no clearance could be measured from the minor phase. Prolonged imaging may allow measurement of this phase with greater accuracy, although two studies followed for 30 or 40 minutes again showed essentially no clearance from this phase. Continued myocardial extraction of the ^{11}C label from arterial blood might also potentially obscure slow clearance from the minor phase over a longer imaging period. Alternatively, there may be little metabolism to $^{11}CO_2$ from the labelled constituents of the minor phase over the period of

measurement, consistent with the observed monoexponential efflux of $^{11}CO_2$ from the heart. In one low work load study the myocardial clearance of ^{11}C label could be fitted only to a monoexponential function consistent with the low rate pressure product and attendant low oxygen consumption observed. Future studies in man may also demonstrate monoexponential clearance due to the low work load at rest compared to instrumented, anaesthetized animals.

Despite the uncertainty regarding the clearance rate from and the source of the minor phase, the correlation between the rate of clearance of the ^{11}C residue (rate constant, major phase) and the rate of efflux of $^{11}CO_2$ indicates that the rate of oxidation of ^{11}C-acetate can be measured non invasively by PET.

Correlation with oxygen consumption and cardiac work. The rate of clearance of the ^{11}C myocardial residue after ^{11}C-acetate administration was shown to be a good index of oxygen consumption and cardiac work in isolated perfused rabbit hearts. Similar results were found in this study using a closed chest canine model over a wide range of oxygen consumption. A close correlation between clearance and both oxygen consumption and cardiac work load is not surprising, given that the rate pressure product has previously been shown to have a close correlation with myocardial oxygen consumption in normal subjects [70]. Although the results in this present study were obtained by correlating global clearance rates with global oxygen consumption, their importance lies in the application of these results to the regional assessment of oxidative metabolism. Regional oxygen consumption is commonly measured in animal models, although the techniques are destructive and accuracy in ischaemic models is impaired by the dilution of blood draining the ischaemic region with blood from non ischaemic regions [71]. Because application of these invasive techniques in patients is not possible, measurement of a regional index of oxidative metabolism with ^{11}C-acetate may provide data that could not be obtained otherwise. Rates of clearance of ^{11}C-radioactivity from multiple regions of interest placed on the left ventricular wall in this study showed no regional difference among lateral, anterior and septal walls, indicating that oxidative metabolism was relatively homogeneous throughout the left ventricular wall.

Data analysis. Data from regions of interest placed on serial tomographic images were corrected for decay, partial volume effects and bidirectional spillover between the left ventricular cavity and the myocardium using constant cardiac dimensions for all studies. Ideally, corrections should be based on the cardiac dimensions present during each study. However a comparison when no corrections were made to the original data (other than decay correction) showed the resulting rate constants to be insensitive to the particular dimensions used.

Corrected data were fitted with multiexponential solutions from the time of maximal $^{11}CO_2$ efflux from the heart to evaluate the relation between the rate of $^{11}CO_2$ efflux and the rate of clearance of ^{11}C-radioactivity from myocardium. This time was found to be similar to the time of maximal change in the residue data, as would be expected given that the majority of the ^{11}C-radioactivity effluxing from the heart was due to $^{11}CO_2$. Hence the time of maximal decrease of the ^{11}C residue approximated the time of peak efflux of $^{11}CO_2$ and could be used for curve fitting in future clinical studies in which *ex vivo* data would not be available.

This series of experiments were published in 1988 [54], and were the first data to validate the concept of using ^{11}C-acetate as a tracer of oxidative metabolism in *in vivo* studies. A subsequent publication by Buxton et al in 1989 [72] also investigated the utility of ^{11}C-acetate with PET in closed chest canine studies. A excellent correlation was found between the rate constant of the early phase of ^{11}C clearance, when measured externally by PET, and myocardial oxygen consumption. These results confirm those reported herein, establishing ^{11}C-acetate as a tracer of oxidative metabolism. Further studies have been reported by Armbrecht et al [73] in 1990, confirming the utility of ^{11}C-acetate over a wider variety of metabolic conditions in the open-chest canine model. Again the rate constant of the rapid phase, measured externally by PET, correlated closely with myocardial oxygen consumption in normal, ischemic, postischemic and hyperemic myocardium. These studies confirm the data derived from the isolated perfused rabbit heart model discussed in the previous Chapter, confirming that ^{11}C-acetate is a valid tracer of oxidative metabolism in those environments potentially found in patients with ischaemic heart disease.

Chapter 5

Effect of altered myocardial substrate utilization on ^{11}C-acetate tracer kinetics.

Alteration in substrate utilization by myocardium, depending on metabolic conditions such as ischaemia, prevailing arterial concentrations of major substrates and the hormonal environment, has been well documented in Chapters 1 and 2. The effect of myocardial ischaemia on ^{11}C-acetate kinetics has been examined in Chapter 3. Plasma concentrations of major cardiac substrates are altered with fasting, post prandial, with exercise [74] and after alcohol [15], and potentially could alter ^{11}C-acetate kinetics. Specifically, the rate of activation of ^{11}C-acetate to ^{11}C-acetyl CoA could be influenced by substrate competition, although this metabolic step has been thought to be poorly regulated [20]. Additionally the rate of oxidation of ^{11}C-acetate in the citric acid cycle could be influenced by the altered size of pools containing metabolic intermediates, especially acetyl CoA or citric acid cycle intermediates. The latter are known to increase in isolated hearts perfused with supra physiological concentrations of acetate and ketone bodies [20,75,76].

The purpose of this study was to examine the effects of alterations of myocardial substrate use on the rate of oxidation of ^{11}C-acetate and on estimates of oxygen consumption using positron emission tomography. Arterial substrate levels were changed by infusion of glucose or free fatty acids. It was hypothesized that altered arterial substrate levels leading to altered substrate utilization would not effect myocardial residue time activity curves following administration of ^{11}C-acetate, independently of myocardial oxygen consumption or cardiac work load.

Methods

Experimental Preparations. Twelve mongrel dogs weighing 20-31 kg were premedicated with subcutaneous morphine (1 mg/kg body weight) and anaesthetized with intravenous thiopental (12.5 mg/kg) and α-chloralose (60 mg/kg). Catheters were placed into the descending aorta, inferior vena cava and coronary sinus as described in Chapter 4. Physiological variables monitored were again aortic blood pressure, heart rate and the rate pressure product.

Experimental Protocol. Myocardial residue time activity curves were measured twice in each animal after administration of ^{11}C-acetate, at baseline and after alteration of myocardial substrate levels within plasma. Randomization of the order of tomographic scans at baseline and following altered substrate conditions was not possible due to the prolonged time taken for myocardial substrates to return to background levels. Substrate levels were altered either by infusion of glucose, insulin and potassium (50 gm glucose, 100 units soluble insulin and 20 mmol KCl in 100 mls sterile water, infused at 100 mls per hour) or by an intravenous infusion of Intralipid (0.6 mg lipid/kg/60 minutes of a 20% solution of neutral triglycerides consisting predominantly of linoleic, oleic, palmitic and linolenic acids, Kabi-Vitrum Inc., Alameda, CA) designed to raise plasma fatty acid concentrations.

Each substrate study consisted of a [^{15}O]CO scan to delineate the left ventricular blood pool, a [^{15}O]H_2O scan to measure myocardial blood flow and a ^{11}C-acetate scan. The technique used for measurement of myocardial blood flow with [^{15}O]H_2O was developed in this laboratory, and provides an accurate quantitative method in absolute terms [77,78]. Full details may be found in these publications. An interval of 10 minutes after administration of [^{15}O]CO or [^{15}O]H_2O and 100 minutes after administration of ^{11}C-acetate was allowed for decay of the previously injected tracer prior to further tracer administration.

Infusion of either glucose (n = 8) or Intralipid (n = 4) was commenced immediately following completion of the baseline study. After approximately 40 minutes of glucose or Intralipid infusion the [^{15}O]CO and [^{15}O]H_2O scans were repeated followed by a further ^{11}C-acetate scan commencing approximately 60 minutes after the start of the glucose or Intralipid infusion.

Myocardial residue time activity curves could not be measured in one control and one glucose infusion study due to a computer malfunction during acquisition. Myocardial oxygen consumption could not be measured in two dogs in which the coronary sinus catheter slipped out of the coronary sinus prior to ^{11}C-acetate administration, based on oxygen saturation of coronary sinus blood samples and confirmed radiologically at the completion of the study.

PET Procedure. Animals were studied in PETT VI, as described in Chapter 4. The [^{15}O]CO scan was obtained after administration of 50 mCi via the endotracheal tube, and data acquired for 5 minutes. After return of radioactivity to baseline, a further bolus of 40 mCi of [^{15}O]H_2O was administered, and data collected in 5 second frames for 90 seconds following injection. Subsequently a bolus of ^{11}C-acetate (approximately 0.8 mCi/kg) was administered intravenously and data acquired dynamically in 90 second frames for a total of 30 minutes. For analysis of both left ventricular blood flow and oxidative metabolism, 2-3 mid ventricular slices were selected and a large region of interest was placed within the myocardium as defined by the ^{11}C-acetate scan. The same regions of interest were used for analysis of the [^{15}O]H_2O data. An additional region of interest was placed in the centre of the left ventricular cavity defined in the [^{15}O]CO scan, allowing measurement of the ^{11}C-radioactivity content of left ventricular cavity blood. Data from the myocardial wall and blood pool were corrected for physical decay, partial volume and spillover effects as described in Appendix A. Results from each left ventricular slice were averaged.

Substrate Utilization. Aortic and coronary sinus blood samples were taken at the beginning, middle and end of each ^{11}C-acetate scan. Oxygen tension, oxygen saturation and haemoglobin were measured in each blood sample (Instrumentation Laboratory model 282 Co-oximeter, Waltham, MA) and oxygen content calculated from each sample, as described in Chapter 4. Oxygen extraction per ml of blood was calculated from the arterio-venous difference, and the mean of the three measurements per study calculated. Myocardial oxygen consumption (μmol/g/min) was calculated from the product of flow and oxygen extraction.

Arterial and coronary venous samples obtained during each ^{11}C-acetate study were analyzed for fatty acid, glucose, lactate and acetate. Substrate utilization was calculated from the product of blood flow and substrate extraction fraction. Fatty acid, lactate and glucose were assayed as described in Chapter 3, while acetate was assayed as described in Chapter 4.

Results.

Haemodynamics. Infusion of glucose tended to lower heart rate, and increase systolic blood pressure, blood flow and MVO_2, whereas infusion of Intralipid tended to increase heart rate and MVO_2 while decreasing blood pressure (Table 5.1). However, none of these changes were statistically significant.

Substrate utilization. Arterial glucose levels increased fivefold after a mean of 59 grams of glucose were infused prior to the beginning of each ^{11}C-acetate study. Total myocardial glucose extraction increased, although extraction fraction decreased. The fatty acid arterial concentration decreased and, consistent with the increased utilization of glucose, the fatty acid arterio-venous difference fell as did total myocardial fatty acid extraction. Little difference was found in arterial levels or arterio-venous extraction of lactate or acetate during the glucose infusion.

Dogs in the lipid infusion group received a mean of 22 grams of lipid. Arterial concentration of fatty acid increased approximately fivefold and myocardial arterio-venous extraction increased (Table 5.2). Little change in lactate or acetate arterial concentration or arterio-venous extraction was observed during the lipid infusion.

PET Data. All ^{11}C-acetate tomographic images of the left ventricle, either at baseline or following glucose or Intralipid infusion, were of high quality. Myocardial residue time-activity curves were biexponential in all studies, and qualitatively similar to studies in Chapter 4. Representative studies are shown in Figure 5.1 The calculated rate constant of the minor phase was essentially zero in all but three studies, indicating that over the period of measurement no clearance could be measured from this phase. The relative distribution of the ^{11}C label was estimated from the relative size of the major and minor phases. No significant change in the size of the major phase was present with glucose infusion, 82 ± 2 % pre glucose compared to 79 ± 4 % post glucose. Similarly no significant change was present following lipid infusion, 83 ± 1 % at baseline compared to 83 ± 1 % post Intralipid.

After infusion of glucose, a mild increase in the rate constant of the major phase was found, indicating more rapid clearance of the ^{11}C label. The rate constant of 0.17 $\pm$ 0.06 min^{-1} (equivalent to a half time of 4.4 ± 1.7 minutes) at baseline increased to

Table 5.1

Effects of Glucose or Lipid infusion on Haemodynamics, Myocardial Blood Flow (MBF) and Myocardial Oxygen Consumption (MVO_2).

	Heart rate (bpm)	Systolic blood pressure (mm Hg)	Rate-pressure product (mm Hg * rate)	MBF (ml/gm/min)	MVO_2† (μmol/gm/min)
Glucose studies (n=8)					
Baseline	126 ± 47	152 ± 20	19515 ± 7987	0.9 ± 0.4	4.4 ± 1.6
Glucose infusion	112 ± 39	177 ± 22	19928 ± 7351	1.2 ± 0.4	4.8 ± 1.5
Intralipid studies (n=4)					
Baseline	122 ± 69	167 ± 10	18525 ± 9479	0.6 ± 0.2	3.7 ± 1.4
Intralipid infusion	132 ± 32	135 ± 58	16723 ± 6782	0.7 ± 0.2	4.3 ± 1.3

Data are mean ± SD. No changes from baseline to intervention in any of the physiological measurements listed were statistically significant, see text for discussion. † MVO_2 was not able to be measured in two studies following glucose infusion due to movement of the coronary sinus catheter from the coronary sinus

Table 5.2

Effects of Glucose-Insulin-Potassium or Intralipid infusion on Arterial Plasma Substrate Concentration, Myocardial Extraction Fraction and Arterial-Coronary Sinus Difference (A-V Δ).

	Glucose study (n = 6)			Intralipid study (n = 4)		
	Arterial Conc.	Extraction Fraction (%)	A-V Δ	Arterial Conc.	Extraction fraction (%)	A-V Δ
Glucose (mM)						
Baseline	5.4 ± 0.8	9.6 ± 10.4	0.5 ± 0.5	5.2 ± 1.4	10.1 ± 7.5	0.5 ± 0.3
Infusion	25.9 ± 6.7†	3.1 ± 8.3†	0.7 ± 1.7	4.7 ± 0.6	13.8 ± 21.9	0.6 ± 0.9
Fatty acid (μM)						
Baseline	445 ± 182	42.0 ± 6.4	186 ± 79	552 ± 154	32.7 ± 15.5	179 ± 103
Infusion	202 ± 61†	17.4 ± 12.7†	41 ± 39†	2925 ± 1831†	23.1 ± 24.8	603 ± 131†

Data are mean ± SD. † $p < 0.05$ compared to baseline.

Table 5.2 (continued)

Effects of Glucose-Insulin-Potassium or Intralipid infusion on Arterial Plasma Substrate Concentration (Art conc), Myocardial Extraction Fraction and Arterial-Coronary Sinus Difference (A-V Δ).

	Glucose study (n = 6)			Intralipid study (n = 4)		
	Arterial Conc.	Extraction Fraction (%)	A-V Δ	Art Conc.	Extraction fraction (%)	A-V Δ
Lactate (mM)						
Baseline	1.9 ± 0.4	37.6 ± 19.7	0.7 ± 0.4	1.4 ± 0.4	23.8 ± 20.9	0.3 ± 0.2
Infusion	2.3 ± 0.7	44.0 ± 14.2	1.0 ± 0.4	1.7 ± 0.8	11.3 ± 7.7	0.2 ± 0.2
Acetate (μM)						
Baseline	115 ± 25	18.0 ± 13.9	21 ± 16	142 ± 17	23.3 ± 11.8	33 ± 18
Infusion	124 ± 30	27.3 ± 20.5	37 ± 37	156 ± 10	24.4 ± 13.7	38 ± 19

Data are mean ± SD. † $p < 0.05$ compared to baseline.

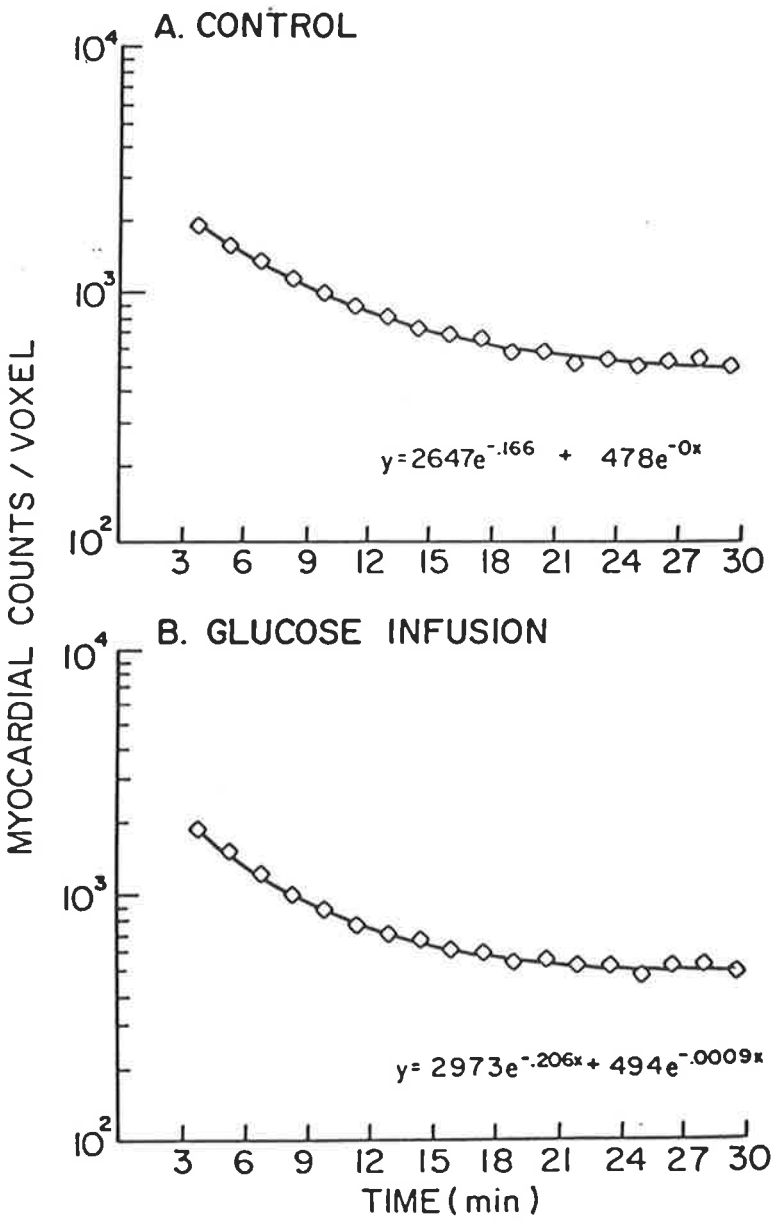

Figure 5.1 Examples of myocardial residue time-activity curves are shown from a control (A) and post glucose study (B). Clearance was biexponential, consisting of a major rapidly clearing phase and a minor phase. In this study rate pressure product was 18,850 and 20,700 mm Hg * bpm at baseline and post glucose, respectively. Measured oxygen consumption was 5.0 and 4.8 μmol O_2/g/min, respectively. No significant differences in rate constants were observed when corrected for differences in rate-pressure product or oxygen consumption, as discussed in the text.

0.21 ± 0.04 min^{-1} (equivalent to a half time of 3.5 ± 0.8 minutes), a significant increase ($p < 0.05$). Clearance of this phase was shown to correlate closely with both oxygen consumption and rate-pressure product in isolated perfused rabbit hearts (Chapter 3) and an identical canine preparation (Chapter 4) over a wide range of cardiac work loads. After normalizing the rate pressure product to a constant rate pressure-product of 20,000 mm Hg * bpm (thereby correcting for minor haemodynamic alterations induced by the glucose infusion), no significant difference between control and glucose studies was found (rate constant at baseline 0.18 ± 0.03 compared to 0.22 ± 0.06 min^{-1} post glucose, half time = 3.9 ± 0.6 minutes and 3.4 ± 0.8 minutes, respectively). Normalization of the clearance rate constant to a constant oxygen consumption of 4 μmol/gm/min again showed no significant difference between groups (rate constant 0.15 ± 0.02 at baseline compared to 0.17 ± 0.03 min^{-1}. Similar rate constants were found before and after Intralipid infusion (0.15 ± 0.06 at baseline compared to 0.14 ± 0.04 min^{-1} after Intralipid infusion, p = ns). No statistically significant differences were found after normalization for rate-pressure product or oxygen consumption. The myocardial clearance rate constant, for studies at baseline and those following glucose or Intralipid, correlated closely with directly measured myocardial oxygen consumption ($r = 0.89$, $p < 0.001$) These data and those obtained in previous canine studies (Chapter 4) are shown in Figure 5.2. Data from Chapter 4 are included to demonstrate the consistency of results. Analysis of covariance showed no significant difference in the individual regression relationships between clearance rate constant and MVO_2 at baseline ($n = 9$, $r = 0.9$, $y = 0.031x + 0.030$), following glucose ($n = 6$, $r = 0.97$, $y = 0.30x + 0.052$) and following Intralipid ($n = 4$, $r = 0.92$, $y = 0.028x + 0.019$). There was also a close correlation in all studies between rate-pressure product, an index of cardiac work that reflects the energy demands of the heart, and MVO_2 ($r = 0.84$, $p < 0.001$). These data and those from previous canine studies are shown in Figure 5.3. Analysis of covariance showed no significant difference in the individual regression relationships between rate-pressure product and MVO_2 at baseline ($n = 11$, $r = 0.90$, $y = 6.45 * 10^{-3}x + 0.044$), following glucose ($n = 7$, $r = 0.80$, $y = 5.84 * 10^{-3}x + 0.082$) and following Intralipid ($n = 4$, $r = 0.97$, $y = 5.66 * 10^{-3}x + 0.042$).

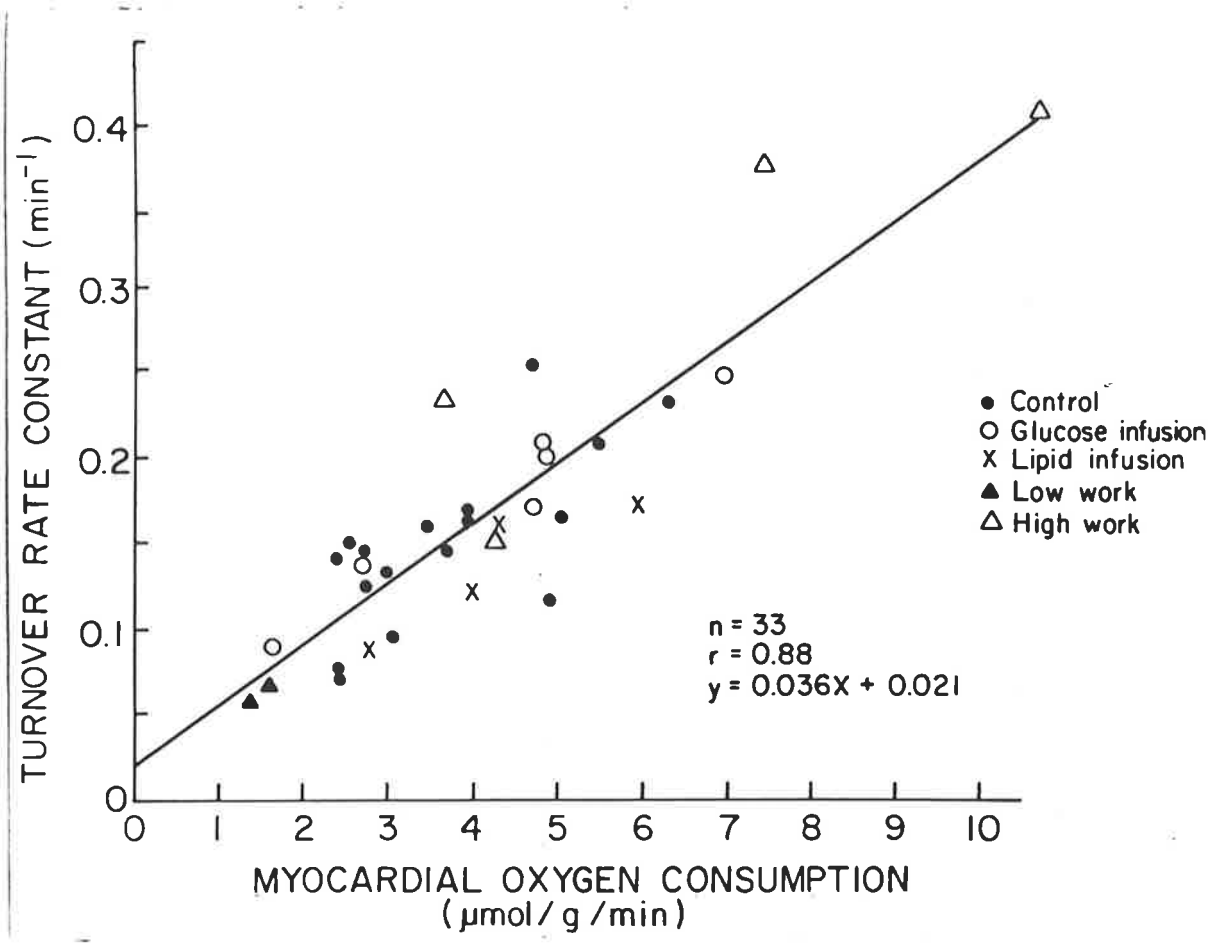

Figure 5.2 The correlation between the rate constant of the rapid phase of clearance of ^{11}C-radioactivity from myocardium and directly measured myocardial oxygen consumption is shown. Results from Chapter 4 are also included, labelled "low" and "high" work load to demonstrate the consistency of results.There was no statistically significant difference between the regression relationship for control studies (excluding data from Chapter 4) with the regression relationship for post glucose studies (control: n = 9, r = 0.90, y = 0.031x + 0.030., post glucose: n = 4, r = 0.92, y = 0.028x + 0.019) by analysis of covariance. The regression relationship shown on the Figure above includes all data, including Chapter 4 data.

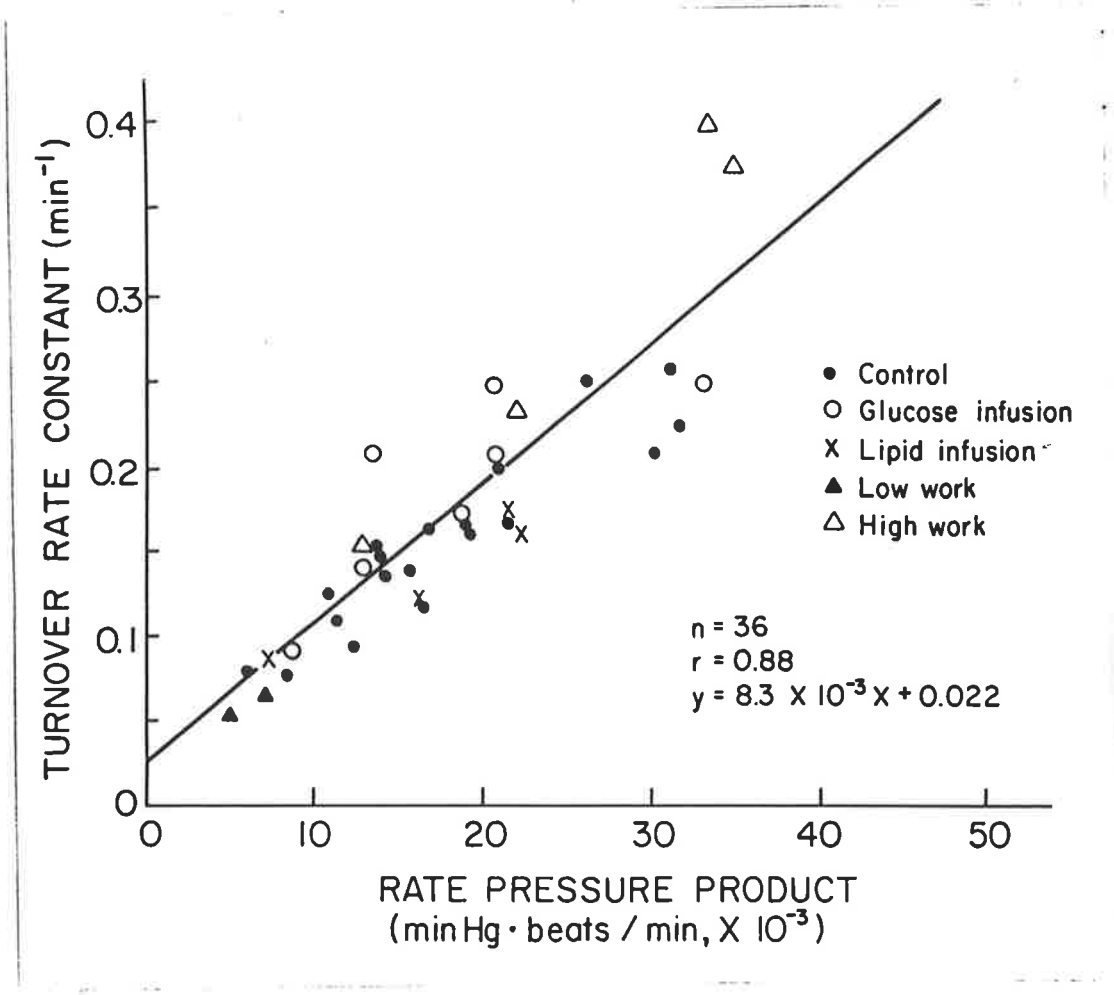

Figure 5.3 The correlation between the rate constant of the rapid phase of clearance of ^{11}C-radioactivity from myocardium and the rate-pressure product, an index of total myocardial work, is shown. Data from Chapter 4 are also included, labelled "low" and "high" work load to demonstrate the consistency of results. There was no statistically significant difference between the regression relationship between control (excluding data from Chapter 4), post glucose and post lipid studies by analysis of covariance. (controls: n= 11, r = 0.90, $y = 6.45 * 10^{-3}x + 0.044$; post glucose: n = 7, r = 0.80, $y = 5.84 * 10^{-3}x + 0.082$; post lipid: n = 4, r= 0.097, $y = 5.66 * 10^{-3}x + 0.042$). The regression relationship shown in the Figure above includes all data., including data from Chapter 4.

Discussion.

The major factor effecting clearance of ^{11}C radioactivity from myocardium after ^{11}C-acetate administration has been shown earlier to be myocardial oxygen utilization. Since myocardial oxygen utilization is determined by energy demand, cardiac work has also been shown to be a determinant of clearance of ^{11}C radioactivity. In this study, after accounting for changes in either cardiac work or oxygen consumption induced by glucose or lipid infusion, no significant changes in clearance rates arising from altered myocardial substrate utilization were evident. The change in arterial concentrations of glucose or fatty acid induced in this study are many times greater than found physiologically in humans. The results indicate that the turnover rate constant of ^{11}C radioactivity after administration of ^{11}C-acetate is insensitive to variations in the pattern of substrate utilization by the heart, and reflects overall myocardial oxygen consumption. This conclusion is limited to those situations where augmented fatty acid or glucose utilization occurs, which is the majority. The effect of augmented lactate or acetate metabolism, as may occur following exercise or heavy alcohol consumption respectively, was not examined in these studies although reported elsewhere (as discussed below).

High plasma concentrations of either glucose or free fatty acid had little effect on the myocardial extraction fraction of unlabelled acetate, suggesting no major competition by other substrates for preferential conversion to acetyl CoA during intermediary metabolism. The distribution of ^{11}C radioactivity between the major and minor phases of ^{11}C clearance curves was also unchanged, suggesting no alteration in the fraction oxidized within the citric acid cycle.

These findings contrast with previous studies examining tracer kinetics of ^{11}C-palmitate [37,79]. After a similar dose of glucose, the major rapid phase of myocardial clearance normally observed after ^{11}C-palmitate administration under fasting conditions and thought to reflect beta oxidation, was either attenuated or not detectable [37]. Similar findings are reported in patients after oral glucose [79]. This change in fatty acid metabolism has been considered to be due to inhibition of beta oxidation with preferential shunting of ^{11}C-palmitate into neural lipid or phospholipid pools. Slow

clearance of tracer subsequently occurs due to slow turnover of these pools. In addition, although rates of beta oxidation can be estimated during normoxia with ^{11}C-palmitate, backdiffusion of unmetabolized tracer results in overestimation of beta oxidation during ischaemia [39].

Estimates of glucose utilization with ^{18}F-fluorodeoxyglucose are also profoundly affected by changes in substrate concentration [80,81,82]. Administration without glucose loading results in diminished uptake of ^{18}F-fluorodeoxyglucose due to preferential metabolism of free fatty acids [80]. Hence neither ^{11}C-palmitate nor ^{18}F-fluorodeoxyglucose alone will provide an overall estimate of oxidative metabolism. However data from ^{11}C-acetate kinetic studies in both isolated perfused rabbit hearts and *in vivo* canine studies are consistent, with early metabolism reflecting citric acid cycle flux. Although no effect of altered substrate concentrations on ^{11}C-acetate kinetics was detected in the above studies, high concentrations of acetate (500 to 5000 μM) in the perfusate have been reported to underestimate citric acid cycle flux using ^{11}C-acetate in isolated rat hearts [65]. These levels are 2 to 20 fold higher than the upper range in man. No effect of altered lactate, β-hydroxybutyrate or palmitate concentrations were evident [65]. Possibly high perfusion concentrations of unlabelled acetate resulted in expansion of the acetyl CoA pool, and hence turnover of ^{11}C-acetate was less for any level of oxygen consumption. Studies with isolated rabbit hearts reported in Chapter 3 compared ^{14}C-acetate kinetics with no added unlabelled acetate compared to 50 μM unlabelled acetate, with no detectable difference found at these lower concentrations.

The studies reported above under Results were published in 1989, and subsequent studies of the effect of varying substrate levels on ^{11}C-acetate clearance in *in vivo* studies have lead to conflicting conclusions. Buxton et al [72] demonstrated an decreased ratio of k/MVO_2 (where k is the rate constant of the rapid phase and MVO_2 is myocardial oxygen consumption) after free fatty acid infusion in a closed-chest canine model, in contrast to a minor increase which may be expected on biochemical grounds. This potential effect of altered substrate levels on the relationship between citric acid cycle flux and oxygen consumption is discussed in Chapter 1. In contrast,

Hicks et al [83] reported a minor increase in the early rate constant of ^{11}C-acetate clearance in humans after infusion of free fatty acid although this occurred at a mildly greater rate pressure product. No direct measurement of myocardial oxygen consumption was made in this study. The increased rate constant of approximately 9% was statistically significant, and was associated with an increased rate-pressure product of approximately 7%, No correction was made for this change in rate-pressure product, and hence it is unknown if the change in rate constant was independent of haemodynamic changes. The same group, examining the utility of polar co-ordinate maps of ^{11}C-acetate clearance rate constants, also reported an increase in clearance rates from 5 normal subjects following free fatty acid infusion [84]. Haemodynamic data following Intralipid was consistent with a mildly lower cardiac workload, and hence could not explain the minor but significant increase in mean rate constant from 0.053 to 0.061 min^{-1}. Again no independent assessment of oxygen consumption was made.

No significant change in ^{11}C-acetate clearance rates were found in the study reported herein, despite markedly altered arterial substrate concentrations involving glucose or free fatty acids. More recent studies have raised the possibility of alterations in clearance rates induced by preferential fatty acid metabolism, but no unequivocal evidence is available to date from the available published data to confirm this. Hence at the current time it is concluded that myocardial residue time-activity curves after administration of ^{11}C-acetate are either not affected or are insensitive to changes in substrate utilization.

Chapter 6

Comparison of ^{11}C-acetate and ^{11}C-palmitate tracer kinetics after 1 hour of coronary occlusion.

The impact of coronary artery disease on myocardial metabolism in patients with angina or myocardial infarction has previously been assessed with both ^{11}C-palmitate and ^{18}F-fluorodeoxyglucose, and these tracers of fatty acid metabolism and glucose respectively are discussed in Chapter 2. The hypothesis that ^{11}C-acetate kinetics, assessed by PET, provides a non invasive index of oxidative metabolism has been validated in two animal models as discussed in Chapters 3 to 5. The application of this technique to patients with myocardial ischaemia or infarction may potentially define the metabolic impact of coronary artery disease on myocardial oxidative metabolism. Oxygen consumption in "stunned" myocardium following brief periods of ischaemia has previously been reported as reduced [85,86,87], unchanged [88,89,90,91,92] or increased [93,94]. Although such studies are able to define the relationship between oxygen consumption and myocardial contractility in experimental models of stunned myocardium, they are invasive and cannot be applied on a serial basis. Additionally the invasive nature of these techniques precludes their use in patients to assess oxidative metabolism.

^{11}C-acetate clearance kinetics in patients with myocardial ischaemia, induced by exercise, have been assessed in a preliminary report from the Hammersmith Hospital in 1981 [51]. Four normal subjects showed a mean clearance half time of 7.9 minutes during exercise compared to 10.1 minutes in 5 patients with coronary artery disease and exercise induced angina. The authors concluded that this was a promising approach to the regional identification of ischaemic myocardium [51]. At the time that the current series of experiments were undertaken and preliminary results published [95], no data were available examining tracer kinetics of ^{11}C-acetate in the setting of acute myocardial ischaemia. Hence in this study ^{11}C-acetate clearance kinetics were initially examined in myocardium salvaged by reperfusion after a period of coronary occlusion, using a canine model to simulate the successful use of thrombolytic therapy in patients with myocardial infarction. A period of one hour of coronary occlusion prior to reperfusion was chosen

to result in maximum salvage of jeopardized myocardium. The clearance kinetics of ^{11}C-palmitate have been characterized after 20 minutes [96] and 3 hours [45] of coronary occlusion in a canine model. In view of these previous studies, tracer kinetics with ^{11}C-palmitate were compared to those seen with ^{11}C-acetate.

The specific aim of this study was to determine clearance rates of ^{11}C-acetate and ^{11}C-palmitate in largely "stunned" myocardium salvaged after an intermediate period of ischaemia.

Methods. Twelve mongrel dogs were instrumented with aortic, left atrial and inferior vena cava catheters as described earlier, following anaesthesia with thiopental and α-chloralose. A coronary angioplasty guiding catheter was introduced via the left carotid artery and a 3.7 mm coronary angioplasty balloon placed in the mid left anterior descending artery (LAD) under fluoroscopic control following lignocaine 80 mg and heparin 5000 units intravenously.

Experimental Procedure. The LAD was occluded by inflation of the balloon to 10 atmospheres for a period of 60 minutes. Fifty minutes following balloon inflation, regional myocardial blood flow was measured with radiolabelled microspheres, as described earlier. The same ischaemic region identified by radiolabelled microspheres was also demonstrated tomographically with [^{15}O]H_2O and PET. At 60 minutes the balloon was slowly deflated over a period of 5 minutes to allow gradual reperfusion of the LAD, potentially minimizing the risk of ventricular fibrillation, and then withdrawn from the coronary artery. Coronary reperfusion was then confirmed with radiolabelled microspheres and a further [^{15}O]H_2O study performed one hour after coronary reperfusion. Studies with both ^{11}C-acetate and ^{11}C-palmitate were then performed in random order, with an interval of at least 100 minutes between administration of either to allow for decay of previously injected tracer. This interval allowed decay of 95% of previously injected tracer. Approximately 0.8 mCi's/kg of each tracer were injected and serial tomograms performed, each lasting for 90 to 120 seconds with a total imaging time of 30 to 40 minutes. Dogs remained in a Plexiglas shell within the tomograph and hence identical left ventricular wall regions could be compared between ^{11}C-acetate and ^{11}C-palmitate studies.

Animals were sacrificed following these studies for determination of regional blood flow. No attempt to measure infarct size was made, since insufficient time had elapsed to allow the of use of staining techniques such as triphenyl tetrazolium chloride.

^{15}O labelled water studies. The use of this technique is described in more detail in Chapter 5. Briefly [^{15}O]CO was given by inhalation, labelling the blood pool within the left ventricular cavity. Following a delay of approximately 10 minutes to allow for decay of the previously injected tracer, [^{15}O]H_2O was given intravenously. The [^{15}O]CO image was then subtracted from the [^{15}O]H_2O image, leaving an image of the [^{15}O]H_2O content of myocardium. No attempt was made to quantitate regional myocardial blood flow in this study.

Analysis of PET images. The subtracted [^{15}O]H_2O studies during LAD occlusion were first examined to determine the tomographic slices in which a reduction of flow to the anterior wall was shown. Of these, the most basal slice was selected and 3 regions of interest (0.9 cm^3 each) placed on the area of reduced flow, and a further 3 regions of interest placed on each of the lateral and septal walls adjacent to the ischaemic region. Reperfusion was confirmed by microspheres and assessment of the second subtracted [^{15}O]H_2O water study. The nine regions of interest were then placed on the ventricular wall of the same tomographic slice for each of the ^{11}C-acetate and ^{11}C-palmitate studies, and myocardial residue time-activity curves generated for each tracer. Subsequently analysis of these were identical, including correction for decay, partial volume effects (based on fixed dimensions) and spillover as described earlier and detailed in Appendix A.

Results.

Four dogs developed ventricular fibrillation during LAD occlusion or immediately on reperfusion. A further dog showed no evidence of reperfusion following balloon deflation, and at autopsy was found to have a intra-coronary thrombus at the site of the previous balloon inflation. These dogs were excluded, leaving a total of 7 complete studies for further analysis. Data are shown below as mean ± SD.

Haemodynamics and regional blood flow. No significant difference was found at the time of each ^{11}C-acetate or ^{11}C-palmitate study for systolic blood pressure (163 ±

30 vs 155 ± 31 mm Hg respectively), heart rate (109 ± 37 vs 107 ± 30 beats min^{-1}) or rate-pressure product (17416 ± 5522 vs 16274 ± 4316 mm Hg beats min^{-1}) to account for potential differences in myocardial clearance rates of either tracer.

Myocardial blood flow to the ischaemic subendocardial region fell by 85% during LAD occlusion, compared to the non-ischaemic lateral and septal walls, and by 75% to the subepicardial region (Table 6.1). Sixty minutes following reperfusion a hyperaemic response persisted in the subendocardium (although not statistically significant), while subepicardial blood flow had recovered to baseline levels.

Table 6.1 Subendocardial and subepicardial blood flow measured with radiolabelled microspheres during LAD occlusion and 60 minutes after coronary reperfusion.

endocardial blood flow	LAD	LAD
(ml/gm/min)	occlusion	reperfusion
non ischaemic region	1.04 ± 0.19	1.13 ± 0.37
ischaemic region	0.16 ± 0.08 *	2.81 ± 3.50
epicardial blood flow		
(ml/gm/min)		
non ischaemic region	0.95 ± 0.15	0.99 ± 0.36
ischaemic region	0.23 ± 0.08 *	1.11 ± 0.74

*$p < 0.05$ compared to non ischaemic regions.

The stability of arterial substrate concentrations was also determined in 3 dogs, and although this represents a minor sample, no significant change was detected between studies for glucose (3.6 ± 0.8 vs 3.9 ± 0.6 mmol/litre for ^{11}C-acetate and ^{11}C-palmitate studies respectively), non esterified fatty acids (600 ± 220 vs 440 ± 150 µmol/litre), lactate (1.3 ± 0.3 vs 1.3 ± 0.3 mmol/litre) or acetate (110 ± 50 vs 120 ± 30 µmol/litre).

PET studies. All subtracted [^{15}O]H_2O studies showed a reduction of flow to the anterior wall, sufficient to place 3 regions of interest, although the ischaemic region was of variable size. To avoid replication, similar examples during LAD occlusion are shown in Chapter 8.

All ^{11}C-acetate and ^{11}C-palmitate studies showed extraction of tracer in the reperfused region, although peak counts per voxel in the anterior wall were reduced by approximately 20% compared to the lateral and septal walls. Limited subendocardial infarction in the ischaemic region would be expected in this model after 60 minutes of LAD occlusion and may account for the mild reduction in peak extraction of tracer. Alternatively, thinning of the anterior wall relative to other walls which persisted after reperfusion could also account for this difference, due to partial volume effects.

Clearance of ^{11}C-radioactivity from arterial blood was consistently slower after intravenous administration of ^{11}C-palmitate compared to ^{11}C-acetate, as shown in one example in Figure 6.1 below. A minor increase in arterial blood counts was usually seen at approximately 5 minutes in ^{11}C-acetate studies, due to production of $^{11}CO_2$.

Figure 6.1 Decline in arterial blood ^{11}C-radioactivity after intravenous ^{11}C-acetate and ^{11}C-palmitate, as a function of time in one representative canine study. Total ^{11}C-radioactivity was counted *in vitro* from arterial blood samples, and ^{11}C-radioactivity expressed as a percentage of peak counts.

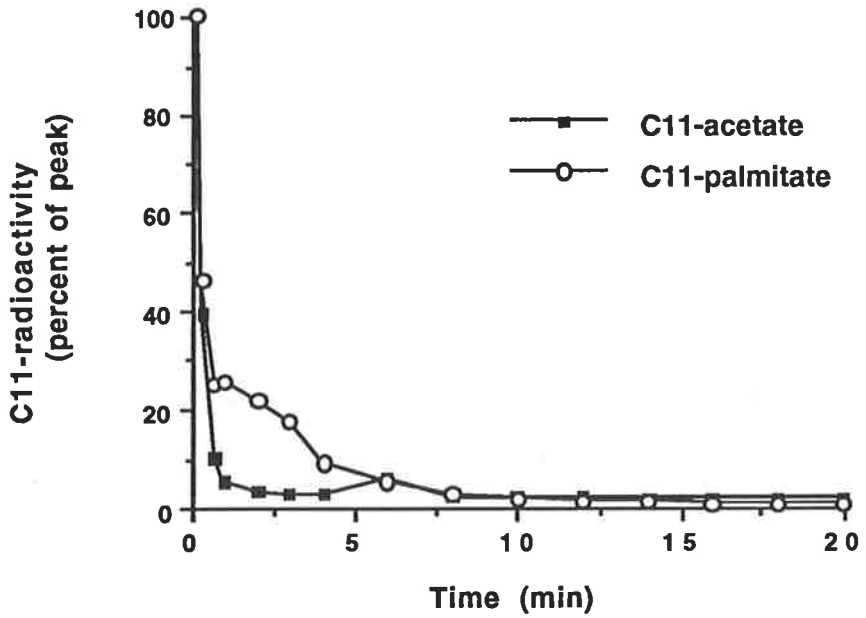

Examples of myocardial time-activity curves for each tracer are shown in Figure 6.2. Clearance of ^{11}C-radioactivity from the previously ischaemic region was impaired for each tracer, and only monoexponential solutions could be obtained. Clearance from normal regions was biexponential, as described in earlier Chapters for ^{11}C-acetate and described previously for ^{11}C-palmitate [96].

The rate of clearance of ^{11}C-radioactivity from myocardium after ^{11}C-acetate (rate constant of the major phase) was obtained as a mean of three regions of interest for the ischaemic region and a mean of 6 regions of interest for the normal or non ischaemic region. The rate constant for normal regions and ischaemic regions was 0.19 ± 0.09 and 0.06 ± 0.03 per minute respectively, corresponding to clearance half times of 4.5 ± 2.1 min and 13.5 ± 5.9 min respectively. Previous studies, described in Chapter 4, defined a regression relationship between MVO_2 and the rate constant of clearance ($MVO_2 = 25.6$ * rate constant - 0.51; units for MVO_2, μmoles O_2/gm/min). The reduction of the rate constant for reperfused regions was consistent with a $69 \pm 23\%$ reduction in myocardial oxygen consumption, compared to normal non-ischaemic regions. A considerable variation in calculated oxygen consumption was found, ranging from 26 to 97% reduction compared to normal regions. Similarly after administration of ^{11}C-palmitate, and for identical regions, the rate constant for normal regions and ischaemic regions was 0.10 ± 0.05 and 0.03 ± 0.11 per minute respectively. These rate constants correspond to clearance half times of 9.3 ± 6.2 min and 42.5 ± 47.0 min respectively. Hence the metabolic rate of clearance of ^{11}C-palmitate is significantly slower in normal myocardium at similar work loads, compared to ^{11}C-acetate ($p < 0.001$, paired t test). Clearance is further slowed in reperfused myocardium, although this may overestimate the degree of impairment of fatty acid oxidation (see Discussion). Differences between ^{11}C-acetate and ^{11}C-palmitate clearance rates may also reflect the different input function of each tracer, as illustrated in Figure 6.1. For example, the slower clearance of ^{11}C-palmitate from arterial blood is likely to result in continuing uptake of tracer by myocardium and hence the myocardial ^{11}C residue will reflect to a greater degree (compared to ^{11}C-acetate) the balance between uptake of ^{11}C-palmitate and efflux of $^{11}CO_2$.

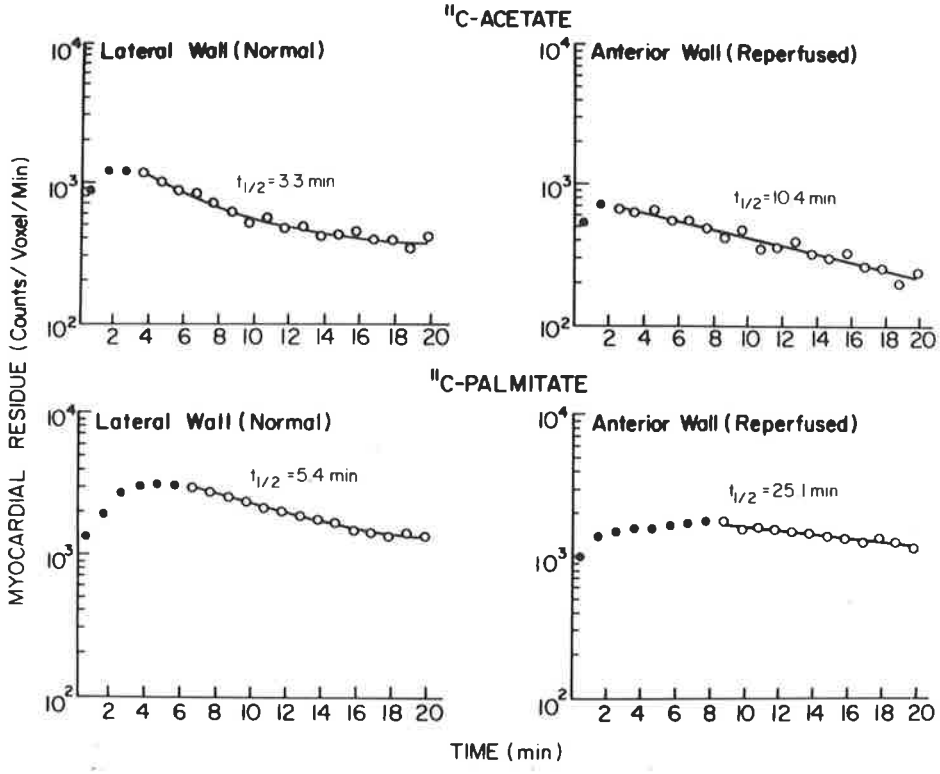

Figure 6.2 Myocardial residue time-activity curves are shown from a representative canine study for both normal and reperfused regions following ^{11}C-acetate (above) and ^{11}C-palmitate (below). The half time of the rapid phase following ^{11}C-acetate was 3.3 minutes in normal regions and compared to 10.4 minutes in reperfused regions, consistent with impaired oxidative metabolism in myocardium reperfused after 60 minutes of coronary occlusion. In contrast the half time of the rapid phase following ^{11}C-palmitate was 5.4 minutes in normal myocardium, compared to 25.1 minutes in reperfused regions. Normal and reperfused regions were identical in both PET studies. Curve fitting was calculated over periods shown by solid lines.

Clearance half times of both ^{11}C-acetate and ^{11}C-palmitate are shown for each region in Figure 6.3, shown on the following page. Clearance from normal regions was relatively homogeneous with ^{11}C-acetate, and less so with ^{11}C-palmitate. Given the resolution of PET, it is possible that "islands" of ischaemic myocardium have been included in the normal zone adjacent to the ischaemic zone (eg., regions 3 and 7) and this may account for the slower clearance seen with ^{11}C-palmitate in region 7.

Discussion.

^{11}C-acetate kinetics. Oxygen utilization of myocardium reperfused after a brief duration of ischaemia has been examined in a variety of animal models by a variety of methods. A majority of studies have demonstrated either no change[88,89,90,91,92] or a reduction of oxygen consumption[85,86,87], although an increase in oxygen consumption has been reported [93,94]. Myocardial contractility has been consistently impaired in these studies, disproportionate to the degree of impairment of oxygen consumption. Typically regional myocardial ischaemia in an animal model (for example a swine [85] or canine [86] model) has involved coronary occlusion or hypoperfusion of 10 to 20 minutes, causing a reduction in oxygen consumption of approximately 20 to 30% [85]. A greater impairment of oxygen consumption (approximately 45%) has been reported in an open chest canine model subjected to 60 minutes of ischaemia prior to reperfusion [5], suggesting that the degree of impairment of oxygen consumption may be related to the severity and duration of ischaemia. A reduction of approximately 70% in estimated oxygen consumption in the reperfused region was seen in this study, based on ^{11}C-acetate clearance rates. The extent of myocardial necrosis is unknown, and may have contributed to a greater impairment of oxidative metabolism compared to studies using a brief period of ischaemia. Potentially, reduced oxidative metabolism could be secondary to diminished delivery of oxygen to the reperfused region or diminished requirement or inability to use oxygen by reperfused myocardium. However myocardial blood flow in this study was greater in the reperfused region compared to normal regions, indicating either a diminished requirement or inability to undertake oxidative metabolism.

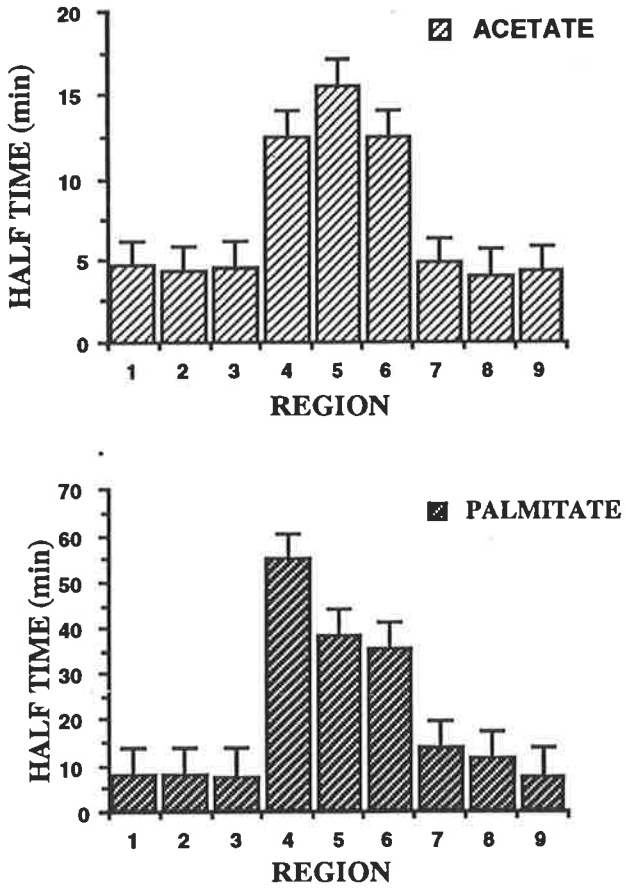

Figure 6.3 Rate of clearance of ^{11}C-radioactivity (major phase) for both ^{11}C-acetate and ^{11}C-palmitate, expressed as mean half times in minutes for each region. Regions 4-6 represent reperfused myocardium in the anterior wall, regions 1-3 normal lateral wall and 7-9 normal septal wall. Data are mean ± SD.

Methodologic Considerations. Previous studies in isolated perfused rabbit hearts, discussed in Chapter 3, have demonstrated the utility of ^{11}C-acetate metabolism to provide a non-invasive index of myocardial oxygen consumption under a variety of diverse conditions, including ischaemic and post-ischaemic states. Validation of this technique was also confirmed in Chapter 4 in a closed chest canine model, although not specifically in the post ischaemic state. However a subsequent report has extended these observations to ischaemic and post-ischaemic myocardium in an open chest canine model [97], confirming ^{11}C-acetate as a tracer of myocardial oxidative metabolism under a wide variety of metabolic conditions.

^{11}C-palmitate kinetics. Tissue kinetics of ^{11}C-palmitate were assessed in both normal and reperfused regions, and compared to tissue kinetics of ^{11}C-acetate. The clearance half time after ^{11}C-palmitate in non ischaemic regions was more than twice that seen with ^{11}C-acetate, reflecting sequential metabolism involving fatty acid oxidation prior to oxidation in the citric acid cycle. Clearance half times were further prolonged in reperfused myocardium. Similar clearance rates have been reported with ^{11}C-palmitate in normal myocardium [37], while prolonged clearance half times in reperfused regions are less than those reported after a more severe ischaemic insult associated with a 3 hour period of coronary occlusion [45].

In contrast to the impression of impaired fatty acid oxidation from ^{11}C-palmitate kinetics, recent studies have demonstrated rapid recovery of directly measured fatty acid oxidation in myocardium reperfused after brief periods of ischaemia [98] with little contribution from glucose [99], pyruvate or lactate [100] towards overall energy production. These discordant conclusions require a careful examination of previous reports of ^{11}C-palmitate kinetics during myocardial ischaemia or reperfusion. Prior studies with ^{11}C-palmitate after a shorter duration of coronary occlusion of 20 minutes have indicated persisting impairment of myocardial clearance rates, despite a paradoxical increase in the proportion of ^{11}C-palmitate assumed to ultimately undergo oxidation to $^{11}CO_2$ [96]. Studies with ^{14}C-palmitate after 60 minutes of coronary occlusion have also suggested slowed fatty acid oxidation (as assessed by the rate of production of $^{14}CO_2$) during reperfusion [5], consistent with the present findings with ^{11}C-palmitate. However the

percentage of tracer ultimately oxidized after reperfusion was very similar to that during control studies [5]. The discrepancy between the apparent reduction in fatty acid oxidation and the fraction of the ^{11}C-label ultimately oxidized may be explained by expansion of intracellular pool of activated and non-activated fatty acid. This expansion is known to accumulate during ischaemia [101,102], and possibly may persist during the early reperfusion period. This expansion would potentially lead to diminished turnover of ^{11}C-palmitate, resulting in lower clearance rates unrelated to impairment of utilization of free fatty acids for oxidative metabolism. However intracellular content of fatty acid in the myocardium during the reperfusion period has not been adequately assessed, and this possibility must remain a hypothesis.

Hence fatty acid utilization, based on ^{11}C-palmitate tracer kinetics, is uncertain in this study and no firm conclusions can be made.

Conclusion. Experiments using a closed chest canine model of stunned myocardium following an intermediate period of coronary occlusion have demonstrated a mean reduction of myocardial oxygen consumption of approximately 70%. The prognostic significance of this degree of inhibition of myocardial oxygen consumption is uncertain, as no assessment of long term recovery of contractility was undertaken in these acute experiments. No previous studies have examined the relationship between oxidative metabolism in stunned myocardium and subsequent recovery of function. Potentially a level of oxidative metabolism may be required in ischaemic or post ischaemic myocardium to preserve tissue viability and result in long term recovery of contractility. This level in ischaemic myocardium may be greater than that required for basal metabolism. Previous studies with myocardial dyskinesis, induced by lignocaine injected directly into the coronary circulation, have demonstrated a 33% reduction of oxygen consumption despite cessation of mechanical activity [103]. This mild reduction of oxygen consumption is less than expected, were oxygen consumed at a level required only for basal metabolism. Hence a testable hypothesis is that assessment of regional oxidative metabolism with ^{11}C-acetate will provide an early indication of late recovery of contractility, and this concept is explored in Chapter 8.

Chapter 7

Assessment of myocardial infarct size with ^{11}C-acetate and ^{11}C-palmitate, using PET.

Tracer kinetics of ^{11}C-acetate in non viable or infarcted myocardium, either extraction or subsequent clearance, are unknown. It is likely that uptake of tracer in viable myocardium will parallel regional myocardial blood flow, since uptake of tracer is dependent on delivery to the myocardium. Additionally it may be anticipated that extraction of tracer requires viable, metabolically active myocardium since sequestration depends on activation of ^{11}C-acetate to ^{11}C-acetyl CoA, which is an energy dependent process. Absent myocardial uptake in viable myocardium would preclude assessment of myocardial oxidative metabolism, while uptake in non viable myocardium would potentially distort the assessment of myocardial oxidative metabolism in viable myocardium or lead to the erroneous identification of viable myocardium. Interpretation of clinical ^{11}C-acetate tomographic images in patients with myocardial ischaemia or infarction optimally requires animal validation of the relationship between ^{11}C-acetate uptake and infarct size. Previous studies in dogs with myocardial infarction resulting from chronic coronary artery occlusion have demonstrated a close correlation between tomographic estimates of infarct size using ^{11}C-palmitate and infarct size measured morphometrically or with creatine kinase depletion [41]. Similar findings with ^{11}C-palmitate have been reported in patients with myocardial infarction, prior to the advent of thrombolysis [104]. The results achieved with ^{11}C-palmitate in these situations of chronic coronary occlusion may reflect myocardial blood flow and hence delivery of tracer. Hence this study was undertaken to assess the accuracy of tomographic estimates of infarct size using ^{11}C-acetate in a reperfusion model of myocardial infarction, comparing ^{11}C-acetate with previously validated ^{11}C-palmitate. Coronary reperfusion following a prolonged period of coronary occlusion may lead to improved myocardial blood flow in the previously ischaemic region [45], although flow may be limited by the "no reflow" phenomenon [105]. Hence uptake of radionuclide in this model may reflect viability rather than delivery of tracer. A four hour period of coronary occlusion was chosen in this study,

as a period of 3 hours followed by reperfusion is documented to cause significant myocardial infarction in a canine model [106].

Methods. Seven mongrel dogs were instrumented with aortic, left atrial and inferior vena cava catheters as described earlier, following anaesthesia with thiopental and α-chloralose. A coronary angioplasty guiding catheter was introduced via the left carotid artery and a 3.7 mm coronary angioplasty balloon placed in the mid left anterior descending artery (LAD) under fluoroscopic control following lignocaine 80 mg and heparin 5000 units intravenously.

Experimental Procedure. The LAD was occluded by inflation of the balloon to 10 atmospheres for a period of 4 hours. Animals were anticoagulated throughout the procedure with heparin 1000 units as a bolus every hour. Ten minutes prior to balloon deflation and anticipated coronary reperfusion, regional myocardial blood flow was measured with radiolabelled microspheres, as described earlier. The region of myocardial ischaemia was not demonstrated tomographically with $[^{15}O]H_2O$ prior to reperfusion. At 4 hours the balloon was slowly deflated over a period of 5 minutes to allow gradual reperfusion of the LAD and then withdrawn from the coronary artery. The animal was then allowed to recover from anaesthesia. The following day the animal was re-anaesthetized after fasting and re-instrumented with aortic, left atrial and inferior vena cava catheters as described above. Persisting coronary reperfusion was then confirmed with radiolabelled microspheres and both a $[^{15}O]CO$ and $[^{15}O]H_2O$ study performed approximately 18 to 24 hours after coronary reperfusion. Studies with both ^{11}C-acetate and ^{11}C-palmitate were then performed in random order, with an interval of at least 100 minutes between administration of either to allow for decay of previously injected tracer. This interval allowed decay of 95% of previously injected tracer. Approximately 0.8 mCi's/kg of each tracer were injected and serial tomograms performed, as described below. Dogs remained in a Plexiglas shell within the tomograph and hence identical left ventricular wall regions could be compared between ^{11}C-acetate and ^{11}C-palmitate studies.

PET Analysis. $[^{15}O]CO$ and $[^{15}O]H_2O$ studies were performed as described in Chapter 4. ^{11}C-acetate and ^{11}C-palmitate studies were then performed in random

order. Each tomographic image was acquired over 60 seconds for ^{11}C-acetate and over 120 seconds for ^{11}C-palmitate, to a total of 20 images for each radionuclide. Early images were then reviewed, and the earliest image with the highest intra-mural left ventricular uptake of radionuclide was chosen for analysis. The tomographic image selected following ^{11}C-acetate was usually at 2-3 minutes, while following ^{11}C-palmitate was usually at 2-4 minutes. Radiation due to ^{11}C radionuclide in the left ventricular cavity and blood pool within the myocardium (due to blood in the myocardial vasculature) was then subtracted from the tomographic image by subtracting the [^{15}O]CO tomographic image. Hence the subtracted tomographic image then identified extracted ^{11}C radionuclide within the myocardium. The inner left ventricular boundary was identified using the ^{15}O-carbon monoxide tomographic image of the left ventricular cavity. In particular the boundary was drawn by trackball where counts per voxel were reduced to 50% of peak counts per voxel in the left ventricular blood pool. The outer left ventricular boundary was drawn in a similar way using the transmission image obtained from the attenuation tomographic image. The anticipated boundaries of the left ventricle were then superimposed on each tomographic slice for both the ^{11}C-acetate and ^{11}C-palmitate scan, and the boundaries standardized for both radionuclide scans. Voxels containing 50-100% of peak counts were identified in the region of interest, and the mean count per voxel calculated. A range of 50-100% was chosen to indicate non infarcted myocardium, as previously described [41]. Total counts expected in the left ventricular region of interest were those expected without myocardial infarction. This assumes that the uptake of ^{11}C-radionuclide is homogeneous within the left ventricular wall. Total expected counts were then calculated from the number of voxels in the left ventricular wall and the mean count per voxel of non infarcted myocardium. Infarct size was then calculated from the actual number of counts in the left ventricular wall compared to the expected counts, had there not been a myocardial infarction (as shown below).

$$\text{infarct size} = 1 - (\text{counts}_{\text{expected}} - \text{counts}_{\text{actual}}) / \text{counts}_{\text{expected}}$$

where $\text{counts}_{\text{expected}}$ = total counts in the left ventricular wall expected without myocardial infarction

$counts_{actual}$ = total measured counts in the left ventricular wall

Post-mortem Analysis. Animals were sacrificed following the last PET scan, and the heart removed. Initially the left anterior descending artery was opened and examined for evidence of residual thrombus associated with the coronary angioplasty site. The right ventricle, right atrium and left atrium were then dissected off the left ventricle, and the left ventricle cut into a series of short axis slices from apex to base of left ventricle. Each slice was approximately 10 mm in thickness. Each slice was incubated in triphenyl tetrazolium chloride (TTC, 5% in buffered phosphate saline) for 20 minutes for determination of infarct size. The outline of the infarct zone on either side of each slice was traced onto clear plastic overlays. The area was subsequently planimetered enabling the area of the non infarct zone and the infarct zone to be calculated. Each slice of left ventricle was then weighed, and the weight of the infarcted region calculated from the product of the percentage of each slice infarcted by planimetry and the weight of each slice. Total infarct size was then calculated from the sum of all left ventricular slices. Following this the infarcted and non infarcted zones in each slice were divided, and regional myocardial blood flow measured for each zone.

Results.

A total of seven dogs were studied, however one died before the second metabolic study and was excluded from analysis. Hence data for a total of six paired comparisons between ^{11}C-acetate and ^{11}C-palmitate are summarized.

Haemodynamic and flow data. Heart rate and systolic blood pressure were stable during the period of ^{11}C-acetate and ^{11}C-palmitate scans (heart rate 164 ± 5 vs 159 ± 5 bpm respectively, p = ns; systolic blood pressure 180 ± 23 vs 174 ± 18 mm Hg respectively, p = ns). Myocardial blood flow measured with microspheres during LAD occlusion was 1.2 ± 0.2 ml/gm/min in the non-ischaemic zone and was 0.07 ± 0.4 ml/gm/min in the ischaemic zone 4 hours after LAD occlusion, a reduction of flow of 99%. Myocardial blood flow in the non-ischaemic zone measured approximately 24 hours later showed a modest increase to 1.8 ± 0.9 ml/gm/min, of marginal statistical significance (p = 0.05). Myocardial blood flow in the ischaemic zone following

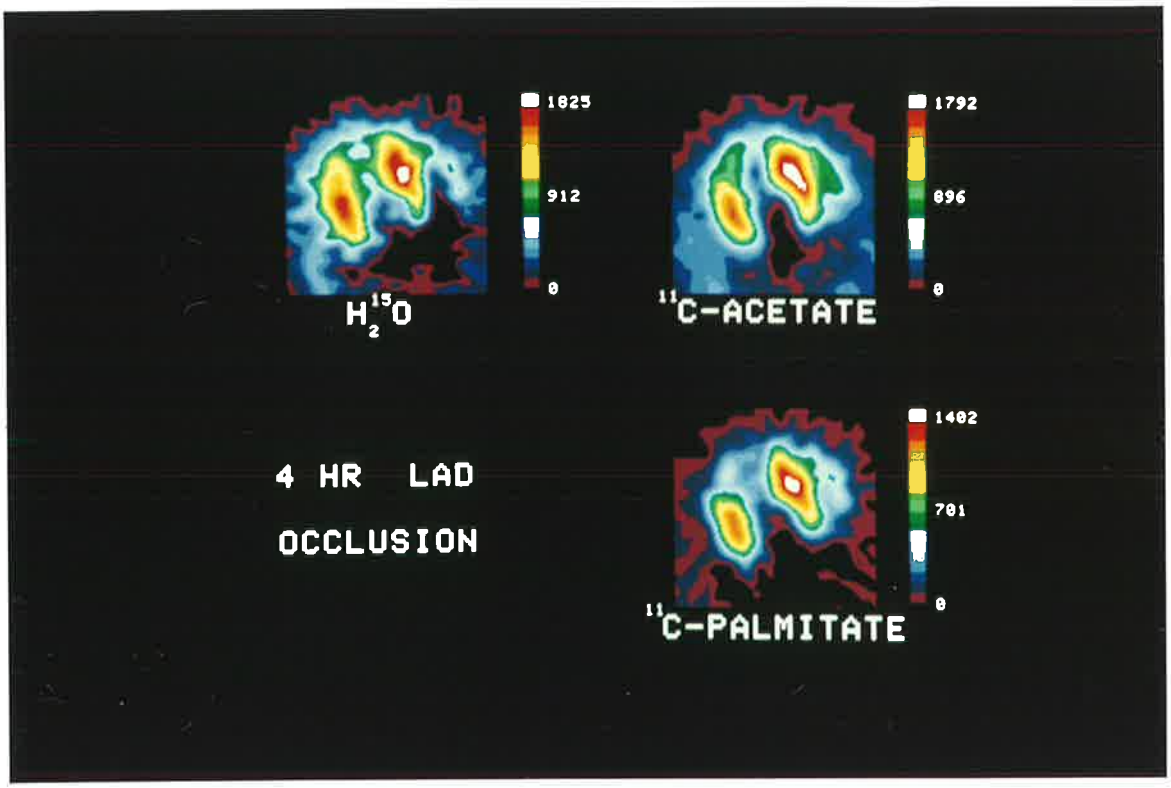

Figure 7.1 A representative subtracted [^{15}O]H_2O,^{11}C-acetate and ^{11}C-palmitate mid-ventricular tomographic image is shown during coronary reperfusion following 4 hours of occlusion of the left anterior descending artery. Myocardial blood flow in the reperfused anterior region was reduced compared to non ischaemic regions despite coronary patency (upper left). Uptake of both ^{11}C-acetate and ^{11}C-palmitate was reduced or absent in the reperfused region consistent with myocardial infarction. However uptake of ^{11}C-acetate was greater, when compared to ^{11}C-palmitate, in peri-infarct regions. Images selected were those with the highest intra-mural left ventricular uptake of radionuclide (see text for discussion).

reperfusion increased significantly from a very low level to 0.5 ± 0.3 ml/gm/min ($p < 0.05$).

Arterial substrate concentration. Concentrations of cardiac substrates, which could potentially influence the extraction of either ^{11}C-acetate or ^{11}C-palmitate, were measured in arterial blood at the onset of each scan (Table 7.1). Glucose levels were marginally lower, and free fatty acids marginally higher than canine studies reported in earlier Chapters. Lactate levels were also lower, consistent with an inverse relationship found between free fatty acid and lactate levels [107]. These minor differences may have been caused by two periods of fasting over sequential days, since fasting raises plasma free fatty acid concentrations. However no significant differences in substrate concentrations were present between ^{11}C-acetate and ^{11}C-palmitate scans, as shown below.

Table 7.1 Arterial substrate concentrations immediately before each PET scan. No significant differences were present.

	^{11}C-acetate	^{11}C-palmitate
glucose (mM)	4.4 ± 0.9	4.9 ± 1.4
FFA (μM)	790 ± 50	690 ± 130
lactate (mM)	1.0 ± 0.1	0.8 ± 0.1
acetate (μM)	100 ± 25	100 ± 15

Infarct Size. Visual inspection of the TTC stained area in each slice showed infarct zones to be largely transmural in 3 hearts, and non transmural in 3 hearts. Infarct size assessed with TTC ranged from 5.8% to 37.4% of the left ventricle, with a mean of 16.3 ± 10.8%.

Representative examples of tomographic images with ^{11}C-acetate and ^{11}C-palmitate during reperfusion are shown in Figure 7.1. Infarct size assessed tomographically with ^{11}C-acetate was 16.8 ± 8.2% of the left ventricle, while ^{11}C-palmitate was 20.5 ± 10.8%. No significant difference in infarct size was present between TTC measured infarct size and either ^{11}C-acetate or ^{11}C-palmitate assessed infarct size, however a difference between ^{11}C-acetate and ^{11}C-palmitate infarct size was found (paired t testing, $p = 0.02$). Infarct size assessed with ^{11}C-palmitate resulted

in a mildly greater estimate of infarct size than ^{11}C-acetate, and visually the difference in part was due to reduced uptake of ^{11}C-palmitate at the "border zone" of the infarct compared to ^{11}C-acetate.

Regression analysis between TTC and ^{11}C-acetate infarct size showed a very good correlation ($r = 0.92$, $p < 0.01$), as did the regression analysis between TTC and ^{11}C-palmitate infarct size ($r = 0.96$, $p < 0.01$). Both regression relationships are shown in Figure 7.2 on the following page.

An alternative method to calculate infarct size from tomographic images was also used, based on the area (number of voxels) of the tomographically defined infarct zone compared to the area (number of voxels) in the entire left ventricular region of interest. This method exaggerated the tomographic assessment of infarct size, a mean (± SD) of 27.9 ± 8.8% for ^{11}C-acetate and 32.4 ± 6.7% for ^{11}C-palmitate, since it assumed that left ventricular wall infarction was complete across the entire left ventricular wall. In practice, this was not usually the case since the subepicardium was frequently spared.

Discussion.

Tomographic estimates of infarct size using ^{11}C-acetate have shown a close correlation with TTC assessment of infarct size, although inspection of the regression equation shows the size of small infarcts is over-estimated with this technique. Similar estimates using ^{11}C-palmitate also show a close correlation, however the size of infarcts is further over-estimated. The significantly greater infarct size seen with ^{11}C-palmitate may be due to a reduction in uptake due to persistently ischaemic myocardium, or to a reduction in uptake in viable but metabolically impaired myocardium after reperfusion. Uptake of fatty acids, and hence ^{11}C-palmitate, is thought to be carrier mediated [34] and potentially ischaemia may impair uptake. Additionally fatty acid oxidation, in particular beta oxidation, is known to be sensitive to ischaemia [102]. Myocardial uptake of ^{11}C-palmitate following 3 hours of coronary occlusion has previously been reported to be depressed in the reperfused region, with a progressive increase in uptake of ^{11}C-palmitate described with serial studies over a 4 week period [45]. Increased uptake of ^{11}C-palmitate over time is consistent with the concept that metabolically injured but

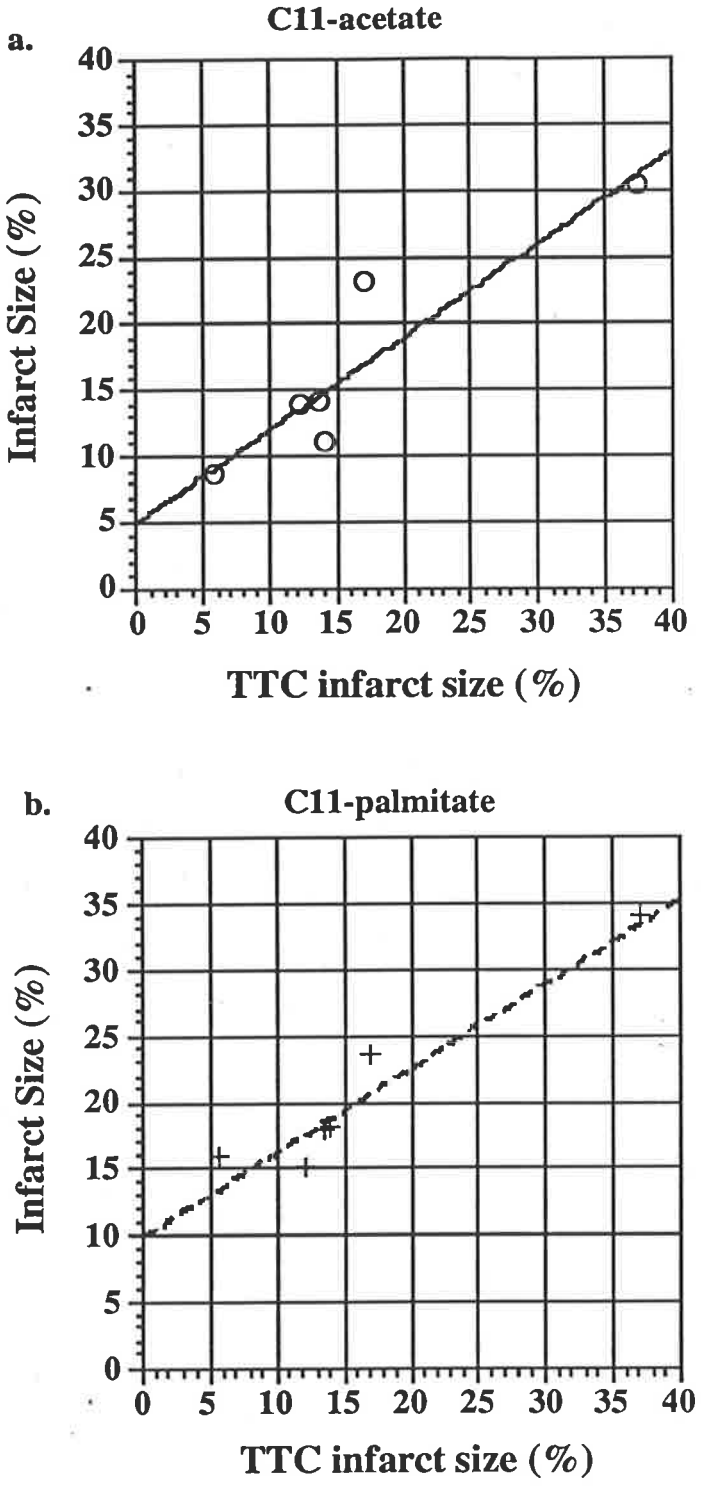

Figure 7.2 Regression relationships are shown **(a)** between TTC infarct size and ^{11}C-acetate ($y = 0.70\ x + 5.05$, $R = 0.92$) and **(b)** between TTC infarct size and ^{11}C-palmitate ($y = 0.63\ x + 9.96$, $r = 0.96$) as described in the text. Data are not superimposed due to overlap.

viable myocardium may demonstrate diminished uptake of ^{11}C-palmitate initially. Alternatively, partial volume effects in thinned left ventricular wall may lead to reduced recovery of counts leading to the impression of reduced uptake of radionuclide. Subsequent normalization of left ventricular wall thickness could potentially lead to apparant increased uptake of radionuclide in the reperfused region.

The method used to analyse tomographic images and assess infarct size is similar to previous reports [41,106], although modified in part. Essentially counts in the left ventricular wall of each tomographic slice were measured, and the counts in this region compared to the expected counts without infarction. Expected counts were derived from the product of counts per voxel in non infarct zones and the number of voxels in the left ventricular wall of each tomographic slice. This assumes homogeneous distribution of tracer throughout the myocardium, and although PET scans were not performed prior to coronary occlusion to demonstrate homogenous uptake of tracer, previous experience has not demonstrated heterogeneity of uptake of either ^{11}C-acetate or ^{11}C-palmitate. The method used has the advantage that "islands" of viable myocardium, which may be present in the infarct zone or viable tissue in the subepicardium, do not contribute to the calculation of infarct size. This may occur if a "boundary" technique is used, where the number of voxels in the infarct zone (as defined tomographically) is compared to the number of voxels outside the infarct zone. This significantly overestimated infarct size, as demonstrated in this study.

Uptake of ^{11}C-acetate has also been reported in a closed chest canine model over a 4 week period following a 3 hour period of coronary occlusion prior to reperfusion [108]. Uptake of both ^{11}C-acetate and ^{13}N labeled ammonia (a tracer of myocardial blood flow) early after reperfusion in reversibly injured myocardium were reduced compared to normal myocardium. This reduction occured despite near normal myocardial blood flow measured with radiolabelled microspheres, when uptake of ^{13}N labeled ammonia would be expected to be normal. Reduced uptake of ^{11}C-acetate and ^{13}N labeled ammonia were possibly due to partial volume effects associated with initial thinning of the left ventricular wall in the reperfused region, as described above.

It is not possible to assess the extent that partial volume effects in the reperfused region may have contributed to impaired uptake of either ^{11}C-acetate or ^{11}C-palmitate in this study. However infarct size measured tomographically with either tracer was closely correlated with infact size measured by TTC. Mean infarct size with TTC was approximately 16% and a very similar result was obtained with tomographic estimates using ^{11}C-acetate.

This latter finding suggests that ^{11}C-acetate is not taken up by non viable myocardium in this reperfusion model of myocardial infarction. Hence tomographic images of ^{11}C-acetate soon after administration in patients following myocardial infarction, particularly when treated with a thrombolytic agent, may indicate viable myocardium. Further delineation of the metabolic activity of reversibly injured myocardium may potentially then be obtained from examining the clearance rates of ^{11}C-acetate from involved regions, and this concept is examined in Chapter 8.

Chapter 8

Long term recovery of oxidative metabolism and contractility after 1 hour of coronary occlusion.

Coronary reperfusion after prolonged coronary occlusion results in diminution of infarct size, both in experimental models and patients with acute myocardial infarction. Recovery of contractility in the ischaemic zone results from salvage of myocardium, although recovery is delayed leading to dissociation between viability and function. This process has lead to the concept of "stunned" myocardium, discussed in Chapter 1 and Chapter 6. A number of diverse aetiologies have been suggested to explain the pathophysiology of myocardial stunning [105,109], including depletion of high energy phosphates and their precursers, myocardial calcium overload leading to dysfunction of mitochondria or sarcoplasmic reticulum, inefficient use of high energy phosphates for contraction or use of high energy phosphates for repair of cellular mechanisms damaged during ischaemia.

Acute recovery of myocardial contractility in perfused rat hearts following global ischaemia requires restoration of oxidative metabolism [110]. Consistent with these results is the finding that anaerobic metabolism in reperfused myocardium contributes only a minor proportion to total energy requirements [5]. However the pathophysiology of the long term recovery of stunned myocardium is unclear. Since recovery of oxidative metabolism predicates recovery of contractility in the short term [110], this may also predict long term recovery after a more severe ischaemic insult.

The aim of this study was to evaluate the rate of recovery of oxidative metabolism compared to the rate of recovery of contractile function over a four week period, following a severe ischaemic insult. Oxidative metabolism was assessed with ^{11}C-acetate and contractility with echocardiography. This relationship was examined in a canine model with LAD occlusion for one hour, a time chosen to achieve maximal metabolic insult with minor associated infarction, and associated with a prolonged duration of functional recovery.

Methods.

Fourteen mongrel dogs weighing 22 to 31 kg were instrumented with a pneumatic occluder and Doppler flow probe, placed on the left anterior descending artery (LAD) distal to the first diagonal artery. Under sterile conditions the chest was opened via a right thoracotomy and the heart suspended in a pericardial cradle. Considerable care was taken to avoid other than transient occlusion of the LAD during placement and testing of the pneumatic occluder. The pericardium was closed, and both pneumatic occluder and connections to the Doppler probe externalized at the back of the animal. Burial in a subcutaneous pouch allowed for subsequent access. The chest was closed and air evacuated. All dogs received intramuscular Combiotic for 3 days followed by oral lincomycin for a further 3 days. Eleven dogs were allowed to convalesce for 5 to 7 days prior to planned investigation, while 3 dogs were studied immediately after closure of the chest. Dogs were premedicated with morphine and anaesthetized with thiopental and α-chloralose as described earlier. After an overnight fast, catheters were placed in the ascending aorta, inferior vena cava and left atrium or ventricle for injection of microspheres. This approach for administration of microspheres was adopted after experience with the placement of a left atrial catheter during surgery in 3 dogs during a preliminary study. Death in all three was considered to be secondary to thrombi on the left atrial catheter. Dogs were similarly reinstrumented the day following coronary occlusion, and with ascending aortic and inferior vena catheters only for PET studies following this.

Experimental Protocol. Baseline two dimensional (2D) echocardiographic images were recorded prior to coronary occlusion, and patency of the LAD confirmed with the Doppler flow probe. Baseline regional myocardial blood flow was measured with radiolabelled microspheres, as described earlier. All dogs received heparin 10,000 units and lignocaine 3 mg/kg bolus IV followed by 1 mg/min infusion prior to LAD occlusion. The LAD was then occluded by inflating the pneumatic occluder for a period of 60 minutes, and occlusion confirmed with the Doppler flow probe. Reperfusion was achieved by slow deflation over 5 minutes, and restitution of coronary flow confirmed by Doppler.

During LAD occlusion the "area at risk" was identified by a $[^{15}O]H_2O$ scan (as described in Chapter 5) five minutes prior to reperfusion, and regional blood flow assessed with radiolabelled microspheres. Fifty minutes after reperfusion the $[^{15}O]H_2O$ scan was repeated to determine the effect of coronary reperfusion on regional blood flow, and flow was again assessed with radiolabelled microspheres. A ^{11}C-acetate scan (0.8-0.9 mCi/kg) was then performed after decay of the previously injected tracer. Immediately following completion of the PET protocol, 2D echocardiography was repeated. Subsequent PET and 2D echocardiography studies were repeated at 1 to 2 days, 7 and 28 days following coronary occlusion. Prior to each study the Doppler probe was exteriorized and patency of the LAD confirmed. Administration of radiolabelled microspheres was repeated at the 1 to 2 day study only.

Positron Emission Tomography. PET scanning in PETT VI was performed in the routine manner, as described earlier. The chest wall was marked during the first PET study and a low powered laser used to reposition the animal at the same level within the tomographic unit on subsequent studies. Each PET study consisted of serial $[^{15}O]CO$, $[^{15}O]H_2O$ and ^{11}C-acetate scans.

Analysis of tomographic data commenced with the selection of a left ventricular tomographic slice containing a hypoperfused region in the anterior wall during LAD occlusion, as assessed from the subtracted $[^{15}O]H_2O$ scan. This region was outlined with a trackball, and the outline used to guide placement of the same region of interest in subsequent tomographic studies. This region of interest was regarded as the "reperfused" region. Nine regions of interest were placed on the left ventricular wall imaged during the ^{11}C-acetate study. Six were placed on normal myocardium, three on the lateral wall and three on the septal wall, and a further three placed on the anterior wall in the reperfused region. A further region of interest was also assigned to the centre of the left ventricular cavity to assess activity of tracer in arterial blood. Counts from each region were decay corrected, and corrected for partial volume and spillover effects as described in Appendix A.

Echocardiographic Analysis. 2D echocardiography was performed using a Hewlett Packard echocardiographic unit and a 64 channel phased array transducer operating at

3.5 MHz. Short axis views of the left ventricle were obtained with dogs on their right side, and the transducer applied to the chest wall from below. Images were all of high quality and were recorded on a Panasonic NV8200 video recorder. Subsequently images were analyzed off line using a Microsonics Dataview System (Indianapolis, Ind.). Short axis views at the mid papillary level were used to define regional contractility. Regional wall motion was initially measured quantitatively using 64 radial chords drawn from the centre of the left ventricle, using the Dataview system [111]. However reproducible results could not be achieved in consecutive sinus beats or on repeat analyses of the same beat. Accordingly a semi quantitative, conventional echocardiographic assessment was performed using two observers blinded to the timing of the echocardiogram and to the results of PET studies. Regional motion for each wall (anterior, septal, posterior and lateral) was graded on a 0 to 4 scale. Hyperkinesis = 0, normal contractility = 1, hypokinesis = 2, akinesis = 3 and dyskinesis = 4. An overall average regional wall motion score was obtained for each echocardiogram. Repeated evaluations of the same images by the same observer at different times yielded measurements that differed by less than 0.2 units.

Morphologic Examination. Animals were sacrificed at the completion of the 4 week study. A left ventricular catheter was inserted into the left ventricle. The pneumatic occluder was inflated and occlusion confirmed with the Doppler probe. Lissamine green (75 ml of 1% solution) was injected into the left ventricle and 1 minute later a lethal dose of saturated potassium chloride administered. The heart was removed, and sectioned into 1 cm slices. The area at risk, as defined by negative lissamine green staining, was planimetered. Each slice was then incubated in TTC as described earlier for determination of infarct size. In three studies a mid ventricular section of 3-4 mm was examined histologically for evidence of myocardial necrosis. Two left ventricular slices, one at mid-papillary level and a more apical slice, were each sectioned into 16 equal segments. Each segment was then divided into endocardial and epicardial samples, and regional blood flow from microspheres calculated.

Results.

Six of the 14 dogs initially instrumented died during the subsequent course; one during the convalescent phase and five either after coronary occlusion or immediately on reperfusion. Two dogs were found to have baseline LAD occlusion associated with regional wall motion abnormalities by echocardiography and were excluded. Six dogs were studied to 4 weeks following one hour of LAD occlusion.

Haemodynamic and Myocardial Flow Data. Haemodynamic data during each ^{11}C-acetate scan are shown in Table 8.1. No significant change in heart rate, systolic blood pressure or rate pressure product was found over the period of follow up. Heart rate during LAD occlusion was a mean of 89 ± 11 bpm and systolic blood pressure was 150 ± 13 mm Hg.

Table 8.1 Haemodynamic data during each ^{11}C-acetate scan on each of the study days, commencing after coronary reperfusion (day 0). HR = heart rate (bpm), SBP = systolic blood pressure (mm Hg), RPP = rate pressure product .

Study	HR	SBP	RPP
day 0	91 ± 14	157 ± 13	14900 ± 3130
day 1-2	89 ± 9	166 ± 13	15180 ± 2610
day 7	88 ± 7	168 ± 11	14880 ± 1721
day 28	67 ± 14	152 ± 12	10640 ± 3115

Coronary flow was measured by Doppler (qualitatively) and radiolabelled microspheres. Coronary occlusion was confirmed acutely by Doppler in all cases, and monitored over the one hour period. Regional blood flow by microspheres in the ischaemic/reperfused zone was corrected for apparent microsphere loss by comparison of myocardial flow in the normal and subsequently ischaemic zone prior to LAD occlusion [112]. Apparent microsphere loss was 16 ± 4% in the subendocardium and 2 ± 8% in the subepicardium. Following LAD occlusion a 71 ± 10% reduction of flow occurred in the subendocardium, compared to a 44 ± 12% reduction in subepicardial flow (Table 8.2). Reperfusion was accomplished by gradual deflation of the pneumatic occluder over 5 minutes, attenuating the hyperaemic response. Coronary flow, assessed

by Doppler, was re-established in all cases. At fifty minutes following reperfusion, myocardial blood flow in the normal and reperfused regions were very similar (p = ns) with no evidence of the "no reflow" phenomenon. Repeated myocardial blood flow measurements at 1-2 days showed blood flow in both normal and reperfused regions similar to baseline.

Table 8.2 Myocardial blood flow measured with radiolabelled microspheres is shown prior to LAD occlusion (baseline), during LAD occlusion (ischaemia) and 1 and 24 hours following coronary reperfusion, for both endocardium and epicardium in normal (N) and ischaemic/reperfused regions (I/R). Units are ml/gm/min. A significant reduction of subendocardial blood flow occurred during LAD occlusion.
(* $p < 0.05$).

		Myocardial Blood Flow	
Time	Region	Endocardium	Epicardium
Baseline	N	0.65 ± 0.17	0.53 ± 0.15
	I/R	0.65	0.53 ± 0.15
Ischaemia	N	0.85 ± 0.25	0.63 ± 0.22
	I/R	0.24 ± 0.08*	0.3 ± 0.07
Reperfusion 1 hr	N	0.66 ± 0.20	0.52 ± 0.19
	I/R	0.71 ± 0.17	0.51 ± 0.14
Reperfusion 24-48 hr	N	0.65 ± 0.27	0.53 ± 0.09
	I/R	0.63 ± 0.11	0.47 ± 0.08

Arterial concentrations of fatty acid, glucose, lactate or acetate during each ^{11}C-acetate scan did not change significantly between studies on different days, and hence data are presented as the mean (± SD) of all studies. Mean fatty acid concentrations were 407 ± 28 μM, glucose 5.3 ± 0.2 mM, lactate 1.4 ± 0.1 mM and acetate 119 ± 2 μM.

PET scans. A [^{15}O]H_2O image of myocardial blood flow during LAD occlusion demonstrated a variably sized defect in the anterior and anterolateral wall in all cases. (Figure 8.1). A repeat study after deflation of the balloon occluder demonstrated

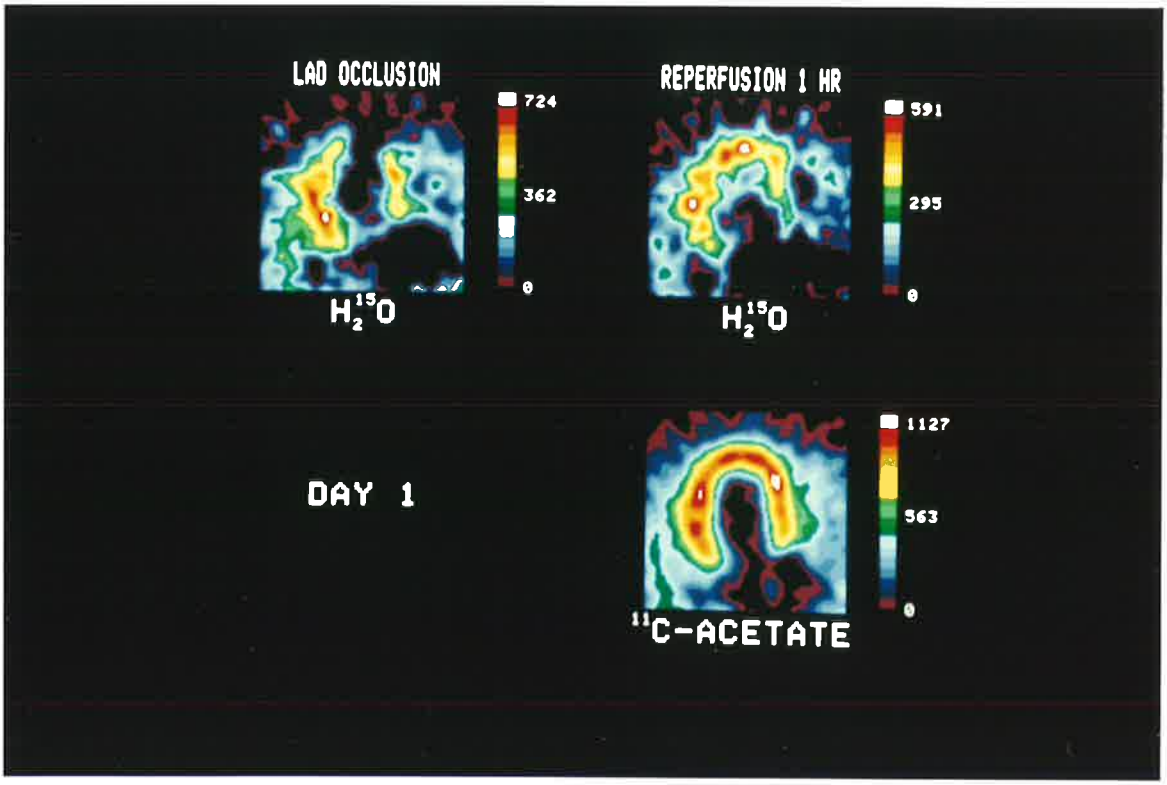

Figure 8.1 Representative examples of PET images are shown for one canine study during LAD occlusion and one hour following coronary reperfusion. A subtracted $[^{15}O]H_2O$ scan (upper left) during LAD occlusion demonstrates reduced perfusion of the anterior wall due to LAD occlusion. Perfusion recovers 50 minutes following LAD reperfusion (upper right). Subsequently a ^{11}C-acetate scan (2 to 4 minutes after IV administration of ^{11}C-acetate, lower right) shows near normal uptake of ^{11}C-acetate in the previously ischaemic anterior wall.

resolution of the defect indicating restitution of myocardial flow, as confirmed with radiolabelled microspheres. Serial [^{15}O]H_2O studies over the course of 4 weeks showed no defect in the previously ischaemic anterior wall. In this analysis, [^{15}O]H_2O scans were used qualitatively rather than quantitatively.

The first ^{11}C-acetate study one hour after coronary reperfusion frequently showed a mild reduction in peak ^{11}C-acetate counts in the anterior wall in comparison to the lateral and septal walls, although this finding was variable (Figure 8.1). Reduction in peak ^{11}C-acetate counts was asociated with minor thinning of the anterior wall, which was not present on subsequent studies, and reduced counts were possibly due to partial volume effects. Studies from day one onwards showed normal peak ^{11}C-acetate concentration in the anterior wall compared to the lateral and septal walls.

Clearance of ^{11}C-radioactivity from normal and reperfused regions was generally biexponential over the 30 minute imaging period, although 4% of normal regions and 14% of reperfused regions could only be fitted with monoexponential solutions. Slow clearance, requiring monoexponential solutions, mostly occurred during the ^{11}C-acetate scan one hour following reperfusion. For biexponential solutions, the major phase accounted for 78 ± 1% of ^{11}C-radioactivity in normal regions and 76 ± 1% in reperfused regions (p = ns).

The half times of the major phase are summarized for lateral, anterior and septal walls at each study time in Figure 8.2. Half times were similar in lateral and septal walls, indicating relatively homogeneous oxidative metabolism. Mean half times were significantly higher in the reperfused region one hour after reperfusion compared to normal regions (10.4 ± 1.4 vs 7.0 ± 0.6 min respectively), indicating impaired oxidative metabolism. When expressed in terms of the original rate constants used to derive these half times, this was equivalent to a 22% reduction in clearance rates in the reperfused region. Derived oxygen consumption from these rate constants (as described in Chapter 6) indicated a 27% reduction in oxygen consumption. Clearance remained significantly impaired in the reperfused region at 1-2 days (half time 8.2 ± 1.05 vs 5.9 ± 0.4 min respectively, $p < 0.05$), equivalent to a 11% reduction in clearance rates. From

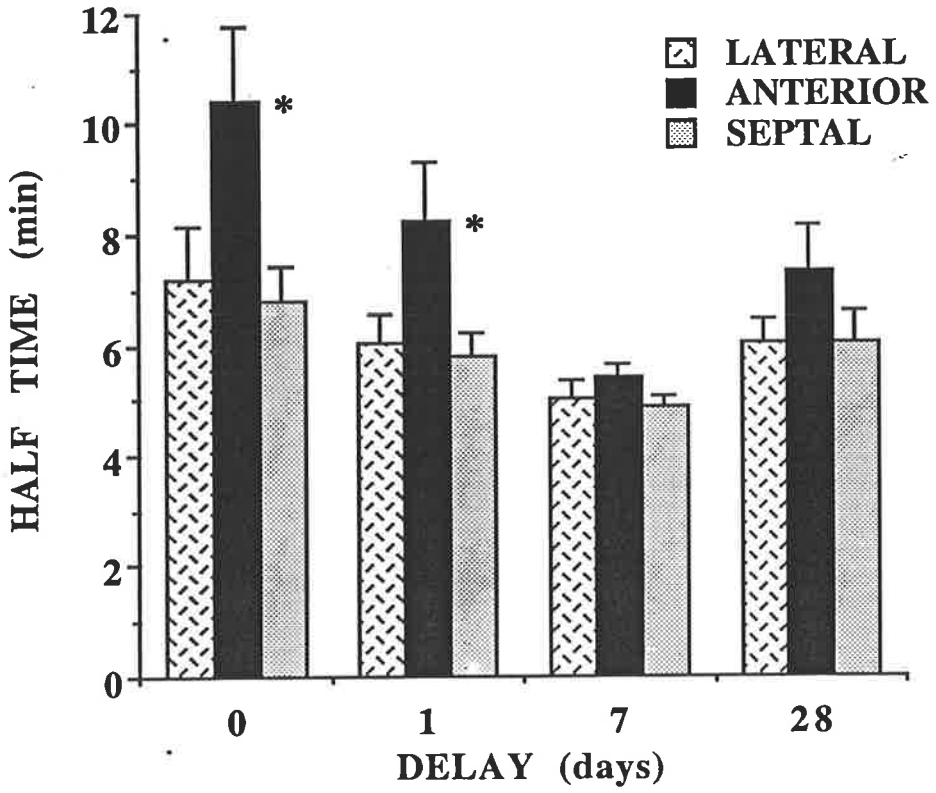

Figure 8.2 Half times for the rapid phase of clearance of ^{11}C-radioactivity from myocardium for non ischaemic regions (lateral and septal) and reperfused regions (anterior) on the day of coronary reperfusion and at 1,7 and 28 days thereafter. Half times for ischaemic regions are significantly greater than for non ischaemic regions on day 0 and 1 ($p < 0.001$).

day 7 onwards no significant difference was present between half times in normal and reperfused regions.

^{11}C-acetate rate constants in normal regions were also compared between different study days to determine if normal myocardium on days 0 and 1 following reperfusion demonstrated an increased metabolic rate to compensate for impaired contractility in the reperfused region. The mean rate constant for normal regions within each animal on study day 0 and 1 was highly correlated with the rate pressure product, as demonstrated in earlier validation studies. Similarly rate constants for normal regions on day 7 and 28 were significantly correlated with the rate pressure product. These particular days were grouped as recovery of contractility in reperfused regions was maximal by 7 days, persisting to 28 days (see below). No significant difference was present between the two regression lines by analysis of covariance, as shown on the following page (Figure 8.3).

Recovery of contractility.

All canine studies prior to coronary occlusion showed normal contractility, hence the wall motion score was 1. Wall motion one hour after reperfusion showed severe hypokinesis to akinesis in the anterior wall, while the mean wall motion score was 2.5 $\pm$ 0.7. Regional contractility improved at 1-2 days, with considerable improvement when compared to 1 hour results by 7 days. No further recovery in the wall motion score occurred by 28 days, as shown in Figure 8.4.

Area at Risk. The area at risk distal to the LAD balloon occluder, identified by the absence of lissamine green, was 12 $\pm$ 6% of the left ventricle. No macroscopic findings of myocardial infarction were present in the anterior wall distal to the site of LAD occlusion, and no negative staining with triphenyl tetrazolium chloride was present. Transverse sections were examined histologically in the last 3 dogs. Only scattered sites of micro infarction were present, immediately beneath the endocardium. However a major proportion of the myocardial wall appeared abnormal, ranging from 30 to 70% of the thickness of the anterior wall, with increased interstitial spaces and intercellular vascularization.

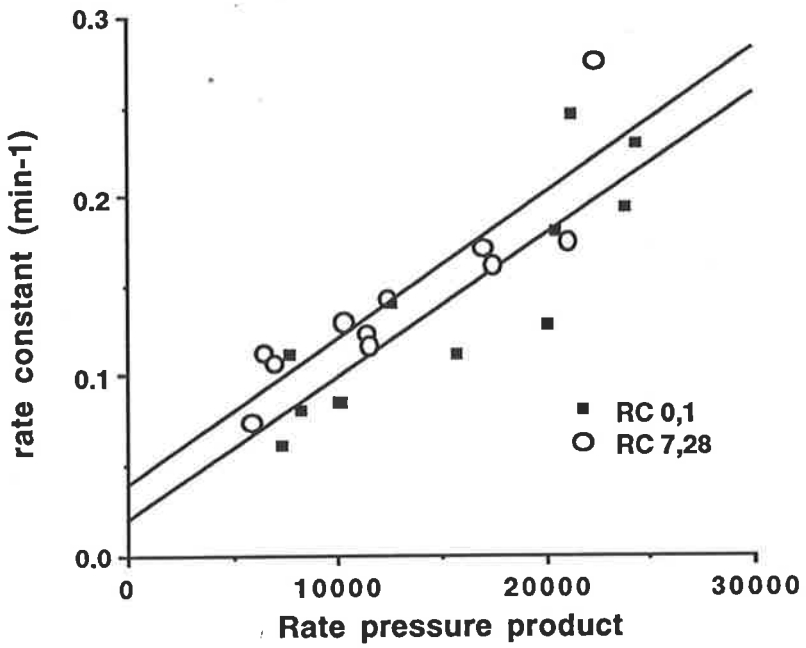

Figure 8.3 Regression relationships are shown between rate pressure product and the rate constant of the rapid phase of clearance of ^{11}C radioactivity in normal myocardium on day 0 or 1 (solid squares, lower regression line, r = 0.87) and days 7 or 28 (open circles, upper regression line, r = 0.89). No significant difference was present between regression lines, either for slope or elevation.

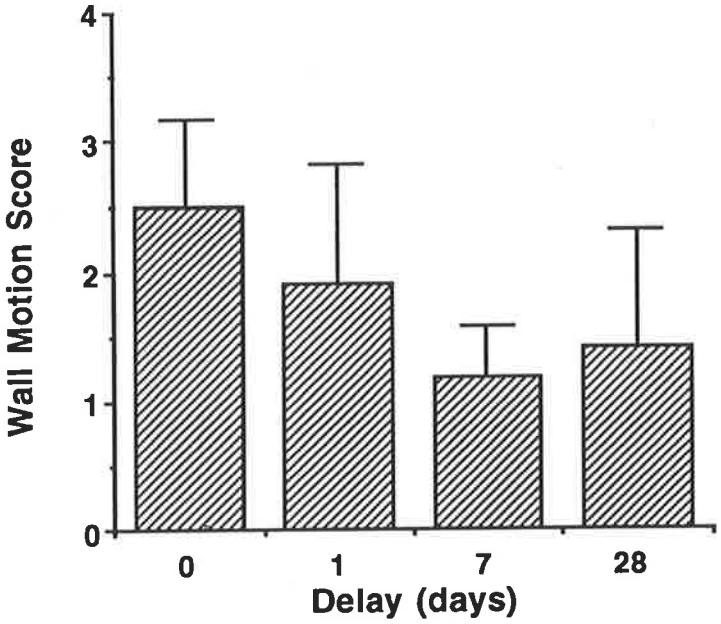

Figure 8.4 The overall wall motion score (as described in Methods) improved over 7 days following coronary reperfusion, with maximal recovery at that time. Normal contractility gave a score of 1.

Discussion.

A reduction of ^{11}C-acetate clearance rates of 27% was seen acutely in myocardium reperfused after 1 hour of coronary occlusion in this model of myocardial ischaemia, when compared to normal myocardium. A 69% reduction was seen in similar canine studies reported in Chapter 6 after the same duration of ischaemia. The greater reduction in earlier studies reflects both higher oxygen utilization in normal myocardium due to increased work load and lower oxygen utilization in reperfused myocardium. Work load, as measured by the rate pressure product, was greater (a mean of 17400 compared to 14900 in this current series) leading to higher ^{11}C-acetate clearance rates in normal myocardium. Hence comparison of absolute ^{11}C-acetate clearance rates, or half times, in reperfused myocardium is more appropriate in these circumstances. A mean half time of 11.4 minutes in reperfused regions in the current study compares to a mean of 13.5 minutes in those reported in Chapter 6, and may

reflect greater preservation of subendocardial and subepicardial blood flow during ischaemia as shown below.

	RPP	regional blood flow		$t_{1/2}$ ^{11}C-acetate
		subendo	subepi	
	(mm Hg*bpm)	(mls/gm/min)		(min)
1 hr LAD occlusion (Chapter 6)	17400	0.16	0.23	13.5
1 hr LAD occlusion (Chapter 8)	14900	0.24	0.30	11.4

Less severe ischaemia is likely to lead to greater recovery of myocardial metabolism following reperfusion. Hence oxidative metabolism in reperfused myocardium in the two series of experiments using different methods of coronary occlusion (coronary angioplasty balloon compared to a largely chronically instrumented model) is similar when the underlying pathophysiological processes are taken into account. Comparison of absolute clearance rates in reperfused myocardium is more appropriate than comparison of relative reductions compared to normal myocardium, since the latter varies widely with cardiac work.

Despite a mild reduction in oxidative metabolism in this study, regional wall motion in the reperfused region demonstrated a severe reduction in contractility consistent with the concept of stunned myocardium. A major improvement in oxidative metabolism had occurred by 1 to 2 days, and maximal recovery had occurred by 7 days which persisted to 28 days. Improved myocardial contractility occurred in parallel to the recovery of oxidative metabolism, with maximal recovery of the latter by 7 days which persisted to 28 days. Although these improvements occurred in parallel, a major recovery of contractility occurred for a minor recovery of oxidative metabolism as the degree of initial impairment of either was disparate. The period of coronary occlusion employed in this series resulted in almost complete recovery of contractility over the four week period, due to the small extent of myocardial infarction created. The látter was confirmed in post mortem analyses. This extent of recovery prevented any conclusion on whether a level of oxidative metabolism early after reperfusion existed to predict ultimate recovery. However these results in combination with a series of

dogs subjected to more prolonged ischaemia [56] have demonstrated that recovery of contractility is predicted and correlates with early recovery of oxidative metabolism. Certainly results from this current series indicate that substantial preservation of oxidative metabolism early after reperfusion predicts ultimate recovery of contractility.

Oxidative metabolism in normal myocardial regions was compared early and late following coronary reperfusion. No significant difference was found in ^{11}C-acetate clearance rate constants in normal myocardium when corrected for cardiac work. Potentially normal regions may show increased contractility to compensate for impaired contractility in the reperfused region. The latter was demonstrated by echocardiography in this series, but the semiquantitative method of assessing contractility used was not sufficiently sensitive to show minor variations in contractility of normal regions. A quantitative method is required to show these minor differences, however initial experience showed poor reproducibility as outlined under Methods. Previous reports have demonstrated variable responses in normal myocardium following coronary occlusion, either showing increased systolic shortening [113] or no change [114,115]. This variable response may reflect the distance of the normal region from the region of impaired contractility, with distant regions showing increased contractility compared to near regions [116]. Oxidative metabolism in normal regions in this study was measured adjacent to the reperfused zone, and possibly the lack of augmented oxidative metabolism found early after reperfusion may reflect the proximity to this hypokinetic region.

These data were first reported in abstract form in 1988 [117], and published in conjunction with a further series of canine experiments subjected to more severe ischaemia (as described above) in 1993 [56]. Similar studies examining the effect of prolonged coronary occlusion followed by reperfusion on regional contractility and oxidative metabolism with ^{11}C-acetate [108] were published in 1992. A 3 hour period of coronary occlusion was used, with follow-up over the following 4 weeks. Neither contractility nor oxidative metabolism returned to normal over this period. Recovery of contractility was more gradual after this more severe ischaemic insult, progressively increasing over the 4 week period. Similarly recovery of oxidative metabolism was

also gradual over the 4 week period, and paralleled the recovery in regional contractility.

Hence it is concluded that oxidative metabolism and contractility recover in parallel in stunned myocardium. Relatively preserved oxidative metabolism predicts late recovery of contractility, and this finding is encouraging for application to future patient studies.

Chapter 9

Initial Human Studies with ^{11}C-acetate.

Preliminary human studies from the Hammersmith Hospital were reported in abstract form in 1980 [50] and 1981[51,52], examining myocardial imaging with ^{11}C-acetate and PET in both normal volunteers and patients with coronary artery disease. These studies demonstrated that myocardium could be successfully imaged with ^{11}C-acetate and that clearance rates at rest were monoexponential, both in normal and ischaemic myocardium. Human studies with ^{11}C-acetate reported herein were the first performed at Washington University, and were undertaken to **a.** confirm the myocardial imaging qualities of ^{11}C-acetate, **b.** characterize the clearance rate constant (and half time) of ^{11}C-acetate in both normal volunteers and patients with acute myocardial infarction and **c.** estimate regional myocardial oxygen consumption based on the relationship between the clearance rate constant and myocardial oxygen consumption previously established in canine studies.

Methods.

Five normal volunteers were studied, ranging in age from 25 to 36 years with no known history of cardiac disease. Three patients with recent myocardial infarction were also studied, ranging in age from 43 to 51 years. The region of infarction was anterior in two and inferior in one, and all were q wave infarction on the electrocardiogram. None had undergone coronary artery bypass surgery or coronary angioplasty. The protocol was approved by the Human Studies Committee of the Washington University Review Board.

All PET studies were performed in Super PETT 1, a time of flight instrument. Patient positioning was enhanced by fabricating a polyurethane mould to stabilize the head, neck and upper torso. Seven tomographic slices were acquired simultaneously in high resolution mode with a full width at half maximum resolution of 13.5 mm. Initially a transmission image was obtained using an external source of germanium-68/gallium-68, and the correct position of the heart in the field of view verified. Subsequently [^{15}O]CO and [^{15}O]H_2O studies were performed to delineate qualitative regional myocardial blood flow, as described in Chapter 5. Ten minutes following the

$[^{15}O]H_2O$ scan, a bolus of ^{11}C-acetate (0.4 mCi/kg) was injected into an antecubital vein and PET data acquired for 30 minutes in list mode.

Tomographic images of $[^{15}O]H_2O$ (after subtraction of the $[^{15}O]CO$ scan) and ^{11}C-acetate were compared. A representative slice of the mid-ventricular region was selected in normals and a slice demonstrating the region of myocardial infarction selected in patients, as defined by the subtracted $[^{15}O]H_2O$ scan. In patients with myocardial infarction, regions were defined as **a.** remote: distant from the infarct region, **b.** peri-infarct: adjacent to the infarct region, but within normally perfused myocardium and **c.** infarct region. Regions of interest, approximately 1 cm^3, were placed circumferentially around the left ventricular wall of the ^{11}C-acetate slice to include remote, peri-infarct and infarct regions. A further region of interest was placed in the centre of the left ventricular cavity. Correction of myocardial counts for spillover from the left ventricular cavity was not performed due to the rapid clearance of ^{11}C-radioactivity from the left ventricular cavity. Myocardial residue time activity curves for each region of interest were then constructed over 30 minutes and mono-exponential solutions fitted to the data, as described in Chapter 4.

Estimated myocardial oxygen consumption was based on the previously established relationship between directly measured oxygen consumption and the clearance rate constant of the rapid phase of the myocardial residue time activity curve. A summary of data, reported separately in Chapters 4 and 5, show the following relationship

$$\text{rate constant} = 0.036 * MVO_2 + 0.021$$

from a total of 33 studies in 19 anaesthetized dogs. The correlation is r = 0.88. Units are rate constant, min^{-1}; MVO_2 , µmol/gm/min. Myocardial oxygen consumption was then calculated from the measured rate constant for each region in human studies, using this regression relationship.

Results.

Haemodynamic Data. Heart rate, systolic blood pressure and rate pressure product were 60 ± 10 beats min^{-1}, 117 ± 8 mm Hg and 6995 ± 1050 beats* mm Hg

min^{-1} respectively in normal volunteers and 112 ± 11, 105 ± 23 and 12360 ± 1650 in patients. Haemodynamics were stable throughout the ^{11}C-acetate scan in all studies.

PET Data. The decline in ^{11}C-radioactivity within the left ventricular cavity, following intravenous injection of ^{11}C-acetate, was rapid. PET derived counts per voxel fell to less than 10% of peak counts within 2 minutes of injection, and a typical example is shown in Figure 9.1 on the following page.

Analysis of myocardial residue time activity curves demonstrated that monoexponential solutions could only be fitted, although an attempt was made to fit biexponential solutions in all regions. Clearance half times for each of nine regions placed on the left ventricular wall in normal volunteers are summarized in Figure 9.2, demonstrating homogeneity of oxidative metabolism present at rest. No significant difference was seen between regions. The co-efficient of variation of half times between regions within each ^{11}C-acetate study ranged from 10.5 to 14.8%, with a mean of 12.4 ± 1.9%. The mean half time calculated from each of 9 regions was very similar to the mean half time calculated from a region of interest encompassing the entire left ventricular wall, 12.4 ± 1.9 minutes compared to 12.4 ± 2.0 minutes respectively (p = ns). This similarity and the homogeneity of clearance between each of the 9 regions indicates that calculation of half times from myocardial residue time activity curves is little effected by fluctuation in counts associated with small regions (approximately 1 cm^3).

Clearance half times in patients following myocardial infarction were influenced by the site of the region of interest in relation to the infarct zone. Clearance half times in regions remote to the infarct zone were a mean of 8.5 ± 0.75 minutes, while half times in peri-infarct regions were significantly increased at 12.9 ± 1.9 minutes ($p < 0.05$). Clearance half times were further increased in the infarct zone, although the degree was variable ranging from 15.7 minutes to 91.4 minutes. These data are summarized in Figure 9.3. Clearance from remote regions in post infarct patients was faster when compared to normal volunteers (mean half time 8.5 ± 0.75 vs 12.4 ± 2.0 minutes in normal volunteers) and was associated with a greater cardiac workload (when measured as the rate pressure product).

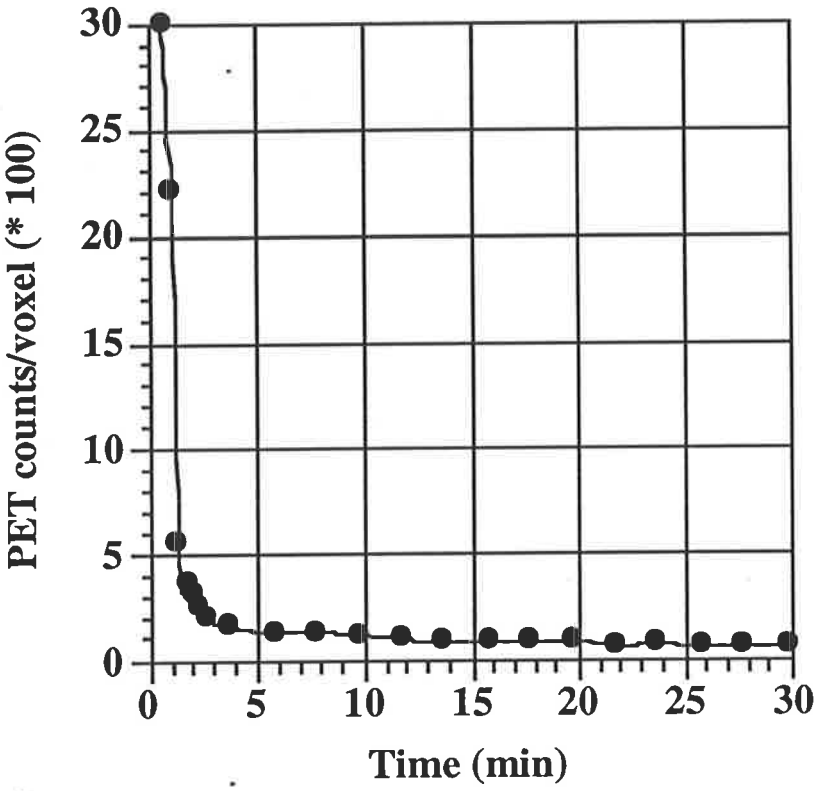

Figure 9.1 PET derived counts per voxel, measured in the centre of the left ventricular cavity, are shown over a period of 30 minutes following intravenous injection of ^{11}C-acetate. The decline in ^{11}C-radioactivity was always rapid, clearing to less than 10% of maximum counts within 2 minutes of injection of ^{11}C-acetate into a antecubital vein.

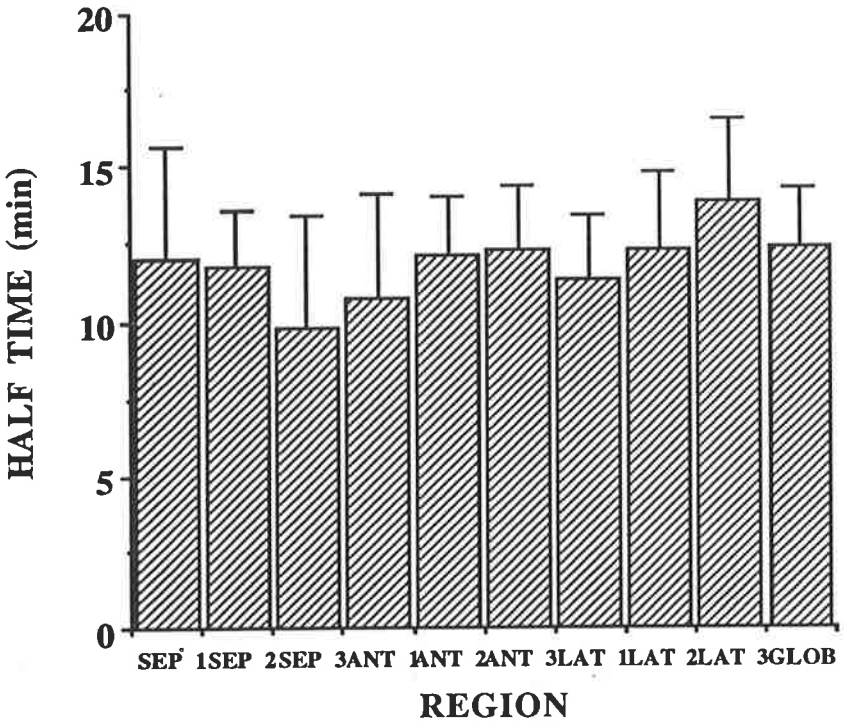

Figure 9.2 The half time of the rapid phase is shown for each of 9 regions of interest placed on the left ventricular myocardial wall, and a further large region of interest (shown as GLOB) encompassing the entire left ventricular wall. Region SEP 1 and LAT 3 are adjacent to the mitral valve. No significant differences are present between regions. Abbreviations SEP = septal, ANT = anterior, LAT = lateral and GLOB = global.

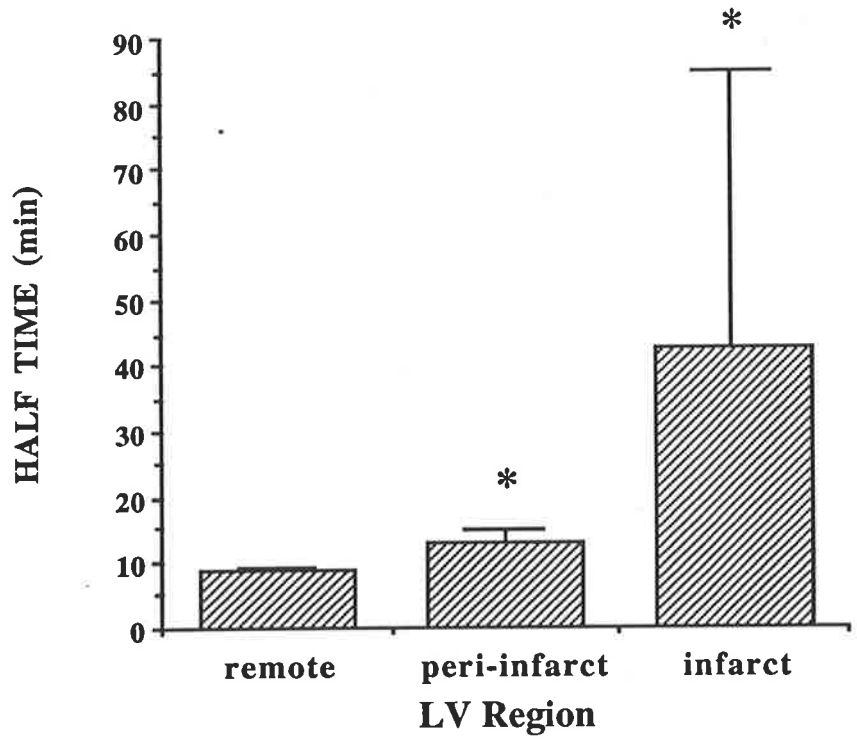

Figure 9.3 Half times are shown for remote, peri-infarct and infarct regions in 3 patients with myocardial infarction. Data are significantly different for peri-infarct and infarct regions compared to remote regions ($p < 0.05$), although in this small sample no significant difference was present between peri-infarct and infarct regions.

The clearance rate constant from normal myocardium in volunteers was significantly correlated with the rate pressure product measured during each study, as would have been anticipated from earlier canine studies although the number of individual volunteer studies was relatively few (shown in Figure 9.4).

Calculated myocardial oxygen consumption in normal volunteers at rest was 0.96 ± 0.23 μmol/gm/min. Calculated myocardial oxygen consumption in patients post myocardial infarction was significantly higher in remote regions (1.73 ± 0.20 μmol/gm/min) compared to peri-infarct regions (0.95 ± 0.24 μmol/gm/min, $p < 0.05$) and also significantly higher compared to infarct regions (0.54 ± 0.49 μmol/gm/min, $p < 0.05$).

Discussion.

Human studies at Washington University have confirmed the excellent myocardial imaging qualities of ^{11}C-acetate, initially reported in preliminary studies from the Hammersmith Hospital. Clearance of ^{11}C-radioactivity from the blood was rapid, and hence no spillover correction from left ventricular cavity to myocardium was made. Clearance from myocardium was monoexponential over a period of 30 minutes, as was seen in canine myocardium at low work loads (see Chapter 4). Possibly biexponential solutions could have been fitted to myocardial residue time activity curves if measured over a longer period, however low count rates over longer acquisition times would be a potential confounding factor due to background "noise". Clearance half times in normal volunteers (mean 12.4 minutes) reported in this series are slower than reported in initial pilot studies [51] involving 4 "healthy subjects" (mean 8.3 minutes). This disparity may be due to a different population of volunteers studied, for example older subjects may have higher heart rates and blood pressure than the relatively young population studied herein. Alternatively a short acquisition time over 12 minutes, utilized in preliminary studies [51], may have lead to errors in curve fitting. The latter is the more likely explanation, since more recent studies in normal volunteers (discussed below) are consistant with the results described herein.

Patients with recent myocardial infarction demonstrated more rapid clearance from myocardium remote to the infarct region, consistent with the higher rate-pressure

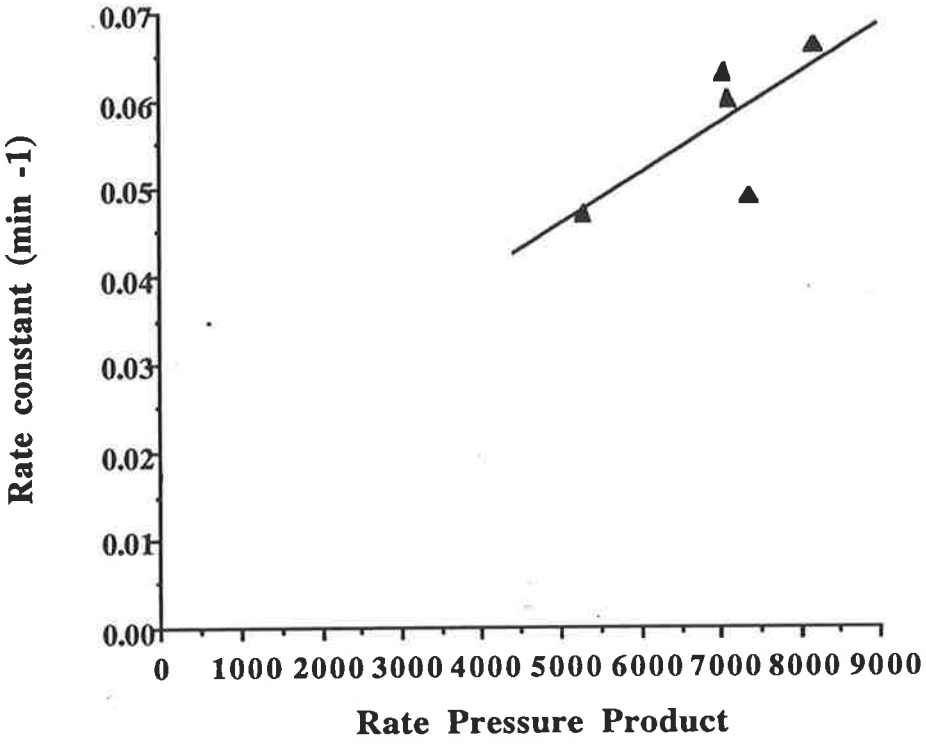

Figure 9.4 The correlation between the rate pressure product and the rate constant of the major phase is shown in 5 normal volunteers at rest ($r = 0.71$, $p < 0.05$). The regression relationship is $y = 5.75E\text{-}6\ x + 0.017$. Units for rate pressure product are mm Hg * bpm

product in these patients compared to normal volunteers. Clearance in the peri-infarct region was significantly impaired compared to remote regions. Potential explanations are inclusion of reversibly injured "islands" of myocardium in the peri-infarct region or alternatively myocardium was "tethered" in the peri-infarct region leading to a reduction in wall thickening and oxidative metabolism. Uptake of ^{11}C-acetate in the infarct region was impaired consistent with the development of irreversibly injured myocardium, as discussed in Chapter 7. Clearance rates from infarct regions were slow, although variable between patients, consistent with impaired oxidative metabolism in remaining viable myocardium.

Technical Considerations.

Myocardial oxygen consumption was calculated in this study based on a previously derived relationship between ^{11}C-acetate clearance rates and directly measured oxygen consumption in canine studies. Previous measurements of global left ventricular oxygen consumption in humans have been based on indicator dilution techniques for the measurement of blood flow and directly measured arterio-venous oxygen extraction. Myocardial oxygen consumption measured in this way is in the region of 6 to 8 mls /100 gm/min in subjects with no evidence of cardiac disease at rest [118], equivalent to 1.5 to 2.0 μmol/gm/min. Similar results have been reported in patients with coronary artery disease at rest [119]. Myocardial oxygen consumption in the current study in volunteers suggested a mean value of approximately 1 μmol/gm/min, lower than that accepted based on directly measured oxygen consumption. This variation may indicate that extrapolation to humans, based on canine data, is inappropriate. Potentially differences in the size of the acetyl CoA pool within the mitochondria, and differences in the size of the pool containing citric acid cycle intermediates, may vary between species. Such differences would potentially alter the relationship between myocardial oxygen consumption and ^{11}C-acetate clearance rates. A definitive answer will require a future comparison of directly measured oxygen consumption in normal volunteers, combined with assessment of ^{11}C-acetate tracer kinetics. Alternatively, lower than anticipated oxygen consumption in this study may reflect the young population sampled. This latter proposition is

supported by the finding that the regression relationship between the rate-pressure product and ^{11}C-acetate clearance rate constant is not significantly different between humans and dogs, as described in a more recent report by Henes et al from Washington University [120]. Hence the ^{11}C-acetate clearance rate constant is similar in both dogs and humans at the same rate-pressure product or cardiac workload. Rate pressure product is closely correlated with myocardial oxygen consumption in subjects with and without evidence of coronary artery disease [119,121], and also canine studies as described in Chapter 4. However it is not clear if the regression relationship between rate pressure product and oxygen consumption is similar between species. Hence extrapolation of canine data to man will require further studies for clarification.

Human studies with ^{11}C-acetate. The results in normal subjects reported herein were reported in 1989 [57], and similar results have subsequently been reported. Hicks et al in 1991 [83] and 1992 [122] reported mean ^{11}C-acetate clearance half times of 13.1 and 13.9 minutes respectively in normal volunteers at rest, and Krivokapich et al [123] in 1993 reported a mean half time of 13.9 minutes in a similar population. Inotropic stimulation with dobutamine, resulting in increased cardiac work, has been shown to increase clearance rates [123]. These results in humans are similar to those observed in canine studies reported in Chapter 4. Further studies at Washington University have been completed in patients with either chronic coronary artery disease [46] or following acute myocardial infarction [124] by Gropler et al. Both studies examined the metabolic capabilities of dysfunctional myocardium that was determined to be either viable or non-viable, based on recovery of contractility following revascularization. Recovery of contractility is generally considered the "gold" standard for the determination of viable myocardium. Dysfunctional but viable myocardium following myocardial infarction was shown to have a level of oxidative metabolism that was moderately impaired in comparison to remote myocardium (a mean of 74% of that of remote myocardium), while non-viable myocardium was severely impaired (a mean of 45% of that in remote myocardium) [124]. It was concluded that preservation of oxidative metabolism was a necessary condition for recovery of contractility consequent to revascularization following myocardial infarction. Similar results were found in patients with chronic

coronary artery disease [46]. Regional utilization of glucose was also examined in each study, using ^{18}F-fluorodeoxyglucose. Uptake of ^{18}F-fluorodeoxyglucose, normalized to relative perfusion (using [^{15}O]H_2O), was very variable in both viable and non-viable regions. Diminished uptake of ^{18}F-fluorodeoxyglucose, without an increase in glucose utilization compared to perfusion, was present in some regions subsequently recognized to be viable following revascularization. Conventionally this pattern of glucose uptake would be interpreted to indicate non-viable myocardium [125]. However oxidative metabolism in these regions was similar to other dysfunctional but viable regions, suggesting that alternative substrates were utilized other than glucose. Conversely increased myocardial utilization of glucose was seen in non-viable regions with severely impaired oxidative metabolism. Potentially anaerobic glycolysis may have been responsible for the increased uptake of ^{18}F-fluorodeoxyglucose, however impaired aerobic metabolism was insufficient to result in functional recovery after revascularization.

Summary. Current human studies have confirmed the excellent imaging qualities of ^{11}C-acetate. Clearance of ^{11}C-acetate was monoexponential at work loads studied, and half times measured in normal volunteers have been confirmed by subsequent investigators. Clearance was greater in normal myocardium post infarction due to greater cardiac work, and peri-infarct and infarct regions demonstrated impaired clearance indicating impaired oxidative metabolism. Calculation of myocardial oxygen consumption based on canine data should be interpreted with caution until confirmed in human studies, although such studies will be difficult to undertake. Subsequent experience with ^{11}C-acetate in patients with myocardial infarction or chronic coronary artery disease has indicated that assessment of oxidative metabolism may be an accurate method of differentiating viable from non-viable myocardium. Confirmation of this potential role of ^{11}C-acetate will require larger studies.

Chapter 10.

Summary

Myocardial utilization of substrates for energy production depends on a variety of factors including the arterial concentration of each substrate, the metabolic environment (for example myocardial ischaemia) and the hormonal environment. Major substrates used are free fatty acids, glucose, lactate and ketone bodies. Preferred substrates under normal resting conditions are free fatty acids, while glucose plays a more major role after a high carbohydrate meal and during ischaemia, and lactate utilization increases during exercise. The variety of substrates utilized by the heart precludes estimation of total metabolic activity from any one substrate alone, and this recognition has lead to the assessment of potential tracers which may measure total oxidative metabolism. Acetate labelled with a positron emitting radionuclide, particularly carbon-11, appeared a ideal agent based on fundamental biochemical principles. Acetate is normally present in low concentrations in plasma, and is readily utilized by the heart. Cellular uptake and activation to acetyl CoA appear to be poorly regulated and are not rate limiting. Subsequent metabolism is limited in comparison to the diversity of metabolites found with glucose or free fatty acids. Acetate is predominantly metabolized in the citric acid cycle, with the production of $^{11}CO_2$ from ^{11}C-acetate. Alternative metabolic routes are incorporation into lipids and amino acids, but prior reports have suggested that these metabolic routes are minor. It was hypothesized that the rate of production of $^{11}CO_2$ would reflect citric acid cycle activity, and that this would reflect oxygen consumption due to tight coupling between citric acid cycle flux and oxidative phosphorylation. Clearance of $^{11}CO_2$ from the heart, after administration of ^{11}C-acetate, could potentially be measured with positron emission tomography from myocardial residue time-activity curves.

Initial studies were performed in isolated perfused rabbit hearts, using both ^{14}C-acetate and ^{11}C-acetate. Clearance of $^{14}CO_2$ from hearts was found to be biexponential, and the rate constant of the initial rapid phase was found to correlate closely with myocardial oxygen consumption. This occurred over a wide range of oxygen consumption, including low and high work loads with normoxia, hypoxia,

ischaemia and reperfusion following ischaemia. Clearance of total ^{14}C-radioactivity was predominantly due to $^{14}CO_2$, and no significant difference was found between rate constants for efflux of total ^{14}C-radioactivity or $^{14}CO_2$. In theory the externally measured clearance of total ^{11}C-radioactivity after administration of ^{11}C-acetate should then indicate the rate of production and efflux of $^{11}CO_2$, and this was shown to be the case. An excellent correlation was found between the externally derived rate of clearance of total ^{11}C radioactivity and myocardial oxygen consumption. Metabolites of ^{14}C-acetate in venous effluent, other than $^{14}CO_2$, were also investigated by high performance liquid chromatography. These were found to be predominantly ^{14}C-hydroxybutyrate and ^{14}C-acetoacetate, with minor quantities of ^{14}C-labelled citric acid cycle intermediates and backdiffused ^{14}C-acetate also present.

These studies indicated that the original hypothesis was correct *in vitro*, when myocardial substrate utilization was constant. The hypothesis was then tested *in vivo*, using a closed chest canine model. ^{11}C-acetate was administered intravenously, and myocardial residue time-activity curves generated by positron emission tomography. Tomograms acquired early following intravenous administration showed excellent left ventricular delineation, with rapid clearance of ^{11}C-radioactivity from the left ventricular cavity. Clearance of total ^{11}C-radioactivity was again found to be biexponential, and was closely correlated with the rate constant of efflux of $^{11}CO_2$ from the coronary sinus. A close correlation between externally derived clearance rates and directly measured oxygen consumption was again confirmed over a wide range of cardiac work loads. Clearance of ^{11}C-acetate was homogeneous throughout the left ventricle, and similar results were later found in human volunteers.

Initial studies in isolated perfused rabbit hearts showed no effect of physiological levels of unlabelled acetate on ^{11}C-acetate kinetics, compared to no added acetate. Further effects of altered substrate utilization were examined in the closed chest canine model by comparing ^{11}C-acetate clearance rates at baseline with those after glucose or free fatty acid infusion, which resulted in preferential utilization of glucose or fatty acid respectively. No significant effect of altered substrate utilization on ^{11}C-acetate tracer kinetics was apparent in these studies. A subsequent

report by other investigators has documented reduced ^{11}C-acetate clearance associated with supra-physiological levels of acetate in isolated perfused rat hearts, possibly due to expansion of the intracellular distribution of the ^{11}C-label. In the same study enhanced free fatty acid utilization had no significant effect in isolated perfused rat hearts, similar to results found herein in *in vivo* canine studies. Although minor changes have been reported in more recent canine and human studies following fatty acid infusion, the direction of these changes has been inconsistent with both a minor decline and increase in ^{11}C-acetate clearance rates reported. In addition a direct assessment of oxygen consumption was not undertaken in these studies, and hence possible effects of altered fatty acid utilization on the relationship between ^{11}C-acetate clearance rates and oxygen consumption can only be inferred. A weighing of the significance of the data published to date, including that described herein, would suggest that ^{11}C-acetate kinetics are either unchanged or are insensitive to changes in substrate utilization.

Hence the utility of ^{11}C-acetate as a tracer of oxidative metabolism has been validated in a variety of animal models over a wide range of cardiac work loads and pathological conditions. The latter include myocardial ischaemia and myocardial reperfusion following ischaemia. Subsequent studies by other investigators have confirmed these results.

This technique was then applied to a canine model of acute myocardial infarction, involving coronary occlusion for 1 hour prior to reperfusion. Calculated myocardial oxygen consumption acutely following reperfusion in the ischaemic region was reduced by 26 to 97%, consistent with the known reduction of oxygen consumption in stunned myocardium. Subsequently oxidative metabolism was examined in a chronic model of acute myocardial infarction, and the recovery of oxidative metabolism compared against the recovery in contractility over a period of 4 weeks. A period of 1 hour of coronary occlusion was again chosen to produced stunned myocardium associated with minor anticipated myocardial infarction. In this model recovery of oxidative metabolism and contractility occurred in parallel over a 4 week period, with recovery of contractility to near normal. Initial depression of contractility

in reperfused myocardium was severe compared to moderate depression of oxidative metabolism, indicating that preserved oxidative metabolism acutely predicates subsequent recovery of contractility.

Myocardial uptake of ^{11}C-acetate was also examined in a canine model of more extensive myocardial infarction, to aid in the interpretation of anticipated patient studies. The size of the defect seen on the left ventricular wall early following intravenous administration of ^{11}C-acetate correlated closely with infarct size measured by TTC. Myocardial uptake of ^{11}C-acetate was also compared with ^{11}C-palmitate, which has previously been investigated in the determination of infarct size. Reduced uptake of ^{11}C-palmitate compared to ^{11}C-acetate was seen in peri-infarct regions, resulting in overestimation of calculated infarct size compared to ^{11}C-acetate. These data suggested that lack of uptake of ^{11}C-acetate in reperfused myocardium was consistent with the presence of non-viable myocardium.

Initial human studies with ^{11}C-acetate confirmed the excellent imaging properties of this tracer. Clearance rates were homogeneous in normal volunteers, indicating homogeneous oxidative metabolism throughout the left ventricle. Myocardial oxygen consumption was calculated from the previously established relationship between clearance rates and oxygen consumption in canine studies, and found in normal subjects to be less than generally accepted from previous direct measurements. Potentially interspecies differences in the intracellular distribution volume of the ^{11}C-label may exist, which alters the relationship between clearance rates and oxygen consumption. Further studies will be required to investigate this relationship further in humans. Three studies were also undertaken in patients following myocardial infarction, and regional oxidative metabolism found to vary depending on the proximity to the infarct zone. Peri-infarct zones showed impaired oxidative metabolism compared to normal zones, with further depression in the infarct zone.

The current investigation of the use of ^{11}C-acetate in conjunction with PET indicates that assessment of oxidative metabolism can be achieved non invasively in normal and diseased states. These findings highlight the future potential for examining

the impact of interventions in the treatment of patients with coronary artery disease and myocardial infarction.

Appendix A.

Volume and Spillover Correction Methods.

Observed blood pool and tissue radiotracer concentration must be corrected for partial volume and spillover effects, since the thickness of left ventricular myocardium is less than two times the full width at half maximum resolution of the tomographic units used in these studies. Four correction factors are defined, as detailed below

recovery coefficient of blood (F_{BB})

recovery coefficient of tissue (F_{MM})

fraction of counts "spilling" into myocardium from LV cavity (F_{BM})

fraction of counts "spilling" into LV cavity from myocardium (F_{MB})

These correction factors were calculated by convolving a Gaussian point spread function in one dimension with a radius of 15 mm (representing the left ventricular cavity) or an annulus with a diameter of 10 mm (representing the left ventricular wall) to obtain image profiles. These profiles were integrated over the width of the region of interest to obtain the correct fractions defined by:

$$F_{BB} = \frac{1}{A.*R}\int_0^R g(x)dx,$$

$$F_{MM} = \frac{1}{B*D}\int_R^{R+D} f(x)dx,$$

$$F_{BM} = \frac{1}{A*R}\int_R^{R+D} g(x)dx,$$

$$F_{MB} = \frac{1}{B*D}\int_0^R f(x)dx,$$

where A = concentration of radioactivity in the left ventricular cavity; B = concentration of radioactivity in the left ventricular wall and g(x) and f(x), the blood pool and tissue analytical profiles, were defined by:

$$g(x) = \frac{A}{\sqrt{2\pi\sigma}} \int_{-R}^{R} \exp\left[-\frac{1}{2}\left(\frac{x-r}{\sigma} \right)^2 \right] dr;$$

$$f(x) = \frac{B}{\sqrt{2\pi\sigma}} \left[\int_{-R-D}^{-R} \exp\left[-\frac{1}{2}\left(\frac{x-r}{\sigma} \right)^2 \right] dr + \int_{R}^{R+D} \exp\left[-\frac{1}{2}\left(\frac{x-r}{\sigma} \right)^2 \right] dr \right];$$

where R = cylinder radius; D = annulus thickness; and σ = standard deviation of the point spread function (FWHM/2.38). These fractions were then used to correct the observed tissue and left ventricular cavity regional counts to estimate true concentration of radiotracer based on the following relations:

$$O_B = F_{BB} * T_B + F_{MB} * T_M$$

and

$$O_M = F_{MM} * T_M + F_{BM} * T_B,$$

where O_B = observed counts in the left ventricular cavity; O_M = observed counts in the left ventricular wall; T_B= true (corrected) left ventricular counts and T_M = true (corrected) left ventricular wall counts. The corrected counts were then used to calculate the turnover rate constant.

Appendix B.

Preparation of ^{11}C-acetate.

Preparation of ^{11}C-acetate was first synthesized by Buchanan et al [126] in 1943, and subsequently by Poe et al [127] and Winstead et al [48]. These workers generally used a methylmagnesium halide to produce ^{11}C-acetate from ^{11}C-labelled carbon dioxide. The technique was refined by Pike et al [49] in 1982, in a detailed description of the production of ^{11}C-acetate from methylmagnesium bromide. Radiochemical purity was reported to be greater than 95%.

A further modification at Washington University enabled the consistent production of ^{11}C-acetate of greater than 99% radiochemical purity. ^{11}C-labelled carbon dioxide was prepared by the ^{14}N (p,α) ^{11}C reaction in the Washington University Centre cyclotron and bubbled through 3 ml of a 0.1 M solution of methylmagnesium bromide (Aldrich Chemical Company, Milwaukee, Wisconsin) in diethyl ether. The product was then hydrolysed with 6 mls of 6N hydrochloric acid, and 6 mls of diethyl ether then added. The sample was vortexed and the organic layer allowed to separate from the aqueous layer. The latter was discarded and 10 mls of 0.9% sodium bicarbonate was added to the organic layer and vortexed. The organic and aqueous phases were again allowed to separate and the aqueous layer removed and bubbled with nitrogen at 50 C for 10 minutes. The latter step allowed the removal of residual ether, which may produce discomfort on intravenous administration to patients. Radiochemical purity also increased due to loss of unknown volatile radiolabelled constituents. Sterility was maintained by serial filtration through 0.45 and 0.2 micron filters.

Each sample intended for an animal study was tested for radiochemical purity. Potential impurities were separated with a SpectroPhysics HPLC system, as described in Chapter 3. Radiochemical purity was consistently greater than 99%, and estimated specific activity was greater than 1 Ci/mmole.

Bibliography.

1. Tennant R, Wiggers CJ. The effect of coronary occlusion on myocardial contraction. Am J Physiol 112:351-361, 1935
2. Braunwald E, Kloner RA. The stunned myocardium: prolonged, post-ischemic ventricular dysfunction. Circulation 66:1146-9, 1982
3. Rahimtoola SH. The hibernating myocardium. Am Heart J 117:211-221, 1989
4. Tillisch J, Brunken R, Marshall R, Schwaiger M, Mandelkern M, Phelps M, Schelbert H. Reversibility of cardiac wall motion abnormalities predicted by positron tomography. N Engl J Med 314:884-888, 1986
5. Myears DW, Sobel BE, Bergmann SR. Substrate use in ischemic and reperfused canine myocardium: quantitative considerations. Am J Physiol:Heart Circ Physiol 253:H107-H114, 1987
6. Parker JA, Beller GA, Hoop B, Holman L, Smith TW. Assessment of regional myocardial blood flow and regional fractional oxygen extraction in dogs, using ^{15}O-water and ^{15}O-hemoglobin. Circ Res 42:511-518, 1978
7. Opie LH. Effects of regional ischemia on metabolism of glucose and fatty acids. Circ Res 38:I52-68, 1976
8. Drake AJ, Haines JR, Noble MIM. Preferential uptake of lactate by the normal myocardium in dogs. Cardiovasc Res 14:65-72, 1980
10. Barnes RH, Mackay EM, Noe GK, Visscher MD. Utilization of betaoxybutyric acid by isolated mammalian heart and lungs. Am J Physiol 123:272-279, 1938
11. Williamson JR, Krebs EA. Acetoacetate as fuel of respiration in the perfused rat heart. Biochem J 80:540-547, 1961
12. Hall LM. Preferential oxidation of acetate by the perfused heart. Biochemical and Biophysical Research Communications 6:177-179, 1961
13. Bassenge E, Wendt VE, Schollmeyer P, Blumchen G, Gudbjarnason S, Bing RJ. Effect of ketone bodies on cardiac metabolism. Am J Physiol 208:162-168, 1965
14. Williamson JR. Effects of insulin and starvation on the metabolism of acetate and pyruvate by the perfused rat heart. Biochem J 93:97-106, 1964

15. Lindeneg O, Mellemgaard K, Fabricius J, Lundquist F. Myocardial utilization of acetate, lactate and free fatty acids after injestion of ethanol. Clin Sci 27: 427-435, 1964

16. Bartelt U, Katterman R. Enzymatic determinations of acetate in serum. J Clin Chem Clin Biochem 23: 879-81, 1985

17. Williamson JR. Glycolytic control mechanisms. I. Inhibition of glycolysis by acetate and pyruvate in the isolated perfused rat heart. J. Biol. Chem. 240:2308-2321, 1965

18. Outlines of Biochemistry. eds Conn EE, Stumpf PK, Bruening GE, Doi RH. John Wiley and Sons New York, p 407

19. Scholte HR, Wit-Peeters EM, Bakker JC. The intracellular and intramitochondrial distribution of short chain acyl CoA synthetases in guinea pig heart. Biochim. Biophys. Acta 231:479-486, 1971

20. Randle PJ, England PJ, Denton RM. Control of the carboxylic acid cycle and its interaction with glycolysis during acetate utilization in rat heart. Biochem J 117:677-695, 1970

21. Bergmeyer HU, Moellering H. Enzymatishe Bestimmung von acetat. Biochem Z 344:167, 1966

22. Bremer J, Osmundsen. H. Fatty acid oxidation and its regulation. in Fatty Acid Metabolism and Its Regulation. ed Numa S. Elsevier Science Publishers B.V. 1984

23. Knowles SE, Jarrett IG, Filsell OH, Ballard OH. Production and utilization of acetate in mammals. Biochem. J. 142; 401-411,1974

24. Gercken G, Trotz M. Fatty acid synthesis in the arrested rabbit heart during ischemia, PflÚgers Arch 398:69-72, 1983

25. Lehninger AL. Principles of Biochemistry. New York, 1982, Worth Publishing Co., p437

26. Bailey IA, Gadian DG, Matthews PM, Radda GK, Seeley PJ. Studies of metabolism in the isolated perfused rat heart using 13C NMR. FEBS Letters 123:315-318, 1981

27. Chain EB, Mansford KRL, Opie LH. Effects of insulin on the pattern of glucose metabolism in the perfused working and langendorff heart of normal and insulin-deficient rats. Biochem J. 115: 537-546, 1969

28. Taegtmeyer H. Myocardial Metabolism. in Positron Emission Tomography and Autoradiography: Priciples and Applications for the Brain and Heart. eds Phelps M., Mazziotta J. and Schelbert H. Raven Press, New York 1986

29. Whereat AF,Chan A. Effects of hypoxemia and acute coronary occlusion on myocardial metabolism in dogs. Am J Physiol 223: 1398 ,1972

30. Stern JR, Coon MJ, Del Campillo A. Enzymatic breakdown and synthesis of acetoacetate. Nature 171:28, 1953

31. LaNoue K, Nicklas WJ, Williamson JR. Conrol of citric acid cycle activity in rat heart mitochondria. J Biol Chem 245:102, 1970

32. Ghosal J, Whitworth T, Coniglio JG. Biosynthesis of fatty acids from [1-^{14}C]acetate in the perfused rat heart. Biochim Biophys Acta 187:576-578,1969

33. Harris P, Gloster J. The effects of acute hypoxia on lipid synthesis in the rat heart. Cardiology 56: 43-47, 1971/72

34. Stremmel W. Fatty acid uptake by isolated rat heart myocytes represents a carrier mediated transport process. J Clin Invest 81:844-852, 1988

35. Klein MS, Goldstein RA, Welch MJ, Sobel BE. External assessment of myocardial metabolism with ^{11}C-palmitate in rabbit hearts. Am J Physiol(Heart Circ Physiol) 237:H51-H58, 1979

36. Schon HR, Schelbert HR, Najafi A, Robinson G, Huang SC, Barrio J, Phelps ME. C-11 labeled palmitic acid for the noninvasive evaluation of regional myocardial fatty acid metabolism with positron computed tomography: I. Kinetics of C-11 palmitic acid in normal myocardium. Am Heart J 103:532-547, 1982

37. Schelbert HR, Henze E, Schon HR, Najafi A, Hansen HW, Selin C, Huanh SC, Barrio JR, Phelps ME. C-11 palmitate for the non-invasive evaluation of regional myocardial fatty acid metabolism with positron computed tomography. III. In vivo demonstration of the effects of substrate availability on myocardial metabolism. Am Heart J 105:492-504, 1983

38. Lerch RA, Bergmann SA, Ambos HD, Welch MJ, Ter-Pogossian MM, Sobel BE. Effect of flow-independent reduction of metabolism on regional myocardial clearance of ^{11}C palmitate. Circulation 65:731-738, 1982

39. Fox KAA, Abendschein DR, Ambos HD, Sobel BE, Bergmann SR. Efflux of metabolized and nonmetabolized fatty acid from canine myocardium. Implications for quantifying myocardial metabolism tomographically. Circ Res 57:232-243, 1985

40. Rosamond TL, Abendschein DR, Sobel BE, Bergmann SR, Fox KAA. Metabolic fate of radiolabeled palmitate in ischemic canine myocardium: implications for positron emission tomography. J Nuc Med 28:1322-1329, 1987

41. Weiss ES, Ahmad SA, Welch MJ, Williamson JR, Ter-Pogossian MM, Sobel BE. Quantification of infarction in cross sections of canine myocardium in vivo with positron emission transaxial tomography and ^{11}C-palmitate. Circulation 55:66-73, 1977

42. Gambirr SS, Schwaiger M, Huang SC. Simple noninvasive quantification method for measuring myocardial glucose utilization in humans employing positron emission tomography and flourine-18-deoxyglucose. J Nucl Med 30:359-366, 1989

43. Choi Y, Hawkins RA, Huang SC. Parametric images of myocardial metabolic rate of glucose generated from dynamic cardiac PET and 2-[^{18}F]fluoro-2-deoxy-d-glucose studies. J Nucl Med 32:733-738, 1991

44. Marshall RC, Tillisch JH, Phelps ME, Huang SC, Carson RC, Henze E, Schelbert HR. Identification and differentiation of resting myocardial ischaemia and infarction in man with positron computed tomography 18F-labelled flourodeoxyglucose and N-13 ammonia. Circulation 64:766-778, 1981

45. Schwaiger M, Schelbert HR, Ellison D, Hansen H, Yeatman L, Vinten-Johansen J, Selin C, Phelps ME. Sustained regional abnormalities in cardiac metabolism after transient ischemia in the chronic dog model. J Am Coll Cardiol 6:336-347, 1985

46. Gropler RJ, Geltman EM Sampathkumaran K, Perez JE, Moerlien SM, Sobel BE, Bergmann SR,Siegal BA. Functional recovery after coronary revascularization for

chronic coronary artery disease is dependent on maintenance of oxidative metabolism. J Am Coll Cardiol 20:569-577, 1992

47. Lathrop KA, Harper PV, Rich BH, Dinwoodie, Krizek H, Lembares, N, Gloria I. Rapid incorporation of short-lived cyclotron-produced radionuclides into radiopharmaceuticals. J Radiopharmacueticals and Labeled Compounds 1:471-481, 1973

48. Winstead MB, Doughtery DA, Lin TH, Khentigan A, Lamb JF, Winchell HS. Relationship of molecular structures to *in vivo* scintigraphic distribution of carbon-11-labeled compounds: 1.^{11}C-carboxylates. J Nuc Med 14:747-754, 1973

49. Pike VW, Eakins MN, Allan RM, Selwyn AP. Preparation of [1-11C]acetate - an agent for the study of myocardial metabolism by positron emission tomography. Int J Appl Radiat Isot 33:505-512, 1982

50. Allan RM, Selwyn AP, Pike VW, Eakins MN, Maseri A. In vivo experimental and clinical studies of normal and ischemic myocardium using ^{11}C-acetate. Circulation 62:III-74,1980 (abstract)

51. Selwyn AP, Allan R, Pike V , Fox K, Maseri A. Positive labeling of ischemic myocardium: a new approach in patients with coronary disease. Am J Cardiol 47:481, 1981 (abstract)

52. Allan RM, Pike VW, Maseri A, Selwyn AP. Myocardial metabolism of 11C-acetate: experimental and patient studies. Circulation 64:IV-75, 1981 (abstract)

53. Brown M, Marshall DR, Sobel BE. Delineation of myocardial oxygen utilization with carbon-11 labelled acetate. Circulation 3:687-696, 1987

54. Brown MA, Myears DW, Bergmann SR. Noninvasive assessment of canine myocardial oxidative metabolism with carbon-11 acetate and positron emission tomography. J Am Coll Cardiol 12;1054-63, 1988

55. Brown MA, Myears DW, Bergmann SR. Validity of estimates of myocardial oxidative metabolism with carbon-11 acetate and positron emission tomography despite altered patterns of substrate utilization. J Nucl Med 30:187-193, 1989

56. Weinheimer CJ, Brown MA, Nohara R, Perez JE, Bergmann SR. Functional recovery after reperfusion is predicated on recovery of myocardial oxidative metabolism. Am Heart J 125:939-949, 1993

57. Walsh MN, Geltmann EM, Brown MA, Henes CG, Weinheimer CJ, Sobel BE, Bergmann SR. Noninvasive estimation of regional myocardial oxygen consumption by positron emission tomography with carbon-11 acetate in patients with myocardial infarction. J Nucl Med 30:1798-1808, 1989

58. Bergmann SR, Clark RE, Sobel BE. An improved isolated heart preparation for external assessment of myocardial metabolism. Am J Physiol 236: H644, 1979

59. Benson JR, Woo DJ. Polymeric columns for liquid chromatography. J Chromatogr Sci 22:386, 1984

60. Bligh EG, Dyer WJ. A rapid method of total lipid extraction and purification. Can J Biochem Physiol 37:911, 1959

61. Wallenstein S, Zucker CL, Fleiss JL. Some statistical methods usefull in circulation research. Circ Res 47: 1-9, 1980

62. Bieber LL, Fiol CJ. Fatty acid and ketone metabolism. Circulation 72 (Supp IV):IV-9, 1985

63. Brown MA, Marshall Dr, Sobel BE, Bergmann SR. Assessment of myocardial oxidative capacity with radiolabeled acetate. Circulation 74 (Suppl II):513, 1986 (abstract)

64. Buxton DB, Schwaiger M, Phelps ME, Schelbert HR. Myocardial acetate kinetics and tricarboxylic acid cycle. Circulation 74 (Suppl II):211, 1986 (abstract)

65. Buxton DB, Schwaiger M, Nguyen A,Phelps ME, Schelbert HR. Radiolabeled acetate as a tracer of myocardial tricarboxylic acid cycle flux. Circ Res 63:628-634, 1988

66. Ter-Pogossian MM, Ficke DC, Hood JT, Yamamoto M, Mullani NA. PETT VI: a positron emission tomograph utilizing cesium fluoride scintillation detectors. J Comput Assist Tomogr 6: 125-33, 1982

67. Bergmann SR, Carlson E, Dannen E, Sobel BE. An improved assay with 4-(2-thiazolylaso)-resorcinol for non-esterified fatty acids in biological fluids. Clin Chim Acta 104: 53-63, 1980

68. Bergmeyer HU, Mollering H. Acetate. In: Bergmeyer HU, ed. Methods of Enzymic Analysis. Weinheim:Verlag-Chemie, p 628-639 1984

69. Heyman MA, Payne BD, Hoffman JIE, Rudolph AM. Blood flow measurements with radionuclide-labeled particles. Prog Cardiovasc Dis 20:55-78, 1977

70. Nelson RR, Gobel FL, Jorgensen CR, Wang K, Wang Y, Taylor HL. Hemodynamic predictors of myocardial oxygen consumption during static and dynamic exercise. Circulation 50: 1179-89. 1974

71. Opie LH, Owen P, Riemersma MA. Relative rate of oxidation of glucose and free fatty acids by ischemic and non ischemic myocardium after coronary artery ligation in the dog. Eur J Clin Invest 3:419-435, 1973

72. Buxton DB, Nienaber CA, Luxen A, Ratib O, Hansen H, Phelps ME, Schelbert HR. Noninvasive quantitation of regional myocardial oxygen consumption in vivo with [1-^{11}C]acetate and dynamic positron emission tomography. Circulation 79:134-142, 1989

73. Armbrecht JJ, Buxton DB, Schelbert HR. Validation of [1-^{11}C]acetate as a tracer for noninvasive assessment of oxidative metabolism with positron emission tomography in normal, ischemic, postischemic, and hyperemic canine myocardium. Circulation 81:1594-1605, 1990

74. Astrand PO, Rodahl K. Lactic acid distribution and clearance. in Textbook of Work Physiology. McGraw-Hill Inc, New York 1970 p 290

75. Garland PB, Randle PJ, Newsholme EA. Citrate as an intermediary in the inhibition of phosphofructokinase in rat heart muscle by fatty acids, ketone bodies, pyruvate, diabetes, and starvation. Nature 200: 169-170, 1963

76. Peuhkurinen KJ, Hassinen IE. Pyruvate carboxylation as an anapleurotic mechanism in the isolated perfused rat heart. Biochem J 202, 67-76, 1982

77. Herrero P, Markham J, Bergmann SR. Quantitation of myocardial blood flow with $H_2{}^{15}O$ and positron emission tomography: assessment and error analysis of a mathematical approach. J Comput Assist Tomogr 13:862-73, 1989

78. Bergmann SR, Herrero P, Markham J, Weinheimer CJ, Walsh MN. Noninvasive quantitation of myocardial blood flow in human subjects with oxygen-15-labeled water and positron emission tomography. J Am Coll Cardiol 14:639-52 1989

79. Schelbert HR, Henze E, Sochor H, Grossman BG, Huang SC, Barrio JR, Schwaiger M, Phelps ME. Effects of substrate availability on myocardial C-11 palmitate kinetics by positron emission tomography in normal subjects and patients with ventricular dysfunction. Am Heart J 111:1055-1064, 1986

80. Phelps ME, Hoffman EJ, Selin CE, Huang SC, Robinson G, MacDonald N, Schelbert H, Kuhl DE. Investigation of [^{18}F]2-fluoro-2-deoxyglucose for the measure of myocardial glucose consumption. J Nuc Med 19:1311-1319, 1978

81. Krivokpaich J, Huang SC, Selin CE, Phelps ME. Fluorodeoxyglucose rate constants, lumped constant, and glucose metabolic rate in rabbit heart. Am J Physiol:Heart Circ Physiol 252:H777-H787, 1987

82. Merhige ME, Ekas R, Mossberg K, Taegtmeyer H, Gould KL. Catecholamine stimulation, substrate competition, and myocardial glucose uptake in conscious dogs assessed with positron emission tomography. Circ Res 61(Suppl II):II124-129, 1987

83. Hicks RJ, Herman WH, Kalff V, Molina E, Wolfe ER, Hutchins G, Schwaiger M. Quantitative evaluation of regional substrate metabolism in the human heart by positron emission tomography. J Am Coll Cardiol 18:101-111, 1991

84. Kotzerke J, Hicks RJ, Wolfe E, Herman WH, Molina E, Kuhl DE, Schwaiger M. Three-dimensional assessment of myocardial oxidative metabolism: a new approach for regional determination of PET derived carbon-11-acetate kinetics. J Nucl Med 31:1876-1893, 1990

85. McFalls EO, Duncker DJ, Krams R, Sassen Lm, Hoogendoorn A, Verdouw PD. Recruitment of myocardial work and metabolism in regionally stunned porcine myocardium. Am J Physiol 263(6 Part 2): H1724-31, 1992

86. Schulz R, Janssen F, Guth BD, Heusch G. Effect of coronary perfusion on regional myocardial function and oxygen consumption of stunned myocardium in pigs. Basic Res Cardiol 86:534-43, 1991

87. Laster SB, Becker LC, Ambrosio G, Jacobus WE. Reduced aerobic metabolic efficiency in globally "stunned" myocardium. J Mol Cell Cardiol 21:419-26, 1989

88. Dean EN, Shlafer M, Nicklas JM. The oxygen consumption paradox of "stunned myocardium". Bas Res Cardiol 85:120-131, 1990

89. Laxson DD, Homans DC, Dai XZ, Sublett E, Bache RJ. Oxygen consumption and coronary reactivity in postischemic myocardium. Circ Res 64:9-20, 1989

90. Ohgoshi Y, Goto Y, Futaki S, Yaku H, Kawaguchi O, Suga H, Increased oxygen cost of contractility in stunned myocardium of dog. Circ Res 69:975-988, 1991

91. Kawashima S, Satani A, Tsumoto S, Kondo T, Ikeoka K, Morita M, Iwasaki T. Coronary pressure flow, pressure-function and function-myocardial oxygen consumption relations in postischaemic myocardium. Cardiovasc Res 25:837-43, 1991

92. Schott RJ, Rohmann S, Brawn ER, Schaper W. Ischemic preconditioning reduces infarct size in swine myocardium. Circ Res 66:1133-42, 1990

93. Krukenkamp IB, Silverman NA, Sorlie D, Pridjian A, Feinberg H, Levitsky S. Characterization of postischemic myocardial oxygen utilization. Circulation 74 (Suppl III):III125-129, 1986

94. Stahl LD, Weiss HR, Becker LC. Myocardial oxygen consumption, oxygen supply/demand heterogeneity, and microvascular patency in regional stunned myocardium. Circulation 77:865-872, 1988

95. Brown MA, Myears DW, Herrero P, Bergmann SR. Disparity between oxidative and fatty acid metabolism in reperfused myocardium assessed with positron emission tomography. Circulation 76 (Suppl IV):4, 1987 (abstract)

96. Schwaiger M. Schelbert HR, Keen R, Vinten-Johansen, Hansen H, Selin C, Barrio J, Huang S-C, Phelps ME. Retention and clearance of C-11 palmitic acid in ischemic and reperfused canine myocardium. J Am Coll Cardiol 6:311-320, 1985

97. Armbrecht JJ, Buxton DB, Schelbert HR. Validation of [1-^{11}C]acetate as a tracer for noninvasive assessment of oxidative metabolism with positron emission tomography in normal, ischemic, postischemic, and hyperemic canine myocardium. Circulation 81:1594-1605, 1990

98. Liedtke AJ, DeMaison L, Eggleston AM, Cohen LM, Nellis SH. Changes in substrate metabolism and effects of excess fatty acids in reperfused myocardium. Circ Res 62:535-542, 1988

99. Renstrom B, Nellis SH, Liedtke AJ. Metabolic oxidation of glucose during early myocardial perfusion. Circ Res 65:1094-1101, 1989

100. Renstrom B, Nellis SH, Liedtke AJ. Metabolic oxidation of pyruvate and lactate during early myocardial reperfusion. Circ Res 66:282-288, 1990

101. van der Vusse GJ, Roemen THM, Prinzen FW. Uptake and tissur content of fatty acids in dog myocardium under normoxic and ischemic conditions. Circ Res 50:538-546, 1982

102. Liedtke AJ. Alterations of carbohydrate and lipid metabolism in the acutely ischemic heart. Prog Cardiovasc Dis 23:321-9, 1981

103. Gayheart PA, Vinten-Johansen J, Johnston WE, Hester TO, Cordell AR. Oxygen requirements of the dyskinetic myocardial segment. Am J Physiol 257:H1184-1191, 1989

104. Ter-Pogossian MM, Klein MS, Markham J, Roberts R, Sobel BE. Regional assessment of myocardial metabolic integrity in vivo by positron-emission tomography with ^{11}C-labeled palmitate. Circulation 61:242-255, 1980

105. Opie LH. Reperfusion injury and its pharmacological modification. Circulation 80:1049-1062, 1989

106. Bergmann SR, Lerch RA, Fox KA, Ludbrook PA, Welch MJ, Ter-Pogossian, Sobel BE. Temporal dependence of beneficial effects of coronary thrombolysis characterized by positron tomography. Am J Med 73:573-581, 1982

107. Gertz EW, Wisneski JA, Neese R, Houser A, Korte R, Bristow JD. Myocardial lactate extraction: multi-determined metabolic function. Circulation 61:256261, 1980

108. Buxton DB, Vaghaiwalla F, Krivokapich J, Phelps ME, Schelbert HR. Quantitative assessment of prolonged metabolic abnormalities in reperfused canine myocardium. Circulation 85: 1842-1856, 1992

109. Schaper W. Molecular mechanisms in "stunned" myocardium. Cardiovasc Drugs Ther 5:925-932, 1991

110. Taegtmeyer H, Roberts AFC, Raine AEG. Energy metabolism in reperfused heart muscle: metabolic correlates to return of function. J Am Coll Cardiol 6:684-670, 1985

111. Parisi AF, Moynihan PF, Folland ED, Feldman CL. Quantitative detection of regional left ventricular contraction abnormalities by two-dimensional echocardiography. Circulation 63:761-767, 1981

112. Buckberg GD, Luck JC, Payne B, Hoffman JIE, Archie JP, Fixler DE. Some sources of error in measuring regional blood flow with radioactive microspheres. J Appl Physiol 31:598-604, 1971

113. Lew WYW, Ban-Hayashi E. Mechanisms of improving regional and global ventricular function by preload alterations during acute ischemia in the canine left ventricle. Circulation 72:1125-1134, 1985

114. Lange R, Ware J, Kloner RA. Abscence of a cumulative deterioration of regional function during three repeated 5 or 15 minute coronary occlusions. Circulation 69:400-408, 1984

115. Weiner JM, Apstein CS, Arthur JH, Pirzada FA, Hood WB, Jr. Persistence of myocardial injury following brief periods of coronary occlusion. Cardiovasc Res 10:678-686, 1976

116. Brown MA, Norris RM, Takayama M, White HD. Post-systolic shortening: a marker of potential for early recovery of acutely ischaemic myocardium in the dog. Cardiovasc Res 21:703-716, 1987

117. Brown MA, Nohara R, Vered Z, Perez JE, Bergmann SR. The dependence of recovery of stunned myocardium on restoration of oxidative metabolism. Circulation 78 (Suppl II):467, 1988 (abstract)

118. Honig CR. Modern Cardiovascular Physiology. Little, Brown and Company, Boston 1981 p 222

119. Gobel FL, Nordstrom LA, Nelson RP, Jorgensen CR, Wang Y. The rate-pressure product as an index of myocardial oxygen consumption during exercise in patients with angina pectoris. Circulation 57:549-556, 1978

120. Henes CG, Bergmann SR, Walsh MN, Sobel BE, Geltmann EM. Assessment of myocardial oxidative metabolic reserve with positron emission tomography and carbon-11 acetate. J Nucl Med 30:1489-1499, 1989

121. Kitamura K, Jorgensen CR, Gobel FL, Taylor HL Wang Y. Hemodynamic correlates of myocardial oxygen consumption during upright exercise. J Appl Physiol 32:516-522, 1972

122. Hicks RJ, Savas V, Currie PJ, Kalff V, Starling M, Bergin P, Kirsch M, Schwaiger M. Assessment of myocardial oxidative metabolism in aortic valve disease using positron emission tomography with C-11 acetate. Am Heart J 124:653-664, 1992

123. Krivokapich J, Huang S-C, Schelbert HR. Assessment of the effects of dobutamine on myocardial blood flow and oxidative metabolism in normal human subjects using nitrogen-13 ammonia and carbon-11 acetate. Am J Cardiol 71:1351-1356, 1993

124. Gropler RJ, Siegal BA, Sampathkumaran K, Perez JE, Sobel BE, Bergmann SR, Geltman EM. Dependence of recovery of contractile function on maintenance of oxidative metabolism after myocardial infarction. J Am Coll Cardiol 19:989-997, 1992

125. Schelbert HR and Schwaiger M. PET studies of the heart. Positron emission tomography and autoradiography. Priciples and Applications for the Brain and Heart. eds Phelps M., Mazziotta J. and Schelbert H. Raven Press, New York 1986

126. Buchanan JM, Hastings AB, Nesbett FB. The role of carboxyl-labeled acetic, propionic, and butyric acids in liver glycogen formation. J Biol Chem 150:413-425, 1943

127. Poe ND, Robinson GD, MacDonald NS. Myocardial extraction of variously labelled fatty acids and carboxylates. J Nucl Med 14:440, 1973 (abstract)